INFORMATION TO USERS

This manuscript has been reproduced from the microfilm master. UMI films the text directly from the original or copy submitted. Thus, some thesis and dissertation copies are in typewriter face, while others may be from any type of computer printer.

The quality of this reproduction is dependent upon the quality of the copy submitted. Broken or indistinct print, colored or poor quality illustrations and photographs, print bleedthrough, substandard margins, and improper alignment can adversely affect reproduction.

In the unlikely event that the author did not send UMI a complete manuscript and there are missing pages, these will be noted. Also, if unauthorized copyright material had to be removed, a note will indicate the deletion.

Oversize materials (e.g., maps, drawings, charts) are reproduced by sectioning the original, beginning at the upper left-hand corner and continuing from left to right in equal sections with small overlaps.

Photographs included in the original manuscript have been reproduced xerographically in this copy. Higher quality 6" x 9" black and white photographic prints are available for any photographs or illustrations appearing in this copy for an additional charge. Contact UMI directly to order.

Bell & Howell Information and Learning
300 North Zeeb Road, Ann Arbor, MI 48106-1346 USA
800-521-0600

OBJECTIVE ASSESSMENT OF STATIC AND DYNAMIC SEATS UNDER VEHICULAR VIBRATIONS

Vladimir Tchernychouk

A Thesis

in

The Department

of

Mechanical Engineering

Presented in Partial Fulfillment of the Requirements

for the Degree of Master of Applied Sciences at

Concordia University

Montreal, Quebec, Canada

May 1999

ABSTRACT

Objective Assessment of Static and Dynamic Seats under Vehicular Vibrations

Vladimir Tchernychouk

Automotive driver/passenger comfort is strongly influenced by the perception of whole-body vehicular vibration, which is further related to the body posture, static and dynamic properties of the seat, and characteristics of vibration at the body-seat interface. In view of the complexities associated with the biodynamic response behavior of the human body, the comfort assessments of the automotive seats are invariably accomplished through laboratory or field experimentation of the seat-human system. Laboratory experiments with human subjects involve certain safety and ethical concerns, while field measurements yield difficulties in interpretation of the results due to lack of controlled conditions. It is thus desirable to develop experimental and analytical procedures that can eliminate or reduce the need for seat testing with human subjects. In this dissertation, currently used experimental and analytical procedures for performance assessment of automotive seats are reviewed. The static and dynamic properties of seat cushions are identified through systematic experimental studies under a wide range of operating conditions. These properties are characterized by nonlinear analytical models involving excitation frequency and amplitude. Nonlinear analytical models of the seat-load and seat-occupant systems are developed by integrating the human body models of different complexity with a seat model. The analytical models are analyzed under harmonic and field measured random excitations, using local equivalent linearization and numerical integration techniques. Laboratory experiments are performed on the seat-load and seat-

human systems to evaluate their vibration transmission performance under harmonic and random excitations. The analytical response characteristics of the models involving human body models of varying DOF are compared with the measured response to assess the validity of the models. From the comparison, it is concluded that a single-DOF biodynamic model yields good agreement with the measured data.

A comparative study of vibration transmission performance of the seats obtained with a number of subjects representing 50^{th} percentile male population and with an equivalent passive load is performed. The experimental results are used to identify a Human Response Function to characterize the contributions of the human body. This function is further utilized to estimate the seat-human system performance from measured seat-passive load performance characteristics. A parametric sensitivity analysis is further carried out to investigate the influence of seat cushion parameters on the vibration transmission performance of the seat-human body model. Developments in dynamic seats (suspension seats) are briefly reviewed with special emphasis on their vibration attenuation performance. An analytical model of a vertical seat-suspension is developed using ADAMS software, incorporating the dynamic interactions of human body, variable friction properties and kinematics of the suspension linkages. The analytical model is validated using the results of laboratory tests performed with rigid load and human subjects under deterministic and random excitations. It is concluded that the validated nonlinear model can serve as an efficient design and assessment tool for suspension seats employed in road and off-road vehicles.

ACKNOLEDGEMENTS

I would like to express my sincere gratitude to my thesis supervisors, Dr. Subhash Rakheja and Dr. Ion Stiharu, for their constant guidance and support throughout the thesis work. Financial support provided by NSERC post graduate scholarship and the support of Institut de recherche en sante et en securite du travail (IRSST) are greatly appreciated. I also would like to acknowledge the constant and reliable help provided by Mr. Danius Juras in the realization of the experimental set-ups.

The completion of this thesis work would not have been possible without the understanding and motivation from my wife Olena. I dedicate this thesis to her and to my daughters Lidia and Veronica.

TABLE OF CONTENTS

CHAPTER 3

ESTIMATION OF VIBRATION TRANSMISSION CHARACTERISTICS OF STATIC SEATS

CHAPTER 4

VIBRATION TRANSMISSION ANALYSIS OF DYNAMIC SEATS

CHAPTER 5

CONCLUSIONS AND RECOMMENDATIONS FOR FUTURE WORK

LIST OF FIGURES

LIST OF TABLES

LIST OF ABBREVIATIONS AND SYMBOLS

Symbol	Description
ADAMS	Automated Dynamic Analysis of Mechanical Systems
$a_s^2(\bar{f}_j)$, $a_f^2(\bar{f}_j)$	mean squared accelerations of the seat and floor vibration, respectively, $(m/s^2)^2$
BS	British Standards Institution
C_{1A}, C_{1B}	bleed- and blow-off damping coefficients of shock absorber, N.s/m
C_1, C_2	damping properties of human body model, N.s/m
C_C	equivalent viscous damping coefficient, N.s/m
$C_{EQ}(\omega, Z_1)$	equivalent viscous damping coefficients of the cushion, N.s/m
C^0_{EQ} , K^0_{EQ}	initial assumed values for equivalent viscous damping and stiffness coefficients, N.s/m
$[C_{NOM}]$	array of local nominal equivalent damping constants
DOF	degree-of-freedom
DRI	Dynamic Response Index
ΔE	energy dissipated per cycle of vibration, N.m
ε_K , ε_C	magnitude of errors between the assumed and computed values
F_{DC}	dissipative force, N
FDP	Fatigue-decreased-proficiency
$F(x, \dot{x}, t)$	nonlinear damping force due to shock-absorber, N
$F_{CUSHION}$	dynamic force due to a cushion, N
F_F	magnitude of the friction force, N

f	frequency of vibration, rad/s
$\bar{f}_j$	center frequency of a selected band, rad/s
f_l, f_u	respective lower and upper limits of the frequency band, rad/s
H(f)	linear transfer function of the seat
$[H(j\omega)]$	complex matrix representing the frequency response function to the seat-human body model
ISO	International Standards Organization
K_C	equivalent stiffness coefficient, N/m
$K_{EQ}(\omega, Z_1)$	equivalent viscous stiffness coefficients of the cushion, N/m
K_B , C_B	visco-elastic properties of a single DOF human body model, N/m
K_1, K_2	stiffness properties of human body model, N/m
K_4^*, C_4^*	equivalent restoring and dissipative properties at a driver-seat interface, N/m
K_{EQ}, C_{EQ}	local constants which are considered valid for certain narrow frequency band, N/m
$[K_{NOM}]$	array of local nominal equivalent stiffness constants
K_{1A}	stiffness coefficient due to primary suspension spring, N/m
K_{1B}	stiffness coefficient due to bump stops, N/m
M_1, M_2	lower and upper human body masses, respectively, kg
M_0	mass of a common frame, kg
[M], [K], [C]	(n x n) mass, stiffness and damping matrices
n	number of degrees-of-freedom for a model
ϕ	randomly distributed phase angle, rad

μ	friction coefficient
N	element specific reaction force at joint, N
PSD	power spectral density,
ROPS	Roll-over protection structure
rms	root-mean-square
S.E.A.T.	Seat Effective Amplitude Transmissibility
$S_I(\omega)$	PSD of acceleration at the seat base, $(m/s^2)^2/Hz$
T_F	magnitude of the friction torque, N
T	magnitude of the element-specific reaction torque at joint, N
$X_{input}(t)$	displacement time history
V_S	preset velocity of transition from high to low damping constant of the shock absorber, m/s
$W_i(f)$	frequency weighting for the human response to vibration
WBVVS	Whole-Body Vehicular Vibration Simulator
ω_D	discrete excitation frequency, rad/s
ω	circular frequency of excitation in rad/s
$\Delta\omega$	small frequency band around the center frequency, rad/s
$X(\omega_D)$	displacement amplitude at discrete excitation frequency, m
$\{X(j\omega)\}$, $\{Y(j\omega)\}$	Fourier transforms of vectors containing response and excitation variables, respectively
X_1, X_2	displacements of the lower and upper body masses, Respectively, kg
Y	excitation displacement, m

CHAPTER 1

INTRODUCTION AND LITERATURE REVIEW

1.1 General

The vehicle ride quality is a subjective perception, associated with the level of comfort experienced by the driver or passenger. Although vehicle ride quality is a complex function of many design factors, including air quality, noise, vibration, visual field, placement of controls, etc., the perception of comfort is primarily related to the seat design. The enhancement of comfort properties of automotive seats thus forms an important design objective. The occupant comfort, however, is a cumulative function of vibration transmitted to the human body, vibration transmitted to the hands and feet, seat design and its capability to provide postural support, temperature, ventilation, interior space, hand holds and many other factors. The tactile vibration transmitted to the driver's body through the seat is the primary factor most commonly associated with the ride quality. The ride comfort performance in this dissertation thus refers to the nature of vibration transmitted to the occupant.

Static seats are invariably employed in automobiles with low levels of vibration transmitted to seat mounts. Such seats are primarily designed to provide controlled seated posture, limited isolation of high frequency vibration arising from tire-road interactions, and sensation of static seating comfort. Heavy vehicles employed in freight, resource and service sectors transmit high magnitudes of low frequency whole body vibration and shocks, primarily arising from tire/track interactions with the rough terrains [1,2]. Although such vehicles impose complex ride environment along the vertical, longitudinal,

lateral, roll and pitch axes, the human occupant is known to be quite sensitive to vertical vibration. This is mostly attributed to the relatively severe levels of ride vibration along the vertical axis and dominant frequencies of such vibration, which for certain vehicles lie in the vicinity of fundamental natural frequency of the seated occupant. The ride comfort of such vehicles is frequently enhanced by dynamic seats comprising a damped low natural frequency suspension system. Heavy vehicles, such as urban buses, freight vehicles, and off-road vehicles employed in forestry, mining, construction and service sectors, invariably employ a vertical suspension or dynamic seat to attenuate the occupant from severe levels of low frequency whole-body vibration and shocks.

The assessment of comfort characteristics of static and dynamic seats is a highly complex task due to excessive variations in the body sizes and weights, individual preferences, driving conditions, and inter- and intra-subject variations. The comfort characteristics are frequently assessed through subjective and objective studies. Since subjective methods yield inconsistent results due to excessive variations in the individual's preferences, the objective methods are considered more desirable to assess comfort characteristic of the seats. The comfort performance of seats may be evaluated objectively either through fields or laboratory measurements. The field measurements, however, tend to be costly and yield inconsistent information related to relative ride comfort due to lack of repeatability. Alternatively, evaluations performed under carefully controlled conditions can provide effective assessments of comfort in a highly efficient manner. The laboratory assessments of seats have been performed using rigid loads and human subjects. It has been established that human body contributes significantly to the overall comfort characteristics of the seats [3]. The use of human subjects in the laboratory evaluations is

thus considered desirable. The involvement of human subjects, however, poses many ethical concerns related to the safety risks associated with shock and vibration exposure. The variations in subjects weight and built further yields considerable variations in the measured data. Upon recognizing such complexities, many studies have proposed human body models, which may be used in conjunction with analytical models of the seats to derive the comfort characteristics of coupled human-seat system. Such models, however, have not yet proven reliable due to nonlinearities of the seat and human body.

The scope of this dissertation research is thus formulated to derive effective methodologies to assess the comfort performance of both static and dynamic seats. A Human Response Function is proposed to describe the contributions of the seated body to the overall comfort performance to the static seat. The human response function used in conjunction with the seat loaded with a rigid mass can provide effective assessment of the seat-human system. A detailed analytical model of the dynamic seat and human body is further developed and validated using the measured data.

1.2 Review of Relevant Literature

The assessment of comfort characteristics of static and dynamic seats necessitates appropriate considerations of the design factors, vibration attenuation characteristics, human response to vibration, etc. The reported studies related to above aspects are briefly reviewed and discussed in the following sections to formulate the scope of this dissertation research.

1.2.1 Assessment of Ride Comfort: Subjective Methods

While subjective evaluations yield considerable data on relative ride ranking, they do not provide quantitative information to the designer. Furthermore, subjective evaluations are, in general, considered to be complex and expensive, specifically when repetitive tests need to be performed with a large number of seats. The subjective evaluations, however, can be effectively used to obtain ride perception when relatively small number of prototype seats is involved.

Studies in human sensitivity to ride vibration in general focus on tolerance as it relates to discomfort in a seated position [4,5,6,7]. These subjective studies have revealed that human sensitivity to an imposed vibration is not only dependent on the physiological and biomechanical response of the body but also on a number of psychological and environmental factors. It is also concluded that human response to vibration is a function of several factors such as: vibration magnitude and frequency, character (rotational, linear) and direction of vibration, and duration of vibration exposure [8,9,10]. Many investigations carried out on various aspects of human response to vibration have provided the data base to establish ride criteria for preservation of health, comfort and performance. A number of vibration performance criteria have been established based on subjective response, relative ride quality ranking of a group of vehicles, tolerance related to machine productivity, vibration interference with normal driver control tasks, health aspects due to vocational exposure, competitive significance and cost/benefit ratio of potential ride-improvement [4,5,7,11]. Although reasonable similarities among the proposed comfort criteria have been shown with respect to input frequency, the subjective response data have been insufficient and inconsistent to derive a generally acceptable

comfort criteria with respect to intensity of vibration. The inconsistencies inherent to the proposed criteria have a multitude of explanations, namely: semantic problems, age and moods of subjects at the time of experiments, and the like.

1.2.2 Assessment of Ride Comfort: Objective Methods

Objective methods propose direct measures of physical quantities, such as velocity, acceleration, and jerk as ride evaluation criteria, while a good correlation between the subjective human response and the mean square jerk and acceleration has been established [8]. Considerable similarities among different ride evaluation criteria, based upon either subjective or objective measures, have been reported in the literature. A number of objective methods have been proposed to assess the ride vibration environment of vehicles that are discussed in the following subsections.

Ride Vibration: Standards and Experimental Methods

Although a large number of ride comfort criteria have been proposed, a single acceptable criterion has not yet been identified [12]. This can be attributed to many factors including the following, which contribute to the general complexity of ride vibration criteria:

1. Complex nature of human response to vibration and difficulty to achieve precise measurement using linear accelerometers.
2. Use of pure sinusoidal rather than random excitations in the laboratory.
3. Differences in various investigations due to varying objectives, experimental methods, data analysis and data reporting techniques.
4. Lack of standardized test procedures.

5. Variations in approaches to the ride questions (subjective, relative, health aspects, activity disturbance, etc.).

6. Variations in seating positions including posture, positions of arms and legs, backrest angle, etc.

7. Variations in duration of exposure.

Despite many controversies, certain common denominators can be seen in the results from the different studies [5]. Majority of these studies show that the human body is most sensitive to vertical vibration in the frequency range of 4 to 8 Hz, due to vertical resonances of the spine and supporting structure [8,9,13]. Figure 1.1 presents the lines of constant *fatigue decreased proficiency* limits for vertical vibration, related to preservation of working proficiency, established by the International Standards Organization (ISO) [14]. The ISO has set forth three exposure criteria as a function of exposure time in the frequency range 1-80 Hz under horizontal and vertical vibration. The proposed exposure limits are *health* and *safety* limits for occupational exposure, *fatigue decreased proficiency* (FDP) limits associated with preservation of working efficiency, and *comfort* limits. The main thrust of the standard can be summarized as follows:

(i) For seated vehicle operators, the seat-human interface acceleration along the vertical, transverse and longitudinal directions are the parameters of importance.

(ii) The acceleration signals are analyzed to determine the rms acceleration levels in 1/3-octave frequency bands up to 80 Hz.

(iii) The 1/3-octave band intensities are plotted vs frequency and the specified tolerance curves are then superimposed to determine the ride quality for a given exposure time.

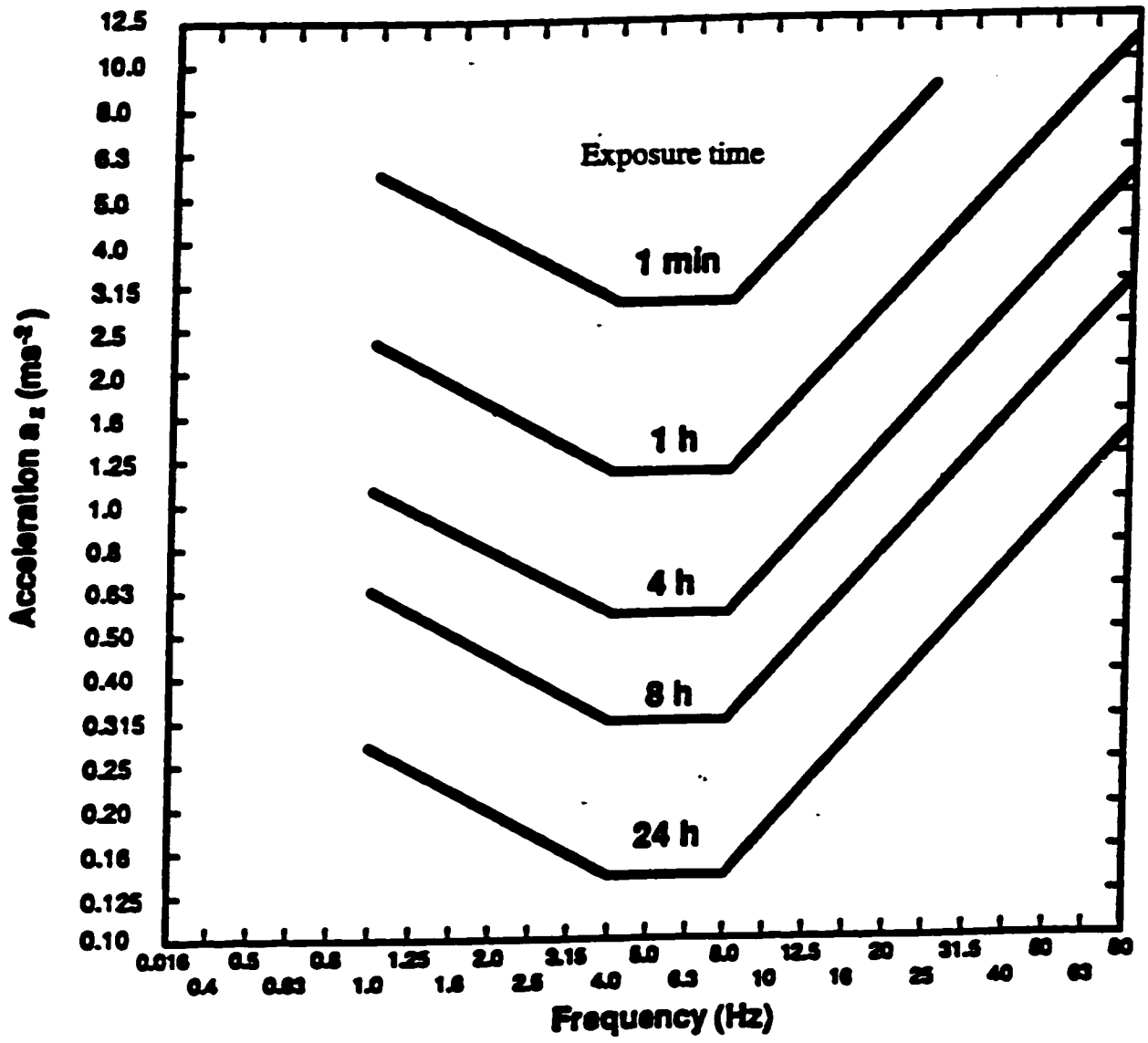

Figure 1.1: Fatigue-decreased proficiency limits as defined in the current ISO 2621/1 standard for vertical (z-axis) vibration [14].

A more fundamental method for assessing the influence of combining vertical and longitudinal vibration emerged from the work of Lee and Pradko [15]. The level of discomfort was related to the level of vibration power dissipated in the subject's body due to vertical, lateral or longitudinal inputs. The measured rms acceleration is weighted along each axis of vibration to compute the average absorbed power for each direction. The total absorbed power quantity is then obtained by summing the absorbed power quantities for three orthogonal axes. The primary limitations of this method have been outlined by Murphy [12]:

1. The weighting curves are based on a single biomechanical criterion, whereas human response to vibration is far more complex, since various parts of the body respond to vibration of different frequencies in different ways.

2. Absorbed power values do not directly relate to subjective response. Absorbed power effectively corresponds to acceleration squared, whereas most evidences point to response being directly proportional to acceleration magnitude.

A number of other criteria have been proposed to assess the ride vibration environment of the vehicles. *K*-factor, as a measure of vibration intensity, function of frequency and rms acceleration, velocity or displacement amplitude has been proposed in Germany [9]. The Dieckman constant and Janeway limits [10], derived from the subjective response, imply that human is most sensitive to vertical vibration below 20 Hz, and were proposed as comfort criteria for automotive passengers. Goldman [13] also established three vibration limits in the vertical mode, such as: perceptible, unpleasant and intolerable, as a function of frequency and peak acceleration response.

Of all these, only ISO-2631 [14] specifies the rms acceleration limits as a function of exposure time under vertical as well as horizontal vibration, and has been most widely

accepted. However, it doesn't define an adequate or reasonable procedure for measuring vibration exposure and specifies vibration limits that are not generally accepted. An alternate ride vibration criteria was proposed by British Standards Institution (BS 6841) [16]. The principal differences between BS 6841 and ISO 2631 can be summarized as follows:

- BS 6841 [16] provides greater guidance on vibration effects without defining vibration limits.
- BS 6841 [16] eliminates the concept of fatigue-decreased proficiency, and proposes a simple time-dependency, and a method for assessing the impact of repeated shocks and intermittent vibration in terms of a vibration dose value (VDV).
- BS 6841 [16] proposes more complete definitions of necessary frequency weightings together with means of assessing the discomfort caused by rotational vibration of the seat, and translational vibration at the feet and seat back of a seated person.
- BS 6841 [16] further proposes more quantitative guidance on motion sickness (i.e. the motion sickness value).

The recently revised version of ISO-2631 has also proposed weighting factors in the frequency range of 1 to 80 Hz in order to quantify the ride quality by a single number [17]. In this method, the measured ride vibration is frequency weighted, using the filters derived from human response to vibration, to compute an overall root mean square (rms) acceleration value. This method of assessing the ride is gaining popularity due to its simplicity. However, there has been a growing controversy associated with the measurement procedures and the vibration limits proposed in ISO-2631 [14]. A study conducted by Boileau [18] has clearly demonstrated the limitations of ISO-2631 [14] for assessment of off-road vehicle vibration with high crest factors. The study summarized the

primary discrepancies arising from ISO-2631 [14] with respect to its frequency weighting, time-dependence relationship, and applicability for motions with large crest factor.

1.2.3 Seat Effective Amplitude Transmissibility (S.E.A.T.)

The comfort performance of static and dynamic automotive seats have been related to their natural frequencies, resonant response, vibration attenuation performance, and static and dynamic relative deflections [4,7,10,11]. Varterasian [19] proposed the use of a "ride number" determined from the resonant frequency of the seat, the transmissibility at resonance and the transmissibility at 10 Hz. The study concluded that the proposed "ride number" provides a better correlation with the subject judgments of ride in different seats than that attained with the measurement of vibration using the method defined in ISO 2631 [14].

The comfort characteristics of seats have been frequently reported in terms of their shock and vibration isolation behavior when loaded with a rigid mass [20]. It has been concluded that human body behaves similar to a rigid mass only at frequencies below 2 Hz. Human body contributes considerably to the overall comfort characteristics of static as well as dynamic seats. Afework [21] analyzed the vibration isolation characteristics of dynamic seats coupled with single- and two-degrees-of-freedom (DOF) human body models. The study demonstrated considerable contributions of the driver to the vibration isolation characteristics of the seats. The contributions of driver have been further concluded through analytical and experimental studies conducted by Boileau [22]. The contributions due to the driver, however, are known to depend upon the nature of vibration excitations and properties of the seat in a highly complex manner. An assessment

of comfort characteristics of a seat thus necessitates appropriate consideration of ride vibration spectrum of the vehicle, the seat response and the occupant response at all frequencies where there is significant vibration.

The comfort characteristics or isolation efficiency of static and dynamic seats may be evaluated in terms of S.E.A.T. (Seat Effective Amplitude Transmissibility), defined as [23]:

$$\text{S.E.A.T.} = \left[\frac{\int G_{ss}(f) W_i^2(f) df}{\int G_{ff}(f) W_i^2(f) df}\right]^{1/2} * 100\% \qquad (1.1)$$

where $G_{ss}(f)$ and $G_{ff}(f)$ are the power spectral densities of accelerations measured at the occupant-seat interface and the floor, respectively. $W_i(f)$ is the frequency weighting for the human response to vibration, and f is the frequency of vibration. Table 1.1 presents the asymptotic values of frequency weighting factors, proposed in BS 6841 [16], for assessment of vibration discomfort along the vertical direction. The S.E.A.T. value of a seat provides a measure of its vibration isolation efficiency, while taking into account the contribution due to input vibration spectrum, seat transfer function and relative sensitivity of the body to different vibration frequencies. An examination of the weighting factors, summarized in Table 1.1, reveals that maximum attenuation is required at frequencies at which the body is most sensitive and where there is maximum floor vibration. There is little need for vibration attenuation at frequencies where there is either no vibration or the body is not sufficiently sensitive.

The integrals in equation (1.1) are determined over the frequency range where there is significant vibration of the floor, often all or part of the range from 0.5 to 80 Hz.

The S.E.A.T. value may be considered to be the ratio of the frequency-weighted ride experienced on the seat to the frequency-weighted ride which would be experienced with a rigid seat. The isolation efficiency of a seat can be conveniently established in terms of S.E.A.T. using either laboratory or field measurements. The measure has been widely used to assess the relative vibration isolation characteristics of various seats [23].

With the application of a frequency weighting appropriate to vibration discomfort, a SEAT value of 100% would indicate that there is no overall improvement or degradation in vibration discomfort produced by the seat, although the seat may amplify low frequency vibration and attenuate high frequency vibration. A SEAT value of 100% thus indicates that sitting on a rigid seat would produce similar vibration discomfort. A SEAT value of greater than 100% indicates that the vibration discomfort has been increased by the seat. A SEAT value less than 100% indicates incresead vibration isolation provided by the seat.

Table 1.1: Asymptotic frequency weightings, $W_i(f)$, used to assess vibration discomfort along Z axis.

0.5<f<2.0	$W_i(f) = 0.4$
2.0<f<5.0	$W_i(f) = f/5.00$
5.0<f<16.0	$W_i(f) = 1.00$
16.0<f<80.0	$W_i(f) = 16.0/f$

The S.E.A.T. value of a seat can also be evaluated using the analytical model of the seat. From equation (1.1), it is apparent that S.E.A.T. is merely the ratio of overall rms value of weighted acceleration at the seat to that due to the base. Since the rms acceleration of the seat is derived from the linear transfer function, *H(f)*, of the seat, and the power spectral density (PSD) of the base acceleration, the S.E.A.T. value of a seat may be computed from:

$$\text{S.E.A.T.} = \left[\frac{\int G_{ff}(f) * |H(f)|^2 * W_i^2(f) df}{\int G_{ff}(f) * W_i^2(f) df}\right]^{1/2} * 100\%$$

(1.2)

Some studies have proposed linear analytical models of static and dynamic seats [24,25]. Griffin [22] derived the transfer function for a driver-seat system through development of a linear analytical model. The S.E.A.T. value of the seat was then derived using Equation (1.2). The S.E.A.T. measure has been used in many studies to determine the relative comfort performance of the seat, and the influence of variations in seat parameters, vehicles and road conditions.

1.2.4 Analytical Methods for Assessment of Seat Performance

Performance characteristics of static and dynamic seats are mostly evaluated through field or laboratory tests. The field tests, in general, yield measurements with low repeatability, which are also difficult to interpret due to lack of controlled test conditions. Alternatively, laboratory assessments of seats involve repetitive tests with human subjects. Laboratory exposure of human subjects to vibration requires careful considerations of safety, ethical, medical and legal issues, and necessitates expensive 'human-rated'

vibrators. Few studies have also proposed analytical models of seats and seated human body to assess their overall comfort performance [21,22,24,26]. The accuracy of such models, however, has been demonstrated in limited cases only. The design and performance characterizations of seats thus continue to rely upon laboratory and field evaluations, primarily due to lack of a reliable human body model that can account for extensive inter-subject variations. The need to develop analytical and empirical procedures to assess the comfort performance of occupant-seat system involving minimal tests with human subjects has been strongly emphasized [22].

Assessment of the effects of vibration on the comfort, performance and health of an occupant seated in a vibration environment necessitates the knowledge of vibration transmission characteristics of the seat. The measurement or analysis of vibration transmission performance of a static or dynamic seat, however, is quite difficult, since it may depend upon the weight and dynamic response of the occupant. Many previous studies have identified a strong need to characterize the vibration comfort offered by a seat without the participation of human subjects due to the associated health, safety and ethical concerns [23,27,28]. A number of analytical and experimental studies have been performed using a rigid mass representation of the human occupant resulting in a single-degree-of-freedom (DOF) model of the seat-occupant system, shown in Figure 1.2 [20,21]. It has been established that such representations of the occupant can be considered valid below 2 Hz, or when the mechanical impedance of the body is insignificant in relation to the mass of the moving components of the seat [3]. Assessment of vibration comfort of seats established either from analysis of single-DOF seat-occupant model or from measurements using an equivalent mass is thus considered inadequate,

since: (i) the seats do not respond as simple ideal frictionless linear systems; (ii) the human body is not a linear system; and (iii) the human body does not respond like a rigid mass under vehicular vibration.

Few studies have thus proposed the use of human body simulator to assess the vibration comfort of seats without involving human subjects in the laboratory. Matthews [29] developed a single-DOF mechanical dummy, comprising a mass suspended by four elastic bands from a rigid frame. The damping was adjusted such that the vibration transmissibility of a suspension seat loaded with the dummy was in agreement with that of the seat loaded with a person.

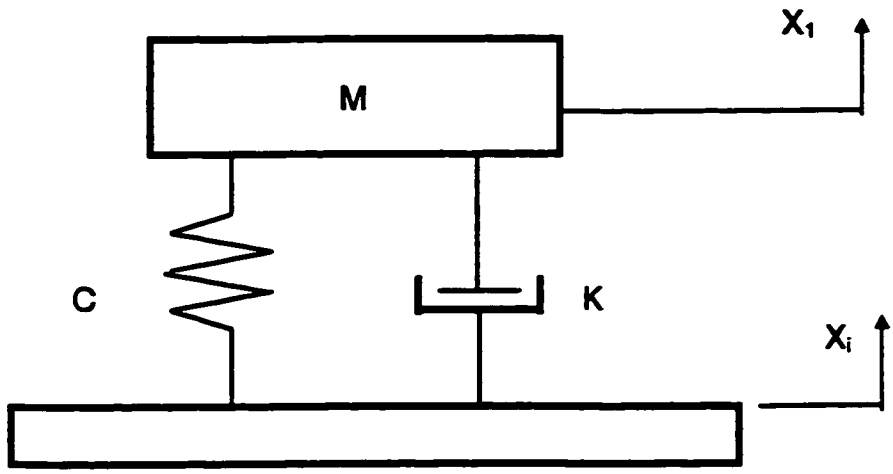

Figure 1.2. A single degree-of-freedom system.

Suggs [27] developed two-DOF human body simulator based upon measured driving point mechanical impedance of the human body. The simulator comprised two masses supported by coil compression springs and viscous dampers on a common rigid frame. For high magnitudes of vibration, the vibration transmissibility of seats measured with these dummies was in reasonable agreement with those measured with a person.

However, both dummies appeared to exhibit more damping at lower magnitudes of vibration.

Non-linear models of vertical seat isolation systems have been devised by Rakheja and Sankar [30]. Patil [31,32,33] developed analytical models for the isolation of vertical and pitch vibration. The modeling of the static and dynamic properties of the foam cushions used in both static and dynamic seats presents many challenges due to their hysteretic nature and excessive variations in the density [34]. Hilyard and Collier [35] have discussed the dynamic response of foams used for vehicle seating and concluded that static response is not a good predictor of the dynamic response of foam. Fairley and Griffin [28] proposed a method to determine the dynamic stiffness of seats using a loading indenter and a linear seat model, which when combined with the dynamic response of the human body, resulted in the vibration transmissibility characteristics of the seat-person system. The proposed method employed the apparent mass of the seated subject. The study described a seat indenter to determine the dynamic stiffness of seats and presented comparisons between the measured and predicted values of the vibration transmissibility of eight different conventional road vehicle seats. The major advantage of the proposed method is that it eliminates the use of human subjects for determination of the dynamic stiffness of the seat.

Fairley [36] extended the above procedure to include the influence of the legs on the prediction of seat transmissibility. The procedure for determining seat dynamic stiffness including the influence of indenter shape and the various assumptions associated with the linear model merit further attention. It has been shown that prediction of similar

accuracy can be obtained by fitting lumped parameter models to both the measured dynamic stiffness of a seat and the apparent mass of the body [37].

1.2.5 Review of Biodynamic Models of Human Body

The vibration transmission properties of the coupled seat-human system can be evaluated using two methods: (i) laboratory or field measurements of the coupled system; and (ii) development and analysis of the coupled seat-human body models. Although the first method can yield reliable assessment of the automotive seats when representative subjects sample and test conditions are employed, the experiments with human subjects involve certain ethical concerns. Alternatively a number of human-body models have been proposed to study the comfort properties of the seats, when coupled with static and dynamic properties of the seats. They range from simple single-DOF to complex nonlinear multi-DOF models. Majority of the models proposed in the literature is lumped-parameter models, where the parameters are identified from measured biodynamic response data. The model parameters are mostly derived from either measured mechanical impedance or vibration transmissibility response characteristics of the human subjects.

The driving-point mechanical impedance is defined as the complex ratio of the driving force to the velocity at the point of entry of vibration within the body, and the seat-to-head transmissibility is defined as the complex ratio of acceleration measured at the head to that of the seat [23]. However, the methodology for derivation of model parameters based upon curve-fitting of the measured characteristics of driving-point mechanical impedance or seat-to-head transmissibility and phase pose two problems: (i)

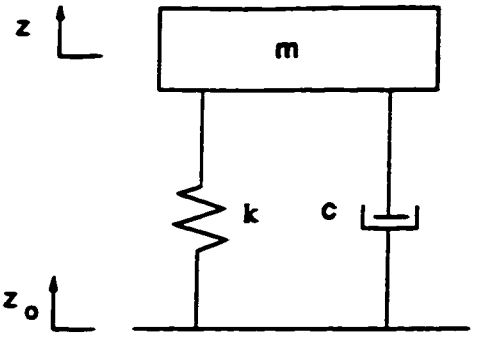

Figure1.3: DRI model [3].

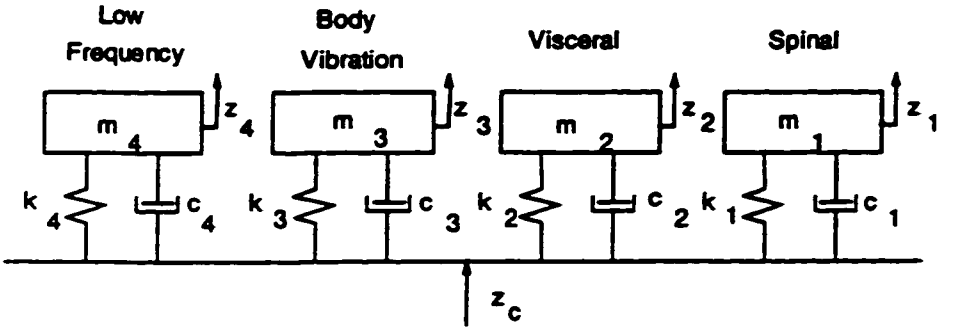

Figure 1.4: Improved DRI model [38].

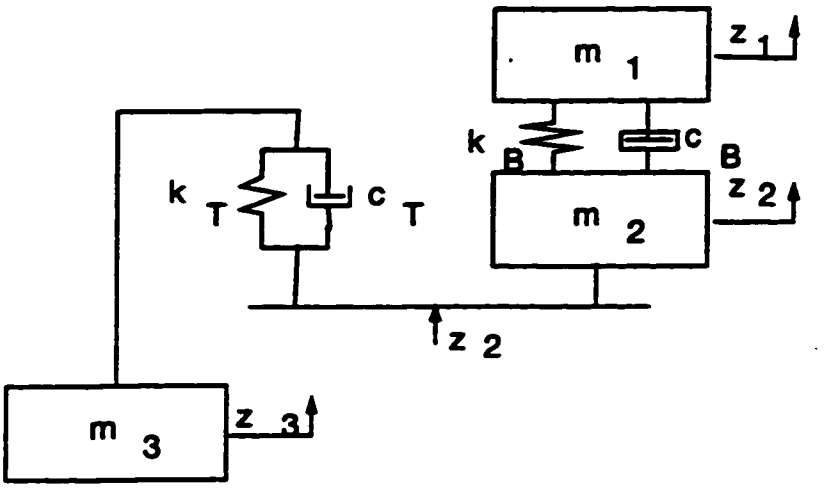

Figure 1.5: Schematic of a mechanical model proposed by Fairley and Griffin [39].

the model may be considered valid only in the vicinity of the test conditions used in the study; and (ii) the model parameters may not relate to any of the body segment characteristics. Consequently, there is a possibility of deriving not one, but multiple sets of model parameters such that the model response correlates reasonably well with the measured data. Furthermore, many models have been devised based on ejection seat data and represent the human response to high level impact [3], while others have been derived from test data acquired with subjects sitting on seats without backrest and subjected to sinusoidal vibration of varying intensity. It may thus be questionable whether these models could be applied in conjunction with vibration environment experienced by vehicle drivers.

DRI model, namely Dynamic Response Index model presented by Coerman [3], is the most widely used single-DOF model (Figure 1.3), which relates to the relative severity of vibration, more particularly the shocks. The mass m of the model represents the mass due to upper torso and the head, while the spring rate k is meant to represent the restoring properties of the spine, and the viscous damping coefficient c is due to the spine and the adjacent tissues. The natural frequency and the damping ratio of the proposed model is 8.42 Hz and 0.2245, respectively. An improved DRI model was proposed by Payne [38] to account for the differences between single events or shocks and continuous vibration. This model consists of four parallel and uncoupled single-DOF models and is realized upon combining the DRI model, also known as "spinal" or "shock response" model, with three additional single-dof models, referred to as "visceral", "body vibration", and "low frequency", as shown in Figure 1.4.

Fairley and Griffin [39] proposed a single-DOF model shown in Figure 1.5, which is based on the measured mean apparent mass of 60 subjects, including male, female and

children, sitting erect without back support. The feet of subjects were vibrated under 1.0 ms^{-2} (rms) random vibration. The seated body is represented by two masses: m_1 being the mass of the upper body moving relative to the platform, and m_2 being the mass due to the lower body and the legs supported on the platform, but not moving relative to the platform. The mass of the legs m_3 was included in the model only when the feet were supported on a stationary footrest. This model, however, did not consider seat-to-head transmissibility data and the effects of back support or the posture.

Suggs [40] proposed a two-DOF biodynamic model of the human body to characterize the response over a frequency range comprising the first two resonant frequencies of the body. The model, shown in Figure 1.6, was derived from the measured mechanical impedance characteristics of 11 male subjects, showing primary and secondary resonances of the seated subjects near 4.5 Hz and 8 Hz, respectively [41]. The tests were performed with subjects seated upright, with feet supported, hands in lap, and exposed to sinusoidal vibration of 2.5 mm (0.1 in) peak-to-peak amplitude in the 1.75 to 10 Hz frequency range. The model comprises two lumped masses, m_1 (pelvis and abdomen), and m_2 (head and chest), suspended from a common rigid frame of mass m_0, representing the spinal column. On the basis of this model a mechanical simulator was constructed to perform vibration testing of seats [42]. While the seat-to-head vibration transmissibility was not considered in deriving the model, the base-to-seat transmissibility characteristics of seats loaded wit the mechanical simulator were reported to be in good agreement with those measured with a person, provided the weight and experimental conditions matched those defined in the model.

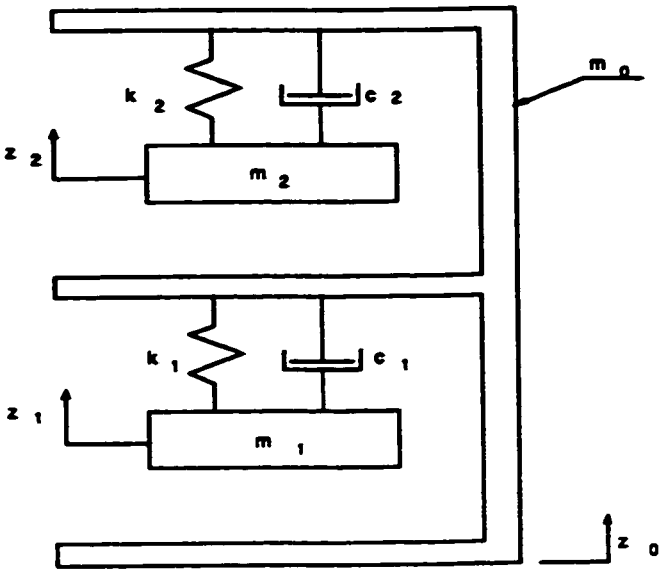

Figure 1.6: A two-DOF model proposed by Suggs [40].

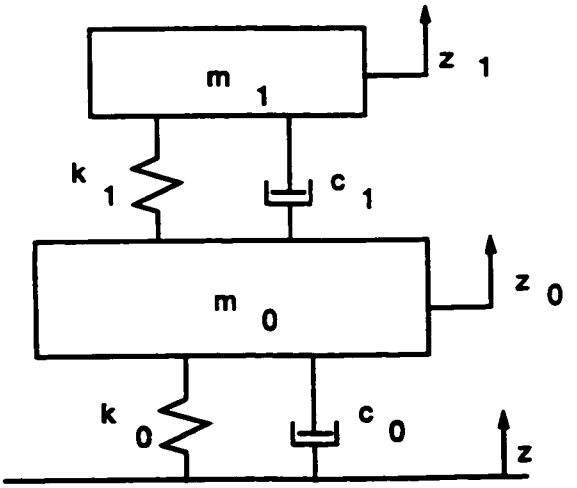

Figure 1.7: A two-DOF model proposed by Allen [43].

Allen [43] derived a two-DOF biodynamic model of the human body using known characteristics of the human body or subsystems. The model, shown in Figure 1.7, consists of a "primary system" to characterize the upper body response, and a "secondary system" representing the head. The model response to sinusoidal excitations was used to derive vibration tolerance curves illustrating the sensitivity of subsystem to vibration within specific frequency ranges. The validation of the proposed model, however, has not been reported.

A number of multi-degrees-of-freedom models of the seated human subjects have been proposed by many researchers. Mertens [44,45] developed a comprehensive biodynamic model involving the comparison of both the impedance and vibration transmissibility magnitude and phase characteristics with the experimental results. The study was intended for ejection seat applications and therefore the experiments were performed with subjects exposed to static acceleration levels ranging from 1g to 4g, superimposed over 0.4g rms acceleration amplitude in the 2 to 20 Hz frequency range. The model, shown in Figure 1.8 comprises five lumped masses due to legs (m_1), buttocks (m_2), abdominal system (m_4), chest system (m_6), and head (m_7). Final model parameters were selected as those, which provided the closest agreement with both measured biodynamic response functions. Under normal gravity, close agreement with the experimentally measured driving-point mechanical impedance and seat-to-head transmissibility magnitude and phase is reported for the chosen model parameters.

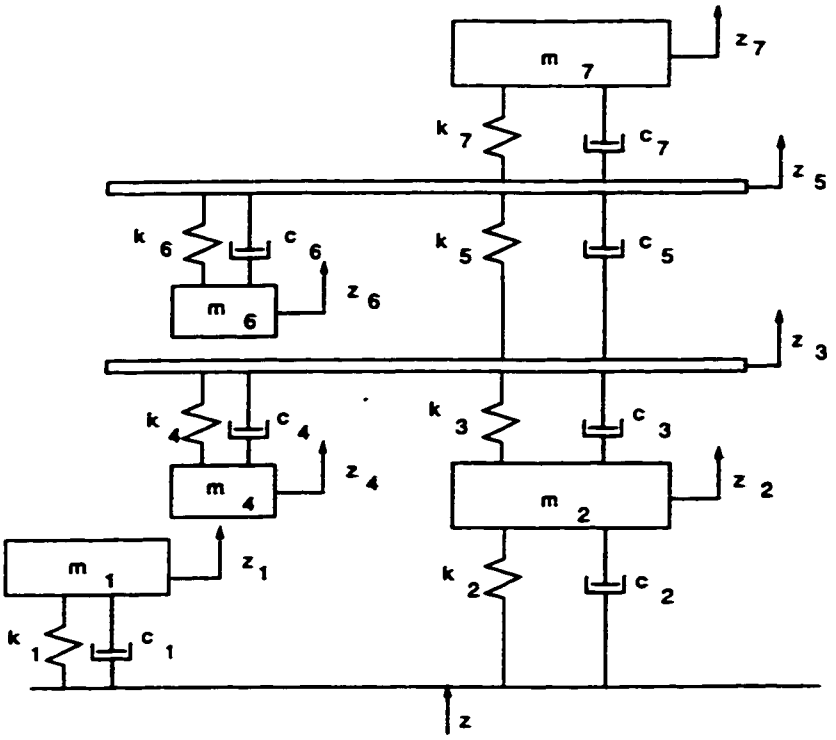

Figure 1.8: A multi-DOF human body model proposed by Mertens [44].

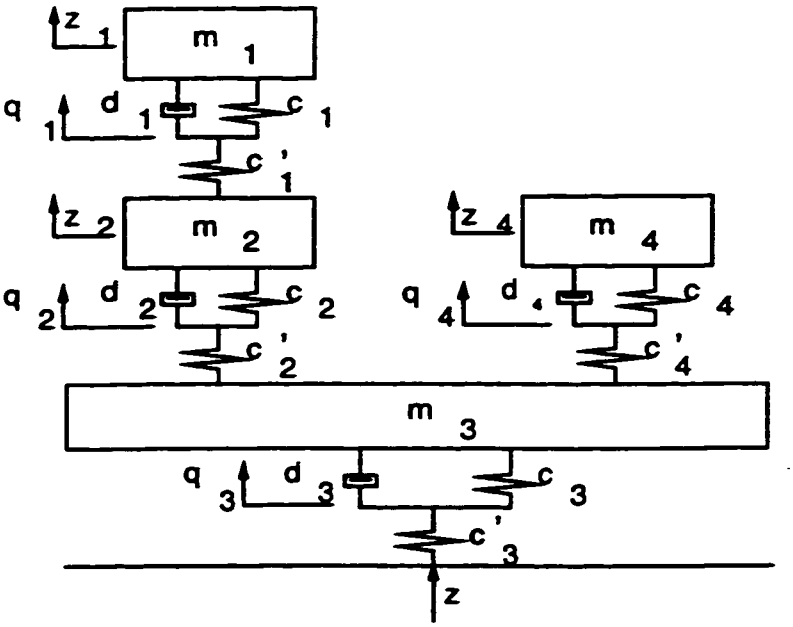

Figure1.9: An ISO CD 5982 model [46].

ISO Committee Draft CD 5982 [46] proposed a four-DOF biodynamic model, shown in Figure 1.9, to characterize both the standardized driving-point mechanical impedance and seat-to-head transmissibility of the human body exposed to vibration. The model represents both seated and standing human subjects, while the model parameters differ depending on the posture. For the seated human body, the masses m_1, m_2, m_3, and m_4 are selected as 8.42 kg, 8.05 kg, 44.85 kg and 13.86 kg, respectively, which are not associated with any specific subsystems of the human body. For the seated human body, the proposed model resulted in relatively good agreement with the standardized mechanical impedance magnitude, though large discrepancies occurred in the impedance phase. Considerable differences in the transmissibility magnitude near the resonant frequency and at frequencies beyond 25 Hz, are also observed. The model response reveals large errors in the transmissibility phase over most of the frequency range considered.

Boileau [22] proposed a four-DOF linear human driver model, shown in Figure 1.10, based upon the magnitude and phase of the measured mechanical impedance and of the synthesized seat-to-head vibration transmissibility. The model comprises four masses, coupled by linear elastic and damping elements. The four masses represent the following four body segments: the head and neck (m_1), the chest and upper torso (m_2), the lower torso (m_3), and the thighs and pelvis in contact with the seat (m_4). The mass due to lower legs and the feet is not included in the model, assuming its negligible contributions to the biodynamic response of the seated body.

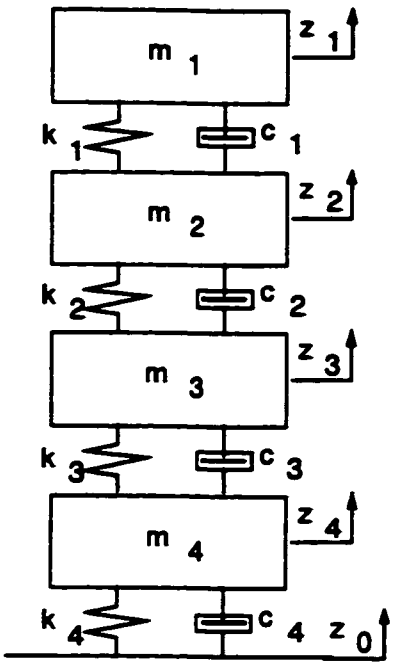

Figure 1.10: Four-DOF biodynamic model of a seated occupant proposed by Boileau [22].

The target values for driving-point mechanical impedance were identified from laboratory measurements performed with seated subjects maintaining various postures under different types of random and sinusoidal excitations within 1.0 to 2.0 ms^{-2} rms acceleration. The target values of seat-to-head transmissibility characteristics were established from the synthesis of published data reported under similar test conditions. The derived model provides closer agreement with the mechanical impedance target values, and the main body resonant frequency predicted from both biodynamic functions was found to correspond within close bounds to that expected for the human body.

The parameters of reported biodynamic human body models discussed above are summarized in Table 1.2. Various biodynamic models of the seated human body may be grouped into four classes, depending on the methodology used for estimating the model parameters:

(i) First class includes models for which parameters identification were based upon measured or reported natural frequencies or transmissibility response of specific segments of human body. Such models were proposed to characterize the response behavior of specific body segments under shock or high intensity vibration, but were rarely validated in terms of the whole-body vibration.

(ii) For the second group of models, parameter identification methodology was based upon magnitude and phase characteristics of the measured or reported whole-body driving-point mechanical impedance or apparent mass. These models relied on data obtained under sinusoidal vibration, and the seat-to-head transmissibility was either not reported or resulted in a poor fit.

(iii) The models belonging to a third class were derived to satisfy the vibration transmissibility response of certain specific segments of the body, while simultaneously matching the driving-point mechanical impedance or apparent mass response characteristics. Although a good agreement is observed with the vibration transmissibility of the body segments, the seat-to-head transmissibility, in general, deviates considerably from the measured data.

(iv) For the fourth group the model parameters were based upon matching the magnitude and phase characteristics of both driving-point mechanical impedance and apparent mass and seat-to-head transmissibility. Although this approach enhances the uniqueness of the models, the complexities associated with curve fitting the four different sets of data increase considerably.

Majority of the above models has been derived from vibration transmissibility and/or driving-point mechanical impedance characteristics measured under excitations and conditions, which are not representative of automobile driving. Vehicle driving usually involves different postures (leaning against a backrest, sitting erect or sitting with a slouched posture), hands in contact with a steering wheel, and feet supported either on the floor or on pedals, while the vibration excitation is random in nature. From the review, it is apparent that none of the models reported in the literature were derived under the conditions encountered in vehicle driving. The validity of these models for applications in automotive environment is thus questionable.

Table 1.2: The parameters of the reported biodynamic driver models (sitting erect, feet supported, hands in lap)

Model	Model Parameters	Mass (kg)	D.O.F.
DRI (1962) [3]	$f_n = 8.42\,Hz, \varsigma = 0.224, m = 55.5kg$ (*For computation*)	Not Reported	1
Improved DRI (1978) [38]	$f_{n1} = 8.42Hz, \varsigma_1 = 0.224, \quad f_{n2} = 4.0Hz, \varsigma_2 = 0.4$; $f_{n3} = 8.42Hz, \varsigma_3 = 1.0, \quad f_{n4} = 0.25Hz, \varsigma_4 = 1.0$ $m_1 = 6.8kg, m_2 = 29.0kg, m_3 = 21.8kg, m_4 = 5.45kg$	Not Reported	4
Fairley and Griffin (1989) [39]	$m_1 = 45.6kg, m_2 = 6kg, m_3 = 0.0kg,$ $\varsigma = 0.475, c_B = 1360 Nsm^{-1}, f_{nB} = 5Hz, \quad k_T = 0.0N/m, \varsigma_T = 0.0$	57-85	2
Suggs (1969) [40]	$m_0 = 5.7kg, m_1 = 36.4kg, m_2 = 18.6kg,$ $k_1 = 25968N/m, k_2 = 41549N/m,$ $c_1 = 485Ns/m, c_2 = 884Ns/m$	58-90	2
Allen 1978) [43]	$m_0 = 50.0kg, m_1 = 5.0kg, \quad \varsigma_0 = 0.3, \varsigma_1 = 0.05,$ $f_{n_0} = 5.0Hz, f_{n_1} = 17.0Hz$	Not Reported	2
Mertens (1978) [44]	$m_1 = 15, m_2 = 10, m_4 = 15, m_6 = 22, m_7 = 7\ kg,$ $k_1 = 47966, k_2 = 250000, k_3 = 200000,$ $k_4 = 17913, k_5 = 160000, k_6 = 42558,$ $k_7 = 89537N/m, c_1 = 678, c_2 = 4000,$ $c_3 = 1000, c_4 = 622, c_5 = 2000, \quad c_6 = 968, c_7 = 633Ns/m$	57-90	5
ISO CD 5982 (1993) [46]	$m_1 = 8.24, m_2 = 8.05, m_3 = 44.85, m_4 = 13.86\ kg,$ $c_1 = 22\times10^6, c_2 = 20.13\times10^4, c_3 = 88.56\times10^3, c_4 = 36.47\times10^3\ N/m,$ $c_1' = 36\times10^7, c_2' = 65\times10^6, c_3' = 52.34\times10^4, c_4' = 69.3\times10^3\ N/m,$ $d_1 = 748.1, d_2 = 578.0, d_3 = 2964.0, d_4 = 901.8\ Ns/m$	51-93.8	4
Boileau (1995) [22]	$m_1 = 5.31, m_2 = 28.49, m_3 = 8.62, m_4 = 12.78kg,$ $k_1 = 310, k_2 = 183, k_3 = 162.8, k_4 = 90kN/m,$ $c_1 = 400, c_2 = 4750, c_3 = 4585, c_4 = 2064Ns/m$	58-81	4

1.2.6 Review of Dynamic Seats

Comfort and safety of off-road vehicle drivers depend highly on the driver environment: visibility, space, placement of controls, noise and ride vibrations. The wheeled off-road vehicles are often unsuspended and large-diameter soft tires offer very light damping. Consequently, the ride vibration of such vehicles can be characterized by lightly damped system resonance occurring at low frequencies. A number of approaches to improve off-road vehicle ride have been proposed, namely: suitable tires, primary-suspension at front and rear axles, cab-suspension and seat-suspension. The ride improvement via tires and primary-suspension, however, has been considered infeasible due to limitations on tire size and requirement of high stability limits [25]. A need to develop effective secondary, seat- and cab-suspension systems has thus been emphasized to accomplish improved ride quality [22,35].

One of the last links in the chain by which vibration is transmitted to the drivers of off-road vehicles is the seat. The seats used in modern tractors range from simple fixed seats to air-suspension seats with automatic compensation for driver weight. A number of studies have reported on developments in suspension seats for off-road and road vehicles, and on the impact of vibration environment on the drivers [47,48,49,50]. The majority of these studies focus on ride improvement offered by vertical seat-suspensions, since the vertical vibration is considered as the most severe.

The vertical vibration of off-road wheeled vehicles predominates in the frequency range 0.5-5 Hz due to the resonance of the pneumatic-tired vehicle. Since human body is most fatigue sensitive to such low frequency vibration, modern off-road vehicles are often

equipped with seat-suspension systems to minimize the transmission of these vibrations arising from tire-terrain interactions and jolting. Seat-suspension systems, invariably, comprise either an air spring or mechanical spring interposed between the seat structure and the base, and a double acting hydraulic damper to absorb vibration energy. Either rubber or metal bump stops are incorporated to prevent excessive relative motion of the low natural frequency suspension. The commercially available seat-suspensions exhibit natural frequencies in the 1-2 Hz range. These low natural frequency suspension designs are also equipped with a weight adjustment mechanism in order to provide either a mid ride or a selected ride height for the drivers in the 50-110 kg weight range.

In an attempt to further improve the vibration isolation performance and to limit the static and dynamic travel of soft passive suspensions, a number of active and semi-active seat-suspension concepts have been investigated [51,52,53]. Active seat-suspensions employ active elements that have the capability of providing or dissipating energy using additional power source and control devices. Active suspensions provide high load bearing capacity at low dynamic stiffness. The relative displacement, therefore, is no longer directly related to the natural frequency of the suspension. Although the active seat-suspensions are capable of providing superior vibration attenuation performance, their application to off-road vehicles has been severely limited due to excessive cost and complexities. In recent years computer modeling techniques have been employed to study vehicle ride performance as affected by vehicle geometry, mass distribution, and tire and suspension characteristics [48, 53, 54]. In general, computer aided analyses free designer from the repetitive tasks of manual design analyses and testing. They permit the analysts to experiment and study system performance, while changing parameters and operating

conditions at will. Further, the systems can be tested beyond the range of normal or safe operation without endangering the lives or property.

A better understanding of the qualitative and quantitative behavior of seat-suspension systems can be obtained by including the nonlinear effects. These nonlinearities refer mainly to the characteristics of shock absorber, cushion, suspension spring, linkage geometry, dry friction, bump stops and human reaction. Rakheja [53, 26] proposed a six DOF rotational seat isolator to attenuate roll, pitch and bounce ride vibration of agricultural tractors, and developed a nonlinear analytical model of the seat. The investigation revealed that a seat-suspension can successfully be employed to improve ride performance in the bounce, longitudinal, and pitch modes. Attenuation of lateral and roll vibrations via passive seat-suspension was considered infeasible due to requirements of extremely low natural frequencies.

Kyeong [54] presented a study on vertical ride simulation of passive, active and semi-active seat-suspension systems for off-road vehicles using linear models. Each suspension model was combined with a three-DOF model of the driver to formulate models of the ride systems of off-road vehicles. The acceleration time histories measured at the base of the seat-suspension of an agricultural tractor during transport and moldboard plowing operations were used to analyze the models. Afework [21] presented a methodology for identifying the static and dynamic characteristics of seat-suspension systems and evaluation of their vibration isolation performance via laboratory testing. A general nonlinear analytical model of a passive seat-suspension system using a rigid body representation of the human driver was developed and validated. The need to incorporate the contributions of the seated human subject to the vibration response of the seat-

suspension was further recognized and Boileau [22] designed and developed a whole-body vehicular vibration simulator (WBVVS) capable of simulating the shock and vibration environment of particular categories of off-road and road vehicles to study the response behavior of drivers and combined driver and suspension seat in the laboratory. Boileau [22] also developed an analytical model of the seated off-road vehicle driver and investigated the contributions of body dynamics to the vibration and shock attenuation performance of the suspension seat.

1.3 Scope and Objectives of the Dissertation Research

The scope and objectives of the research are formulated upon review of published studies on measurements, evaluations and predictions of the dynamic response of static and dynamic vehicle seats. It has been well established that dynamics of coupled seat-body system is a highly complex phenomena due to nonlinear response of seat cushion and human body in particular to vibration input. The reliable assessment of the automotive seats can be achieved through the experiments with human subjects, when representative subjects sample and test conditions are employed. This approach, however, involves certain ethical concerns. The assessment methods, experimental or analytical, which either eliminate or reduce the involvement of human subjects are thus considered highly desirable. The studies on dynamic seats have evolved into measurement methods, and analytical models of the seats and the human occupant. The suspension models, however, include lumped stiffness and damping properties, while neglecting the contributions due to kinematic and dynamic motion of the linkage. The scope of this dissertation is thus further

enhanced to study the role of linkages design and the contribution due to their kinematic and dynamic motion.

The overall objective of this dissertation research is to develop methodologies for objective assessment of performance characteristics of static and dynamic seats subject to vehicular vibration, such that the human exposure to transmitted vibration during evaluations is reduced. This is sought via systematic analytical and experimental analysis of static and dynamic properties of seats, seat-occupant and seat-passive load systems. The specific objectives of the study include the following:

(i) Identify the static and dynamic characteristics of two automotive static seats selected for the study.

(ii) Evaluate the vibration isolation performance of seat-occupant and seat-passive load system via laboratory testing under sinusoidal and field measured random excitations.

(iii) Develop nonlinear analytical models of seat-human body systems incorporating different human body models, and select a most appropriate human body model based upon its validity with respect to the measured data.

(iv) Develop a methodology for identifying a Human Response Function such that the vibration assessment of the seat-human system may be performed by integrating the identified function to the vibration transmission characteristics of the seat-load system.

(v) Perform parametric sensitivity analyses to determine near optimal parameters for the seat cushion under deterministic and random excitations.

(vi) Develop a nonlinear analytical model of a selected dynamic suspension seat system using ADAMS (Automated Dynamic Analysis of Mechanical Systems) software, incorporating kinematics and dynamics of the suspension linkages.

(vii) Integrate a rigid body representation of the human driver as well as a dynamic model of seated human body to the dynamic seat suspension model and validate the models.

1.4 Organization of the Dissertation

This dissertation research is presented in five chapters. The highlights of the reported studies are briefly discussed in appropriate chapters, whenever relevant.

In chapter 2, nonlinear mathematical models of vertical seat-occupant systems are developed incorporating single-, two- and four-DOF human body models. The laboratory test procedures for identifying static and dynamic properties of seats are described and results of these tests are discussed and analyzed to yield the model parameters. The laboratory test methodology and apparatus for determination of vibration transmission performance of seat-human and seat-load systems are also presented along with the description of input excitations. The nonlinear differential equations of motion for the seat-occupant models are solved in time-domain using numerical integration algorithm. The random response analysis in frequency domain is also performed using local equivalent linearization technique. Performance characteristics of various seat-human body models are validated using the experimental data and the most appropriate model is selected.

In chapter 3, the vibration transmissibility characteristics of the seat loaded with a passive load are compared with the mean characteristics of the seat-human system in order to identify the Human body Response Function. The response analysis of the seat-human system integrating the Human Response Function is carried out under sinusoidal and random excitations. The results are compared with those established from the laboratory tests in order to validate the proposed methodology. Furthermore, the sensitivity of the vibration isolation properties of the seat-occupant model to changes in seat cushion parameters is investigated.

In chapter 4, a comprehensive analytical model of a mechanical seat-suspension system incorporating rigid body dynamics, biodynamic response of the human body, and linkage dynamics is formulated using ADAMS software. The vibration response characteristics derived from the model are compared with those derived from the laboratory measurements performed under different types of excitations. The conclusions and recommendations for future work are finally presented in chapter 5.

CHAPTER 2.

DYNAMIC ANALYSIS OF STATIC SEATS

2.1 General

The ride vibration environment of an automobile comprises low frequency vibration arising from the tire-terrain interactions and filtered through the low natural frequency suspension, and medium high to high frequency components arising from the structural deflection modes and the drive-train. While the magnitude of high frequency vibration is often lower than that of the low frequency vibration, the high frequency components contribute to the noise environment of the vehicle. The driver and passenger comfort, among many factors, is strongly related to the intensity of low frequency whole-body vibration [55]. The high sensitivity of the human body to low frequency vibration is primarily attributed to its primary resonance near 5 Hz [22]. Although adequately damped low natural frequency wheel suspensions can provide considerable attenuation of the road induced body vibration, the lower limit on the natural frequency is constrained by the rattle space, and adequate handling and control requirements. The automobile suspension is thus designed to achieve a compromise between the ride quality, handling and directional control performance characteristics [56]. It is thus highly desirable to design seats, which can further attenuate the whole-body vehicular vibration, while providing the controlled comfortable posture for the driver and passenger.

In this chapter, static and dynamic laboratory test procedures to identify seat cushion properties are described. Test matrix and methodology for tests with human subjects are also presented. The seat-human body system is analytically modeled

incorporating three different human body models. The simulation results are compared with the experimental data in order to select the most appropriate human body model.

2.2 Comfort and Design Considerations of Static Seats

The seat is perhaps more closely linked to comfort than any other vehicle component. The seats are designed to maintain acceptable driver and passenger comfort and driver interactions with various controls. The perception of whole-body vehicular vibration and its effects on comfort is related to the magnitude and distribution of vibration in the body. The magnitude and distribution of vibration is determined by the body posture and the characteristics of vibration at the body-seat interface. The design of automotive seats with enhanced comfort characteristics thus necessitates appropriate considerations of the body posture and the vibration transmission characteristics. Automotive seats invariably employ contoured compliant cushions to provide controlled body posture with minimal muscular fatigue, facilitate ventilation, distribute pressure around ischial tuberosities, and attenuate vehicular vibration [57,58,59]. The primary components of a static seat which influencing the comfort characteristics are seat cushion and back rest.

Human occupants normally sit on their ischial tuberosities, which are bony prominences, about 11 cm apart, covered by muscle, fat and skin. They transmit most of the weight of the upper body directly from the spinal column to the seat cushion. The dynamic forces are directly transmitted to these prominences, and thus to the back. The firmness of the seat cushion thus affects the degree of driver's comfort and fatigue. Very hard cushions result in discomfort at the tuberosities, which encourage slouched posture

to shift weight to more fleshy areas [58]. But if the cushion is too soft or too contoured it can lead to possible pain and discomfort in the hip joint [60,61]. The main support provided by the seat cushion must be at or slightly forward to the ischial tuberosities. Care must be taken such that the pressure applied to the thighs close to the knee is not too high, as that may pinch the femoral artery and nerve leading to numbness of the foot and the lower leg [62].

Adequate back rest designs can improve the driver's comfort considerably by providing lumbar support and controlled seated posture. It is generally recognized that in order to minimize discomfort, fatigue and potential damage to the spinal column, the driver's back should maintain its S-shaped normal curvature. A slouched back creates high and uneven pressure in the vertebral discs, leading to increased tension in various spinal ligaments and stress in individual vertebrae, especially in the lower back [61]. The vibration isolation characteristics of seat-operator system are influenced by the operator posture. Erect posture experiences large vibrations corresponding to frequencies greater than 4 Hz, while a slouched posture experience slightly larger vibrations at lower frequencies [63]. Back rests with adjustable lumbar supports have thus been developed to help the drivers in maintaining an adequate S-shaped spinal curve.

The postural and vibration characteristics of the seats are primarily related to stiffness and hysteretic properties of the cushion. The cushion compliance, however, cannot be determined from the vibration attenuation characteristics alone. An appropriate consideration of the distribution of body pressure and postural properties may be necessary for the seat design. The comfort or dynamic efficiency of a seat is primarily determined by three factors: the vibration environment, the seat dynamic response and

the response of the human body. The predominant frequencies and direction of vibration further contribute to the vibration discomfort of a seat occupant. The seats should be designed to minimize the transmission of vibration at frequencies to which human body is known to be most sensitive. Since the ride vibration environment of vehicles varies with the vehicle design and operating conditions, a seat design considered optimal for a specific vehicle may not be the optimum for another vehicle. The 'tuning' or adapting a seat to an environment consists of adjusting the dynamic response of the seat in order to minimize the most important adverse effects of the vibration. This can only be achieved with prior knowledge of the vibration environment and availability of adequate methods of predicting human response to the complex vibration that are transmitted to the seats.

The automotive static seats comprising foam cushions and springs are designed to accommodate a wide range of body weights. The stiffness and damping properties of the air-filled foams are known to be nonlinear functions of body weight, force-deflection and force velocity properties of the foam cushions, which primarily arise from the nonlinear stress relaxation behavior and the visco-elastic nonlinearities present in the stress-strain curves [34]. The results from previous investigations also show that the influence of human whole-body dynamics on seat vibration attenuation performance is very significant [21,22]. Griffin [23] also reported that the influence of whole-body dynamics on the seat attenuation performance is highly dependent on the characteristics of the seat itself. For a relatively stiff seat such as that used by Griffin, with resonant frequency close to 4 Hz, the lightly damped and highly rigid seat-load interface results in significant amplification of the resonant vibration. The elasticity and dissipative properties provided by the human buttocks and thighs contribute considerably to reduce the magnitude of the

resonant peak and the resonant frequency, while impeding the attenuation performance at higher frequencies. The study of the occupant-seat system thus necessitates appropriate consideration of the coupled dynamics associated with the seat and human body, along with the characteristics of the vibration excitation.

2.3 Analytical Modeling of Vertical Seat-Human Body System

In view of the complex human-seat interactions, and highly nonlinear static and dynamic properties of the seats, the design and performance characteristics of the seats are frequently evaluated through field tests. The design practices based upon expensive field trials, however, are known to be demanding on human resources associated with analyses and interpretation. The design approach based upon model development and analyses can be extremely effective and efficient, since it provides a flexible design tool to perform extensive parameter sensitivity analyses. Such a design approach needs to be supported by only a limited number of field tests for product development with optimal characteristics.

Development of analytical model of the seat-human system requires careful considerations of the following:

(i) description of a truly representative excitation at the seat base;

(ii) determination of nonlinear damping and stiffness properties of the seat cushion;

(iii) selection of the most appropriate human body model; and

(iv) determination and interpretation of the dynamic response of the seat-human system.

Three analytical models of the seat-human body systems are developed incorporating different human operator models. The analytical models are realized by integrating four different models of the human operator to the cushion model. These models include: a rigid mass representation of a human body, a single-DOF model, reported by Griffin [39]; a two-DOF model, reported by Suggs and [40]; and a four-DOF model, reported by Boileau [22]. Primary assumptions associated with the models include:

(i) the visco-elastic properties of the foam-cushions along the vertical axis are characterized by equivalent linear stiffness and viscous damping coefficients, within the operating range;

(ii) motions along the generalized coordinate system are considered to be small relative to overall dimensions of the seat;

(iii) the seat and human body models are constrained to move along the vertical direction only.

2.3.1. Static Seat Model with a Rigid Mass Representation of a Driver

A seat model lumped with a rigid mass M is illustrated on Figure 1.2. It should be noted that the force-deflection and force-velocity characteristic of a cushion are known to be a complex function of the seated body weight, excitation frequency and amplitude, and material properties. The cushions are frequently characterized by their equivalent linear stiffness and damping coefficients in order to evaluate their vibration isolation performance. The static seat, comprising a foam cushion, is thus represented by its equivalent stiffness K_C and viscous damping coefficient C_C. The equation of motion for the resulting one-DOF system is:

$$M\ddot{X}_1 + K_C(X_1 - X_i) + C_C(\dot{X}_1 - \dot{X}_i) = 0 \qquad (2.1)$$

where, X_1 is a displacement of the rigid mass and X_i is the excitation displacement.

2.3.2 Static Seat Model with Single-DOF Human Body Model

A seat model lumped with a one-DOF driver model, proposed by Fairley and Griffin, is illustrated on Fig.2.1. The single-dof human operator model was derived using the measured apparent mass data for subjects under random vibration of 1 m/s^2. The human body is represented by the lower and upper body masses (M_1 and M_2 respectively), coupled by the visco-elastic properties (K_B and C_B). The equations of motion for the two-degrees-of-freedom seat-human body model can be derived in the following manner:

$$\begin{aligned} &M_2\ddot{X}_2 + C_B(\dot{X}_2 - \dot{X}_1) + K_B(X_2 - X_1) = 0 \\ &M_1\ddot{X}_1 + C_B(\dot{X}_1 - \dot{X}_2) + K_B(X_1 - X_2) + K_C(X_1 - X_i) + C_C(\dot{X}_1 - \dot{X}_i) = 0 \end{aligned} \tag{2.2}$$

where, X_1 and X_2 are displacements of the lower and upper body masses, respectively, and X_i is the displacement excitation at the seat base.

2.3.3 Static Seat Model with Two-DOF Human Body Model

Suggs proposed a two-DOF seated human body model, comprising two masses suspended from a common frame of mass M_0 representing the rigid spinal column [40]. The lower mass (M_1) represents the pelvis and abdomen, while the upper mass (M_2) represent the mass due to head and chest. A three-DOF seat-human body model is thus derived by integrating two-DOF operator model to the seat model as illustrated in Figure 2.2. The equations of motion for the three-DOF model are derived as follows:

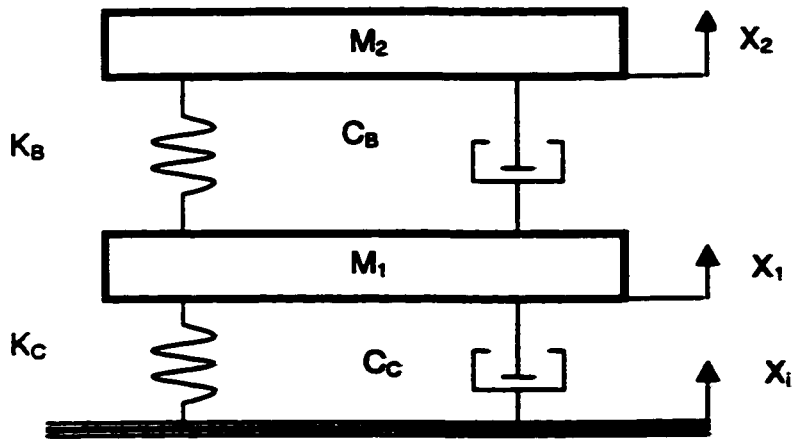

Figure 2.1. Two-degrees-of-freedom seat-human body model [39].

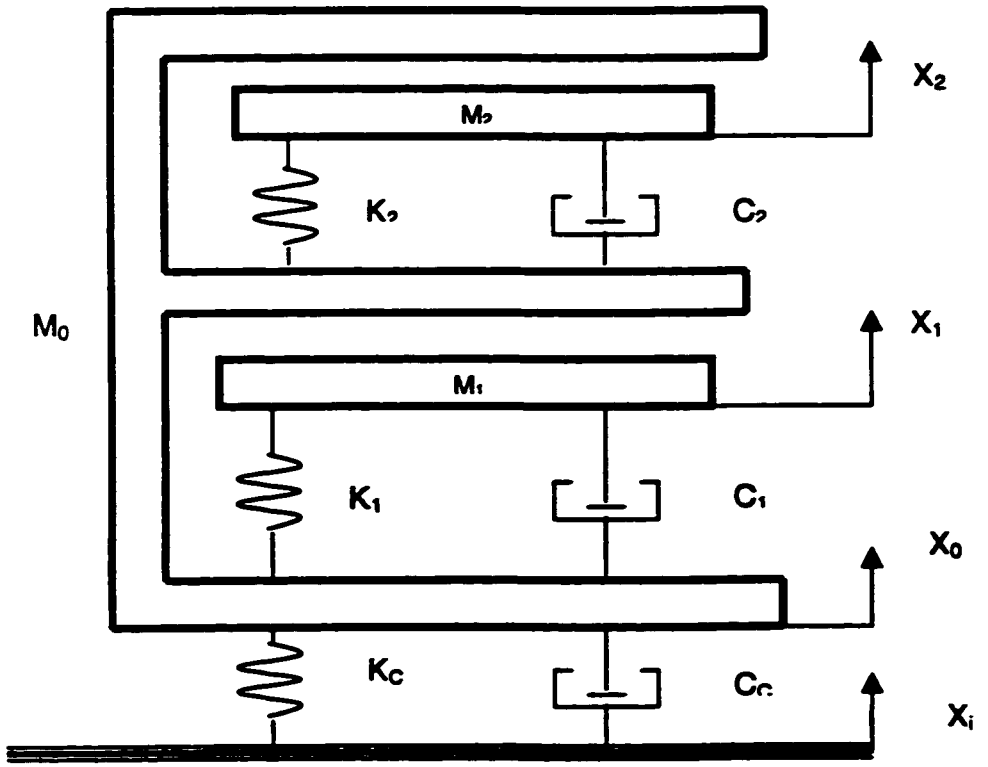

Figure 2.2. Three-degrees-of-freedom seat-human body model [40].

$$
\begin{aligned}
&M_0\ddot{X}_0 + K_C(X_0 - X_i) + C_C(\dot{X}_0 - \dot{X}_i) + K_1(X_0 - X_1) + C_1(\dot{X}_0 - \dot{X}_1) \\
&+ K_2(X_0 - X_2) + C_2(\dot{X}_0 - \dot{X}_2) = 0 \\
&M_1\ddot{X}_1 + K_1(X_1 - X_0) + C_1(\dot{X}_1 - \dot{X}_0) = 0 \\
&M_2\ddot{X}_2 + K_2(X_2 - X_0) + C_2(\dot{X}_2 - \dot{X}_0) = 0
\end{aligned}
\tag{2.3}
$$

where, M_0, M_1, M_2, K_1, K_2, C_1 and C_2 are the inertial, stiffness and damping properties of human body model, summarized in Table 1.2.

2.3.4 Static Seat Model with Four-DOF Human Body Model

Boileau [22] proposed a four-DOF biodynamic model of a seated body based upon measured and synthesized values of diving-point mechanical impedance and seat-to-head vibration transmissibility characteristics. The model, shown in Figure 1.10, comprises masses due to head and neck (M_1), upper torso (M_2), middle torso (M_3), lower torso (M_4), and buttocks and thighs (M_5). The stiffness properties of the model were based upon the spinal data reported in different studies. The Figure 2.3 illustrates a four-DOF seat-human body model, derived upon integrating the proposed human body model to the single-DOF seat model. The equations of motion for resulting four-DOF model are derived as:

$$
\begin{aligned}
&M_4\ddot{X}_4 + K^*_4(X_4 - X_i) + C^*_4(\dot{X}_4 - \dot{X}_i) + K_3(X_4 - X_3) + C_3(\dot{X}_4 - \dot{X}_3) = 0 \\
&M_3\ddot{X}_3 + K_3(X_3 - X_4) + C_3(\dot{X}_3 - \dot{X}_4) + K_2(X_3 - X_2) + C_2(\dot{X}_3 - \dot{X}_2) = 0 \\
&M_2\ddot{X}_2 + K_2(X_2 - X_3) + C_2(\dot{X}_2 - \dot{X}_3) + K_1(X_2 - X_1) + C_1(\dot{X}_2 - \dot{X}_1) = 0 \\
&M_1\ddot{X}_1 + K_1(X_1 - X_2) + C_1(\dot{X}_1 - \dot{X}_2) = 0
\end{aligned}
\tag{2.4}
$$

where, M_1, M_2, M_3, M_4, K_1, K_2, K_3, C_1, C_2 and C_3 describe the inertial, stiffness and damping properties of the human body model, summarized in Table 1.2. The driver-seat interface is represented by the stiffness and damping constants, K_4^* and C_4^*, representing

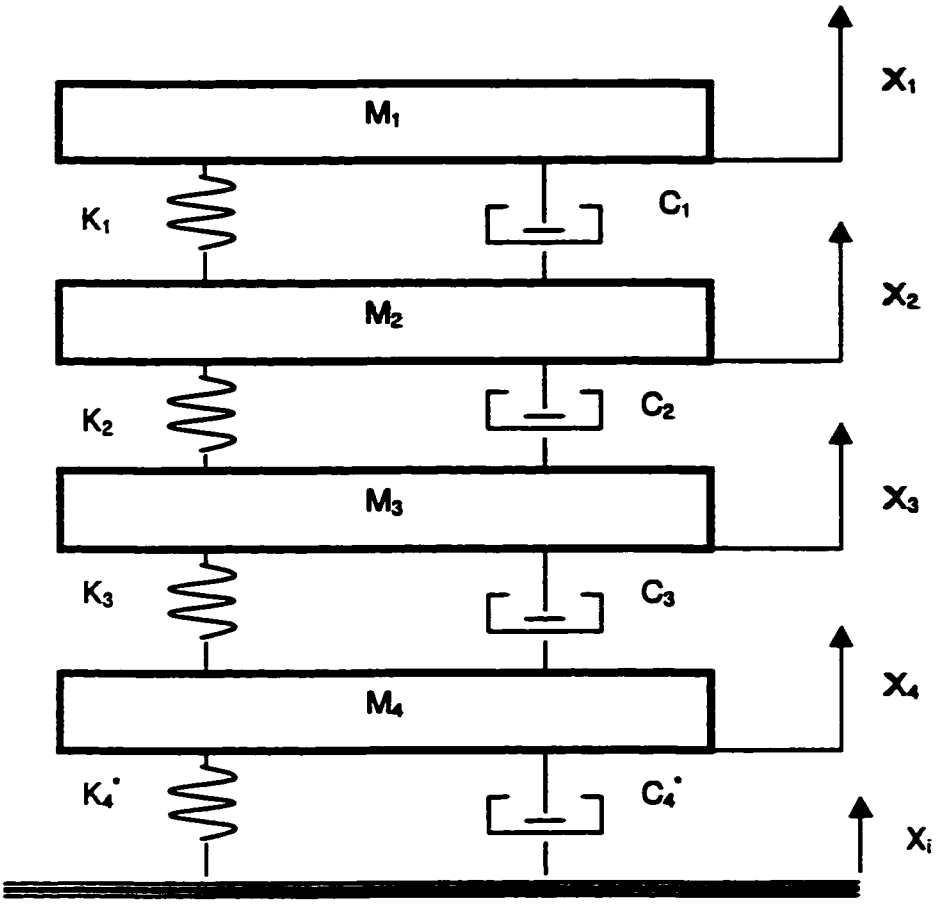

Figure 2.3. Four-degrees-of-freedom seat-human body model [22].

the equivalent restoring and dissipative properties derived for a series combination of cushion, and driver buttocks and thighs stiffness and damping coefficients, expressed as:

$$K_4^* = \frac{K_4 K_C}{K_4 + K_C}; \qquad C_4^* = \frac{C_4 C_C}{C_4 + C_C} \tag{2.5}$$

where K_4 and C_4 are the stiffness and damping properties of the proposed human body model interface. In the above equations, the motion X_4 of mass M_4, representing the buttocks and thighs, serves as an indicator of the vibration exposure of the driver under an excitation represented by X_i.

2.4 Static and Dynamic Properties of the Static Seats

The effectiveness of the combined static seat-human body models is strongly dependent upon the accurate characterization of both the properties of the seat and the seated human body. The biodynamic response behavior of seated human subjects has been reported in terms of driving–point mechanical impedance, apparent mass, and seat-to-head vibration transmissibility. The properties of cushion may depend upon the material, construction and the body weight. Such seat properties may be identified in the laboratory through measurement of static and dynamic force-deflection characteristics of the seat, while the properties of the combined seat-human system may be derived from the response measurement at the human-seat interface.

The automotive seats are designed to accommodate subjects of different weights and are exposed to different vibration environments. The static and dynamic characterization of an automotive seat thus necessitates consideration of variations in the following test parameters:

(i) Preload: The static and dynamic characteristics of the seats should be established for different preloads representing the 5th, 50th and 95th percentile adult male and female population. The corresponding seat cushion load or preload can be estimated as 65% of the total body weight [67]. For this study, however, only measurements representing 50th percentile male population are considered. The average body weight for this category is 75 kg and corresponding seat cushion load is estimated as 48.75 kg.

(ii) Amplitude of Vibration Excitation: The vehicle seats are subject to varying levels of displacement excitations depending upon various vehicle and road factors. Furthermore, the seat cushions exhibit nonlinear stress-strain relationship. It is thus vital to characterize the seat cushions under different amplitudes of vibration excitations. In this study, excitation displacement amplitudes ranging from 2.5 mm to 19 mm are selected to perform the various static and dynamic tests. It is believed that this range represents the vibration environment of wide range of automobiles under different road conditions.

(iii) Frequency of Excitation: The automobile vibrations predominate in the vicinity of sprung mass natural frequencies (≈ 1 Hz) and the wheel-hop frequencies (9-15 Hz). The dynamic characterization of the seats is thus performed at selected discrete frequencies in the 0.625 to 15 Hz frequency range.

2.4.1 Test Apparatus and Methodology

Figure 2.4 illustrates the schematic of the test setup designed to perform the static and dynamic tests. The test setup comprises a vibration platform mounted on an electro-hydraulic vibration exciter. The test seat is installed on the platform, and a load indentor is installed between the cushion and a fixed inertial frame. The load indentor comprises a 20.3 cm (8 in.) diameter flat disk as recommended in the SAE J1051 [64]. The cylindrical joint of indentor permits the measurement of vertical force, irrespective of the cushion contours. A string potentiometer is installed between the fixed inertial frame and the vibration platform to measure the displacement and velocity response of the seat cushion. The deflection response of the seat is also measured using the LVDT integrated within the electro-hydraulic actuator.

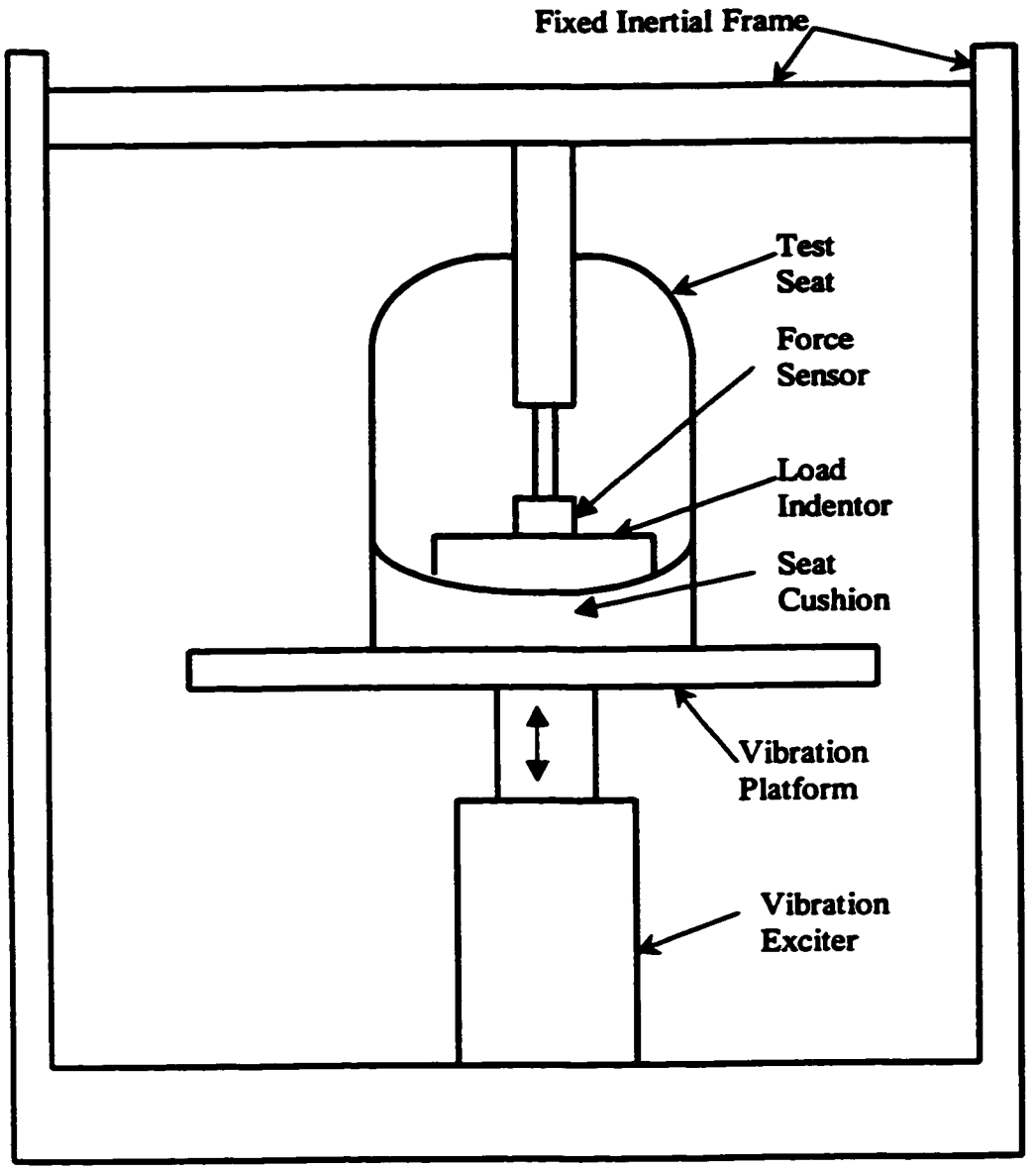

Figure 2.4. Schematic of the test setup for measurement of static and dynamic properties of seats.

The static and dynamic tests were performed in accordance with the procedures outlined in SAE J1051 [64]. It should be noted that the SAE J1051 is proposed for force-deflection measurements of the foam cushion seats employed in off-road machinery. The recommended test specifications are thus modified to adapt for the candidate spring cushion automotive seat. The standard recommends the compression of the seat cushion to nearly 20% of the original thickness under application of 1334 N force. The loading of the car seat under such conditions can result in failure of the seat coverings and the foam. The maximum seat load for the dynamic tests is thus limited to approximately 900 N. The standard further recommends application of force in increments of 222 N, which is considered to be too high for the car seats. In this study, the force is applied in increments of 50 N using the recommended indentor, and the force-deflection properties are measured by varying the force in increasing and decreasing order.

The SAE J1051 recommends 1 minute relaxation duration between each load increment or decrement prior to the measurement of the deflection response. While this practice allows for relaxation and measurement of truly static deflection with minimal contribution due to hysteresis, the validity of the measurement can be argued, when the results are applied under dynamic conditions. The seat cushions subject to vibration environment do not necessarily experience total relaxation. Furthermore, the relaxation duration is most likely dependent upon the behavior of the foam material. The recommended methodology, however, is considered to evaluate the static stiffness characteristics of the seat cushion.

Two different automotive seats are selected for the static and dynamic characterization, which are referred to as 'seat A' and 'seat B'. The dynamic force-

deflection characteristics of the seat cushion subject to the specified preload are measured under sinusoidal excitations of varying frequencies and amplitudes using a 4500 N Sensotech load cell, a built-in Schaevitz LVDT, and a Magnetek string potentiometer, respectively. The string potentiometer was installed to yield displacement and velocity response. The displacement measured using the built-in LVDT, however, was used for the data analysis. The sensors signals are acquired in an analog DMA block of the PC comprising a 4-channel data acquisition board PC-1-204228W-1. The DMA block is linked to a DDE server block, as shown in Figure 2.6. The software performs the A/D conversion, and exports the data into the MS-Excel spreadsheet through Visual Designer software. The data acquisition software is configured to sample each data channel at a rate of 360 samples/cycle. The selection of this sampling rate allowed for desirable variations in the sampling rate with variations in the frequency. The processed data are further manipulated to display the force-deflection Lissajous diagrams and force-velocity characteristics during the tests.

2.4.2 Static Force-Deflection Characteristics of the Seats

The static and dynamic tests were performed on two automotive seats to determine their static and dynamic stiffness and damping properties. To evaluate the static stiffness characteristics of the seat cushion the seat is initially displaced to achieve desired preload and the corresponding static deflection is recorded. The seat is further displaced gradually to increase the force in increments of 45 N. The seat is permitted to relax for a period of 1 minute corresponding to each increment, and the resulting displacement is recorded, as outlined in SAE J1051 [64]. The force-deflection

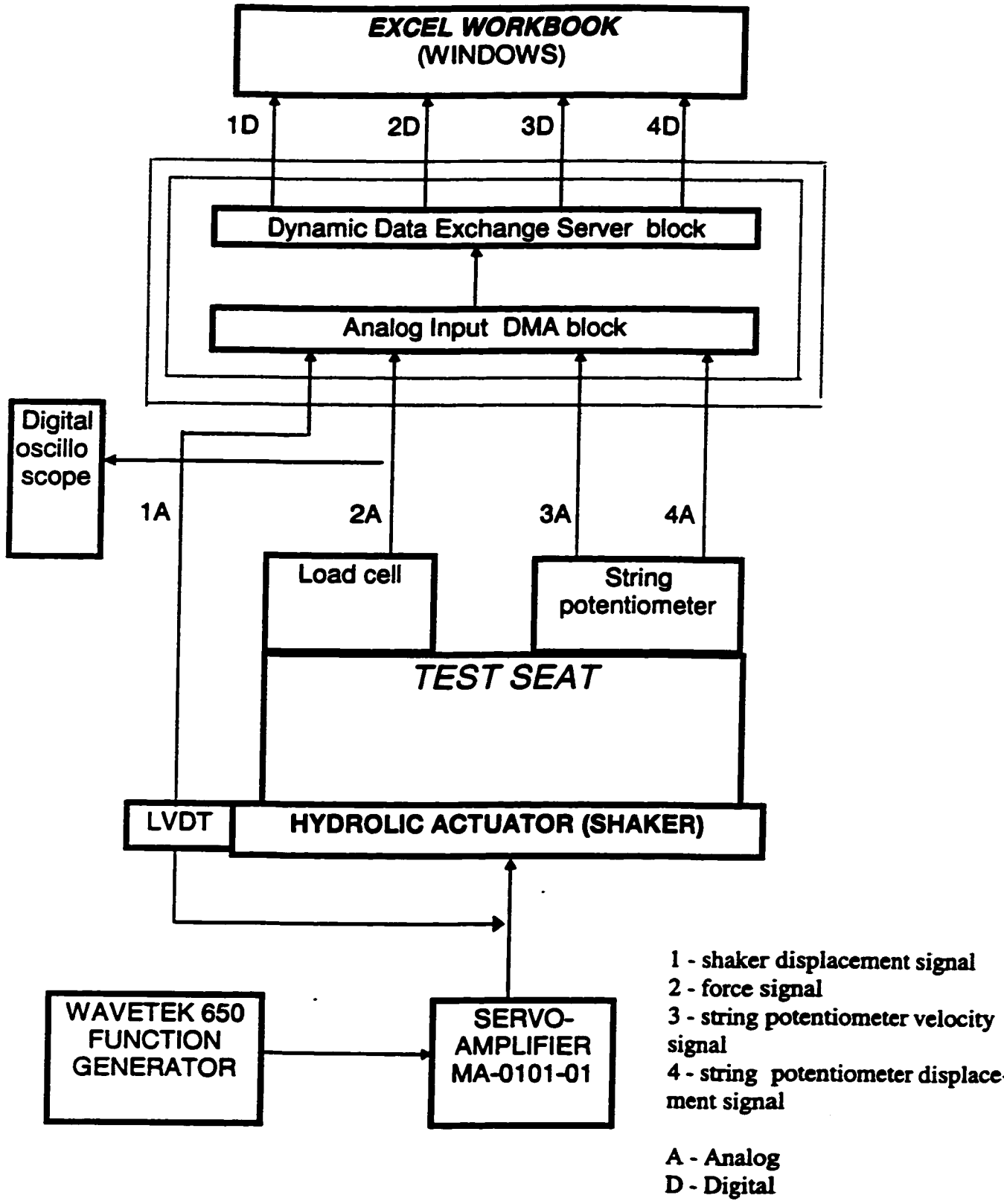

Figure 2.6. Data acquisition and processing chart for static and dynamic testing of automotive seats.

characteristics are measured up to a maximum load of 890 N for seat 'A' and 670 N for seat 'B'. The maximum load for the seat 'B' was selected as 670 N due to its excessive deflection. The seat was then gradually unloaded to zero force in steps of 45 N and the corresponding force-deflection values were recorded.

The static force-deflection characteristics of the two seats, acquired under a preload of 480 N, are presented in Figure 2.7. The seat cushions exhibit considerable hysteresis, as indicated by the difference between the loading and unloading curves. The measured data reveals maximum hysteresis of approximately 75 N for both seats. The cushion employed in seat 'A' reveals higher stiffness compared to that used in seat 'B'. The static force-deflection characteristics clearly reveal the nonlinear visco-elastic nature of seat cushions arising from the nonlinear stress-relaxation and stress-strain properties of the foam. Assuming linear force-deflection properties of the seat cushions for small variations in load around a known preload, the static stiffness of the seat cushions can be computed corresponding to the selected preload values.

2.4.3 Dynamic Force-Deflection Characteristics of the Seats

The dynamic force-deflection characteristics of a seat provide significant information related to its comfort characteristics as a function of the preload, stroke and frequency of excitation. The dynamic stiffness coefficient of a seat is known to differ from its static stiffness value. The dynamic stiffness characteristics of the seats are derived from the measured force-deflection data, as a function of the excitation frequency and amplitude. The dynamic stiffness constants are computed from the mean force-deflection data in the vicinity of the seat preload.

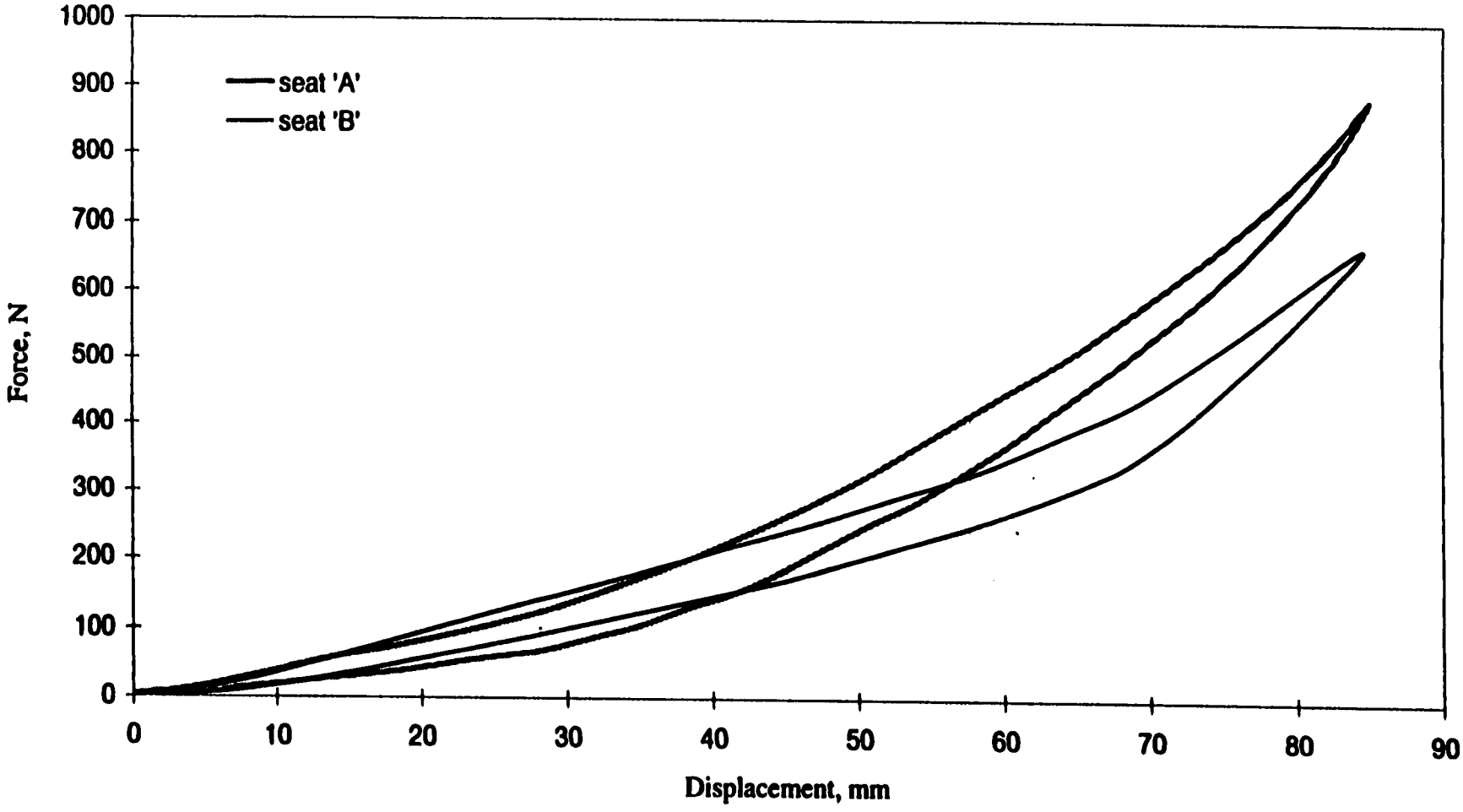

Figure 2.7: Measured Static Force-Deflection Characteristics of the Selected Static Seats.

The typical force-deflection characteristics of the seat, measured under sinusoidal excitations of varying frequency and amplitude, are illustrated in Figures 2.8 and 2.9. The results are presented for excitations at two distinct frequencies, 1.5 Hz and 6 Hz. The results clearly show that the magnitude of hysteresis increases considerably with the increase in the excitation frequency and the amplitude. The dynamic stiffness of the cushion, estimated from the ratio of change in force to the change in deflection, also increases with increase in the excitation frequency and decrease in the amplitude of excitation.

The values for static stiffness coefficients for both seats were derived assuming linear fore-deflection characteristics of the seat cushions for small variations in load around a known preload. The value of preload was selected to be 480 N to represent 50th percentile male category driver weight supported by the cushion. A comparison between static and dynamic stiffness values for seat cushions calculated under different excitation amplitudes and frequencies are presented in Table 2.1. The results show that the cushion stiffness tends to increase with increase in excitation frequency, which can be attributed to lower relaxation period permitted under high frequency excitations. The stiffness coefficients tend to decrease with increase in the deflection amplitude. The influence of excitation amplitude and frequency on the stiffness coefficients for seats 'A' and 'B' for the preload of 480 N (48.75 kg) is further presented in Figures 2.10 and 2.11. These figures clearly illustrate some important trends. The stiffness coefficients obtained under low frequency excitations are quite similar to the corresponding static values. The stiffness characteristics of the cushions, in general, increase with the increase in the excitation frequency and decrease with the increase in the stroke. The seat 'A' reveals

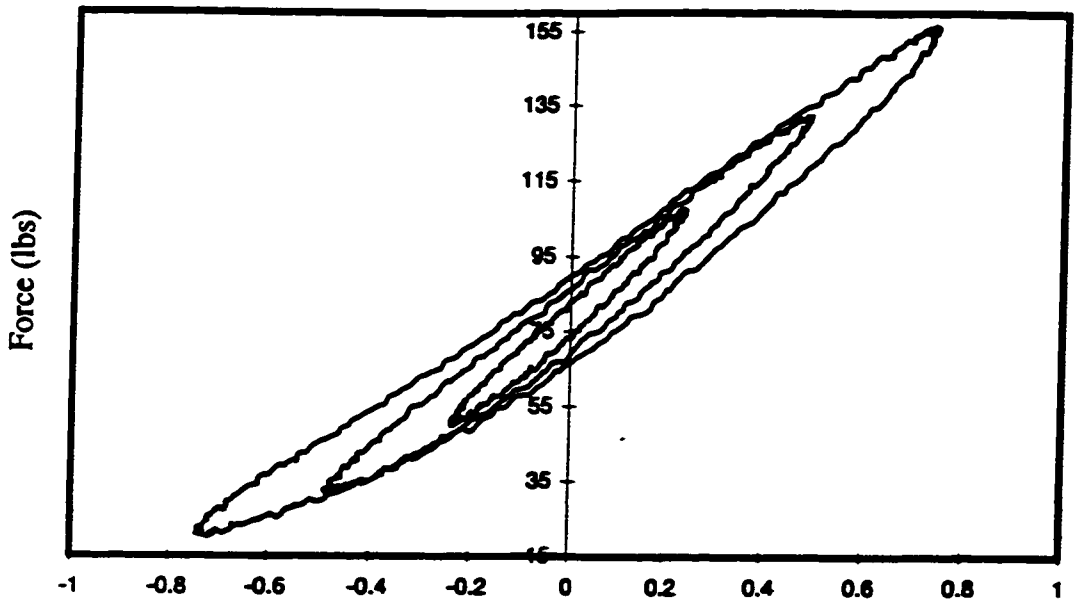

Figure 2.8: Dynamic Force-Deflection Characteristics for Different Excitation Amplitude (seat 'A', excitation frequency 1.5 Hz)

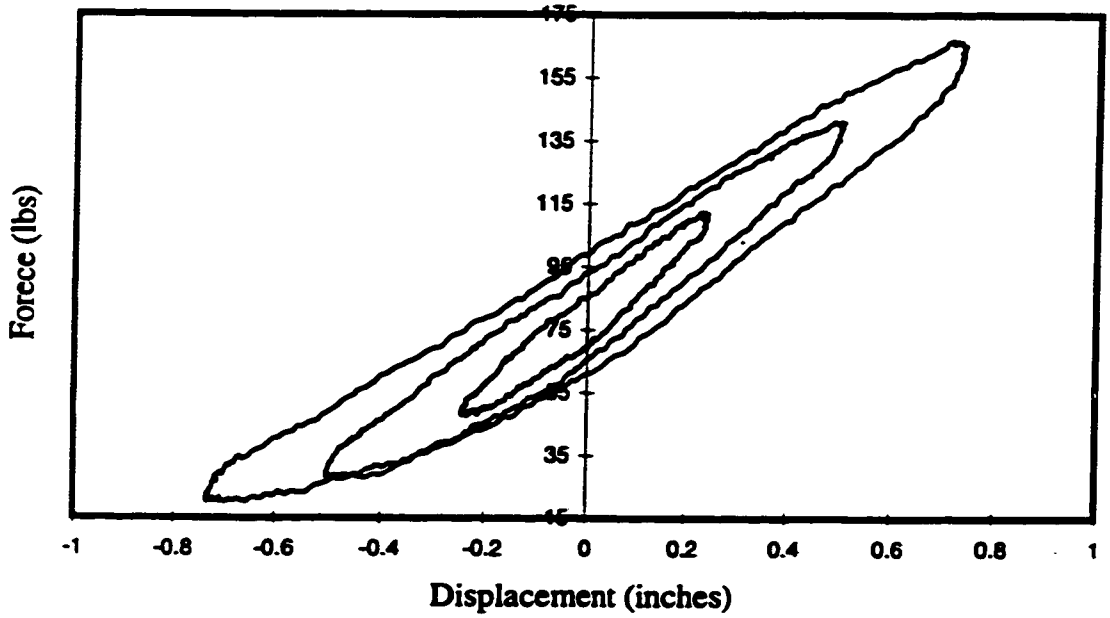

Figure 2.9: Dynamic Force-Deflection Characteristics for Different Excitation Amplitude (seat 'A', excitation frequency 6 Hz)

Table 2.1: A Comparison Between Calculated Static and Dynamic Stiffness Coefficients for Seats 'A' and 'B' (Preload 480 N)

Seat	Static Stiffness N/m	Excitation Amplitude mm	Dynamic Stiffness, N/m									
			Frequency, Hz									
			0.1	1	1.5	2	4	6	8	10	12	15
A	19910	6.4	20962	21557	21522	21662	22450	23028.3	23938.9	23641.2	27056	33343
		12.8	18860	19456	19473	19666	20349	21066.9	21907.5	21609.8	24674	31854
B	21550	2.6	24429	26023	28439	29385	29263	30418.3	29472.7	30716	30944	------
		12.8	18685	18930	19018	21435	20769	21504.7	20611.6	23203.4	24377	------

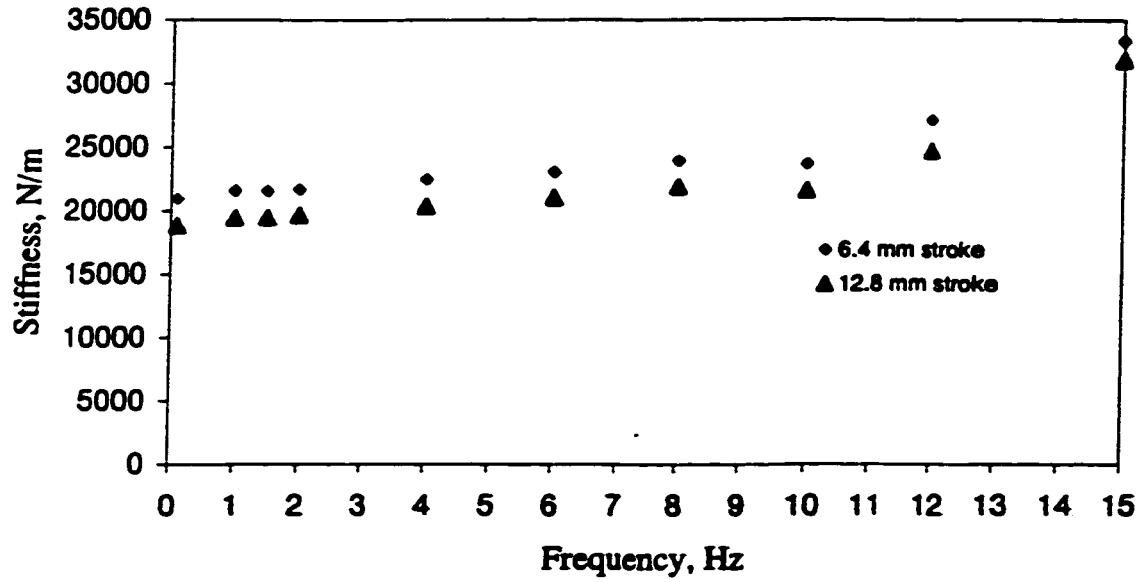

Figure 2.10: Influence of the Excitation Frequency and Amplitude on the Stiffness of seat 'A'.

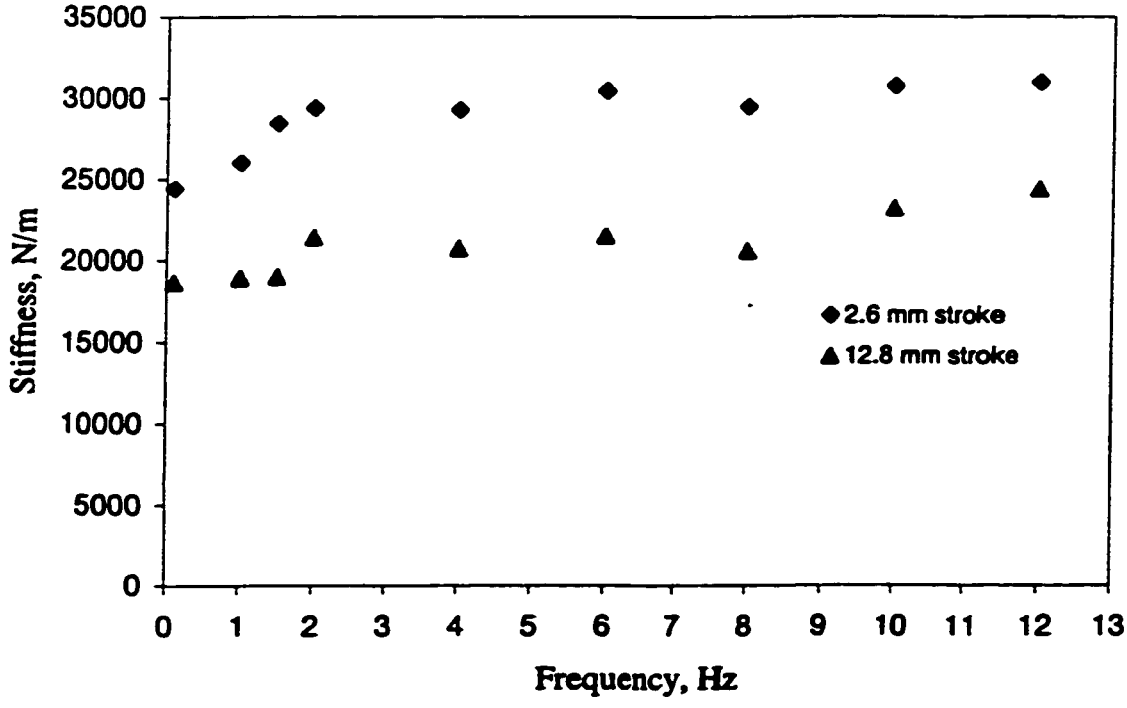

Figure 2.11: Influence of the Excitation Frequency and Amplitude on the Stiffness of seat 'B'.

considerable increase in the stiffness at frequencies above 10 Hz, which may be attributed to the bending deflections of the cushion support structure.

Estimation of Damping Characteristics.

The damping or energy dissipation properties of the automotive seats can be estimated from the force-displacement and force-velocity characteristics acquired from dynamic testing of the cushions. The equivalent viscous damping associated with a cushion can be estimated from the energy dissipated per cycle of vibration by the cushion. The energy dissipated per cycle is derived from the measured force-displacement curves in the following manner [69]:

$$\Delta E = \oint F_{DC} dx \tag{2.6}$$

where ΔE is the energy dissipated per cycle and F_{DC} is the dissipative force. Cushion damping can be conveniently approximated by an equivalent damping coefficient, which may be derived by equating the energy dissipated by the cushion to that of a viscous damper. The energy dissipated per cycle by a viscous damper is given by [65]:

$$\Delta E = \pi C_C \omega X^2 \tag{2.7}$$

where C_C is the equivalent viscous damping coefficient, ω is the circular frequency of excitation in rad/s and X is the peak displacement amplitude. The coefficient C_C is thus referred to as a local equivalent viscous damping coefficient, which is considered valid in the vicinity of selected excitation frequency ω and excitation amplitude X. The equivalent damping coefficient due to cushion is then obtained by equating Equations (2.6) and (2.7):

$$C_C = \frac{\Delta E}{\pi \omega X^2} \tag{2.8}$$

The seat cushions exhibit dissipative properties due to two phenomena: (i) hysteresis of the foam, and (ii) air flow to and from the pneumatic filled foam. Stiff cushions provide large hysteresis damping, while the soft cushions provide higher damping due to air flow. The local equivalent damping coefficients of the seat cushions, as a function of frequency and displacement amplitude, are presented in Figures 2.12 and 2.13. The seat cushions reveal high damping at low frequencies and the damping coefficients decrease rapidly with increase in the excitation frequency. The results also show almost insignificant influence of deflection amplitude on the equivalent viscous damping constants. Seat 'A', however, exhibits lower damping coefficients than seat 'B'. From the results, it is apparent that the damping coefficient of seat cushions is relatively less sensitive to the amplitude of deflection. The damping coefficient is also less sensitive to variation in the excitation frequency at frequencies above 5 Hz. The cushions, in general, yield high damping at lower frequencies, which may be attributed to certain relaxation of the cushion during the vibration cycle.

2.5 Experimental Characterization of the Seat-Human System

The comfort characteristics of the seat in view of its vibration behavior is a complex function of the vibration environment, the dynamic response of the seat and the human body, and the static and dynamic properties of the seat. In view of the complexities associated with dynamics of the human body, the performance of vehicle seats can be evaluated through tests with human subjects. This method can yield reliable assessment of the automotive seats when representative subjects sample and test conditions are employed.

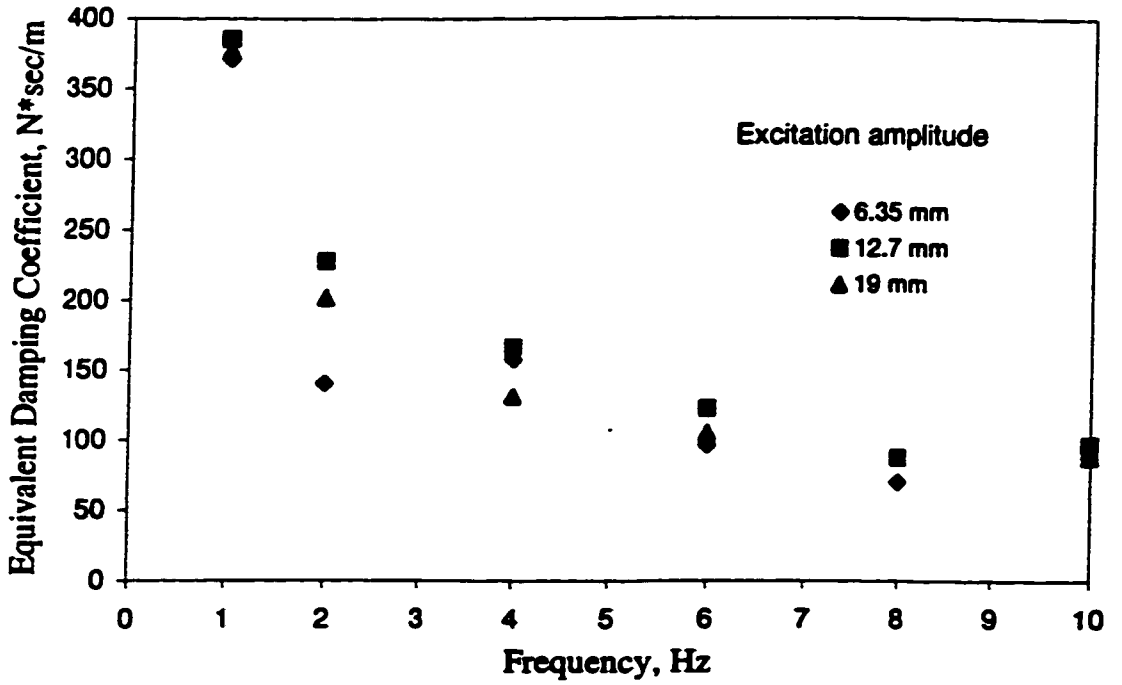

Figure 2.12: Equivalent Viscous Damping Coefficient of Seat 'A'.

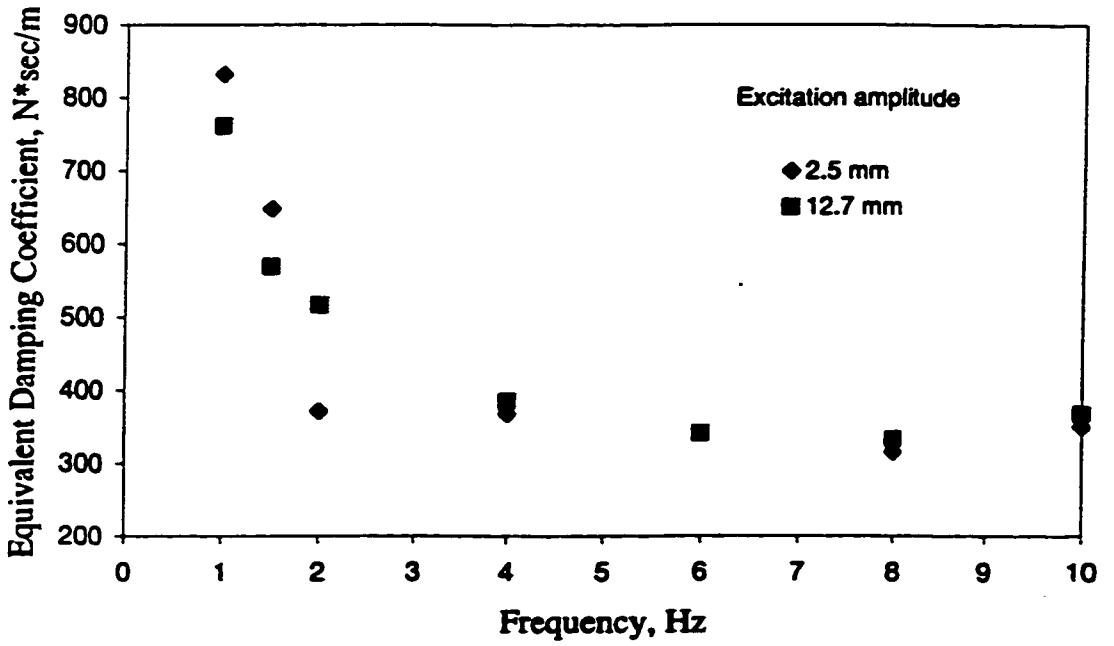

Figure 2.13: Equivalent Viscous Damping Coefficient of Seat 'B'.

2.5.1 Test Apparatus and Methodology

The vibration transmission characteristics of seats 'A' and 'B' were investigated in the laboratory using the whole-body vehicular vibration simulator (WBVVS). The simulator comprises a vibration platform supported on two servo-hydraulic actuators, as shown in Figure 2.14, and a servo-control system interfaced with either an analog or a digital signal generator. Since the vertical vibration encountered in vehicles is among the most severe ones, the WBVVS was configured to simulate vertical vibration alone. The WBVVS was designed with the following considerations to ensure the safety of the test subjects and to meet appropriate vibration requirements for testing seat-driver and suspension-seat-driver systems.

- The magnitude of the compressive and extensive forces generated by the WBVVS are continuously monitored and limited, such that the rms acceleration levels are well below the exposure limit proposed in ISO 2631/1 [14]. Furthermore, the peak acceleration level at any time does not exceed 1.0 g.
- Slow ramp-up and ramp-down circuits must be incorporated to eliminate the undesired transient motions and forces that could arise during start-up, stoppage, and sudden power interruptions.
- Emergency safety switches are provided to the subjects and to the operator.
- The WBVVS is designed to support the load due to the platform, the steering column, the seat and the driver.
- The WBVVS is designed to reproduce the vibration environment of different classes of vehicles, specifically in the 0.5 to 35 Hz frequency range.

The test seat was installed on the force platform of the WBVVS. Each subject was seated in the seat with feet supported on the vibrating platform and hands on the steering wheel. The subjects were advised to assume a driving posture considered most comfortable by the individuals. It was observed that most subjects assumed almost erect posture, while making adequate use of the back support.

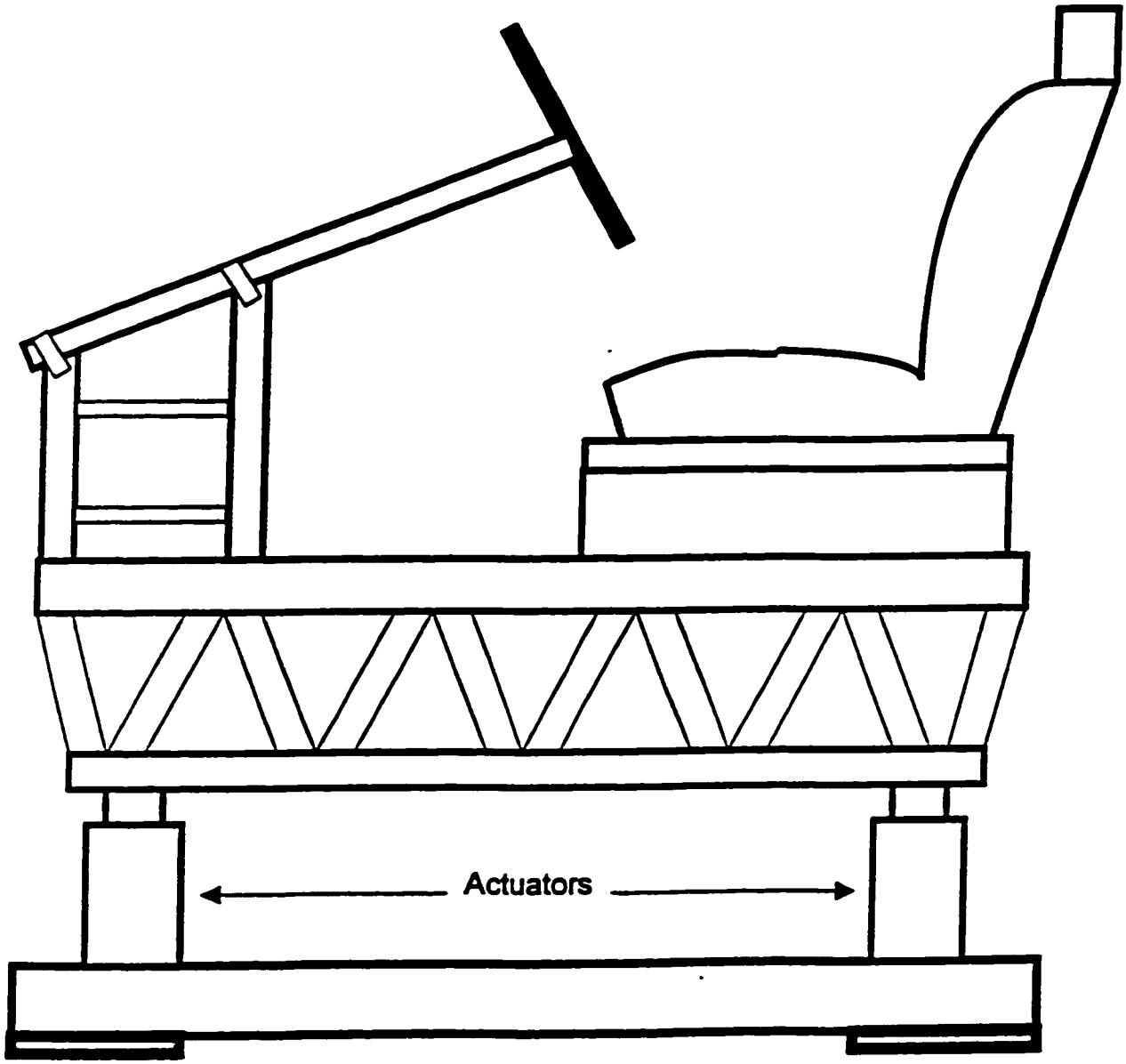

Figure 2.14: Schematic of WBVVS.

The seat and platform were instrumented to measure the acceleration excitation and the response at the subject-seat interface. An accelerometer (B&K 4370) was installed at the platform, while the B&K seat accelerometer pad was positioned at the seat cushion. The accelerometer signals were conditioned using B&K signal conditioners, and filtered using a low-pass filter with cut-off frequency of 40 Hz. The filtered acceleration signal was acquired and analyzed using B&K 2035 signal analyzer. Figure 2.15 illustrates the schematic of the measurement set up.

The WBVVS was also used to investigate the vibration transmission characteristics of seats 'A' and 'B' when loaded with passive loads (sand bags). The methodology for these tests and results are further discussed in Chapter 3.

2.5.2 Description of Test Subjects

A total of 6 male subjects were selected for the study in order to represent the 50th percentile adult male population. The weight of the subjects was permitted to vary within $\pm 10\%$ of the established mean weight for this category (75.3 kg). The weight, height and age of the selected subjects are summarized in Table 2.2. A summary protocol describing proposed experiments together with the participant consent form, approved by the ethical acceptability committee, was provided to each participant for his/her approval.

2.5.3 Vibration Excitations

The ride vibrations encountered at the seat base of the vehicle arise from various sources, which can be classified in two broad classes:

(i) tire interactions with road

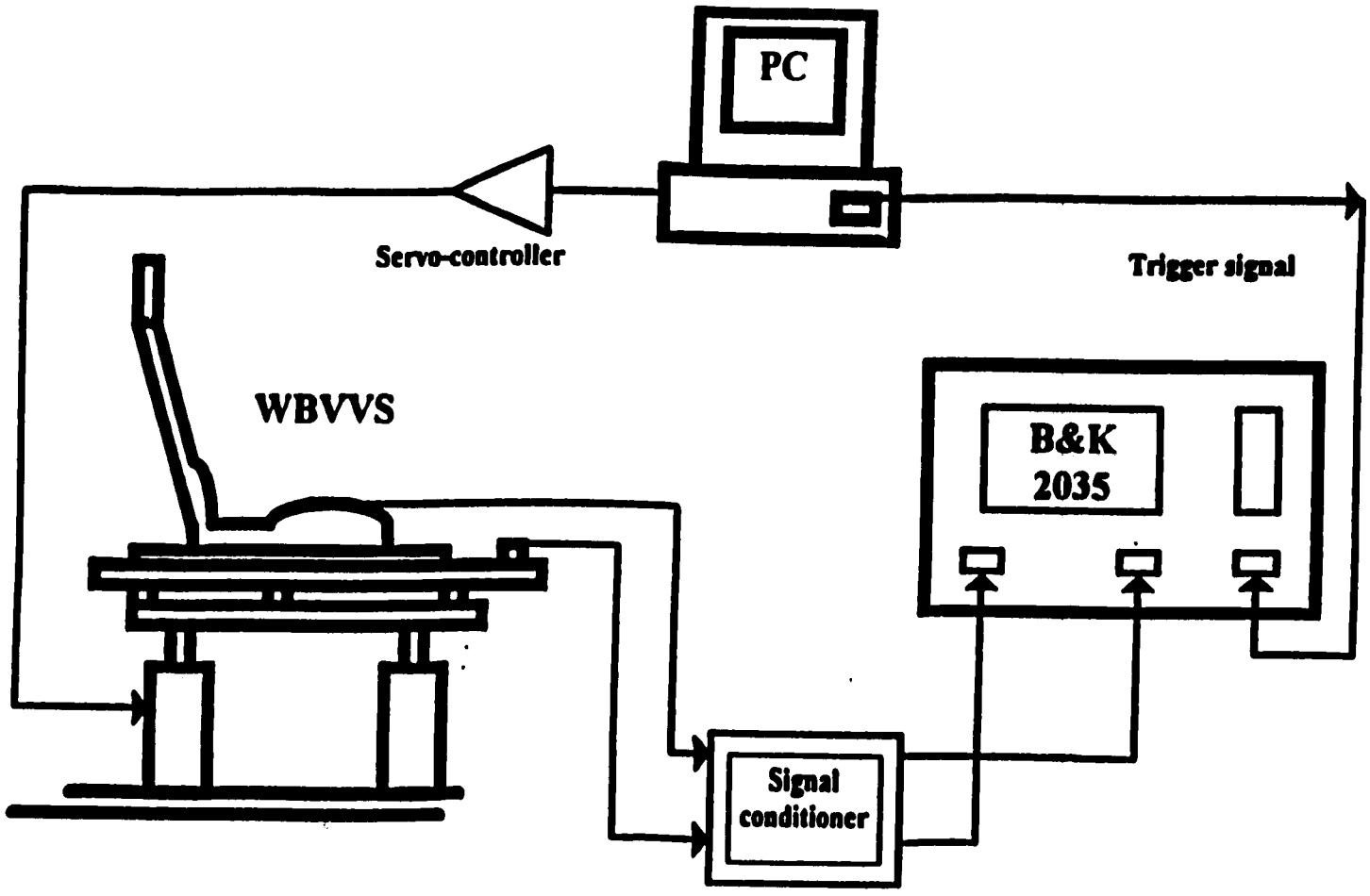

Figure 2.15: Schematic of the measurement and data analysis set-up.

(ii) on-board sources.

The on-board sources include the structure and rotating components, such as tire/wheel assemblies, drive line, engine, and the like. The vibration originating from on-board sources often predominates around higher frequencies, while the ride vibration induced by the road predominates around the low frequencies to which human body is most fatigue sensitive. Furthermore, the amplitude of road induced vibration is considerably larger than that induced by the on-board sources. The road induced vibrations, encountered at the vehicle floor, thus need to be quantified in order to evaluate the performance characteristics of the seat-human body system.

TABLE 2.2: Weight, height and age of 6 male subjects selected for the study.

1	74.1	174	41	74.2
2	79.5	162	26	
3	68.2	175	31	
4	79.5	182	38	
5	69.1	181	34	
6	75.0	181	30	

Random vibrations more closely represent the true vibration environment in which the seat-occupant system must operate. Two different vibration spectra for seats 'A' and 'B' were derived from the field-measured data and synthesized in laboratory using the WBVVS and digital signal processing (DSP) software. Figures 2.16 and 2.17

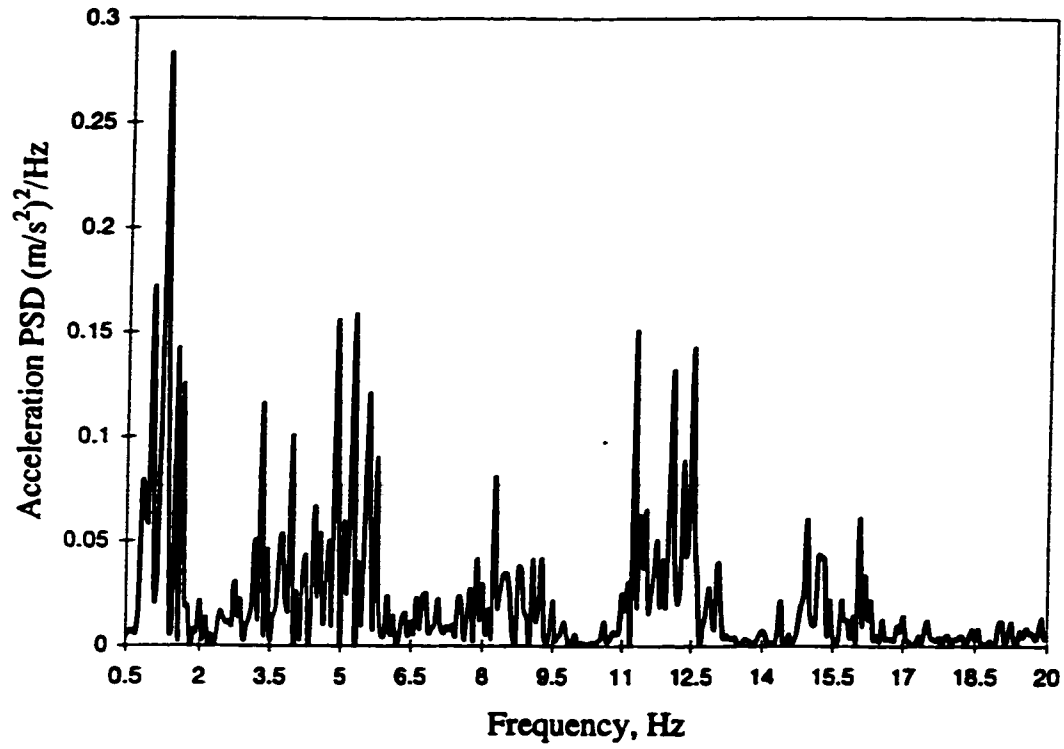

Figure 2.16: Synthesized Acceleration PSD Spectra for Seat 'A'.

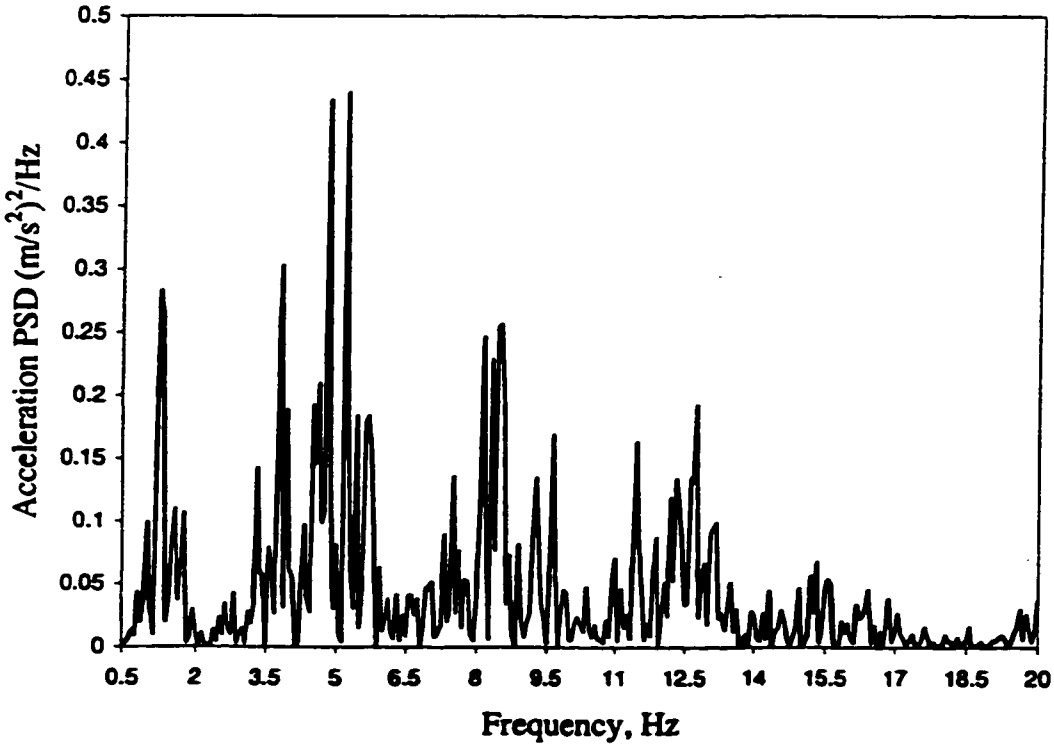

Figure 2.17: Synthesized Acceleration PSD Spectra for Seat 'B'.

present the acceleration PSD of the measured spectra. The spectra synthesized for seat 'A' reveals dominant vibration around 1.25, 5.0 and 12.5 Hz bands. The spectra for the seat 'B' reveals additional components dominant around 8.0 Hz.

To assess the relative vibration transmissibility of the seats under controlled excitations, a swept sinusoidal excitation spectra was also generated, using the DSP software. The excitation signal was synthesized to sweep in the 0.625 Hz to 10 Hz frequency range at a rate of 1 octave per minute. Based on WBVVS capabilities, the signal was synthesized to yield a constant 6.5 mm peak displacement in the 0.5 to 2 Hz range, followed by a constant peak acceleration of 0.1g (1 m/s^2) between 2 and 10 Hz. The various steps involved in the synthesis of the sweep signal consist of the transformation of acceleration sweep into a displacement sweep through double integration, filtering, scaling and concatenation of the samples.

2.5.4 Analysis of Measured Data

The acceleration response characteristics measured under harmonic excitations can be analyzed to yield the following:

(i) Frequency response characteristics of the candidate seats to establish their vibration isolation performance and the resonant frequency for the coupled seat-human system.

(ii) W_B-weighted and unweighted overall rms acceleration response to carry out relative performance evaluations.

(iii) S.E.A.T. based upon W_B-weighted and unweighted rms acceleration for relative performance evaluations.

The measured vibration excitation and response data under the synthesized field measured vibration are analyzed to determine the following:

(i) 1/3-octave band rms acceleration spectra to study the frequency contents of the weighted and unweighted vibration.

(ii) W_B-weighted and unweighted overall rms acceleration due to vibration excitation and response to estimate the VDV (Vibration Dose Value).

(iii) S.E.A.T. performance based upon W_B-weighted and unweighted VDV or the overall rms acceleration.

The S.E.A.T. of a seat is defined as the ratio of vibration dose value (VDV) or the overall weighted rms acceleration of vibration transmitted to the seat to that of the vibration encountered at the seat base, according to Equation (1.1), section 1.2.3. For discrete frequency bands the Equation (1.1) can be expressed in the following manner:

$$\text{S.E.A.T.} = \left[\frac{\sum_{j=1}^{n} \int_{f_l}^{f_u} G_{ss}(\bar{f}_j) W_b^2(\bar{f}_j) df}{\sum_{j=1}^{n} \int_{f_l}^{f_u} G_{ff}(\bar{f}_j) W_b^2(\bar{f}_j) df} \right]^{1/2} \tag{2.8}$$

where $\bar{f}_j$ is the center frequency of a selected band and n is the number of frequency bands. f_l and f_u are the respective lower and upper limits of the jth frequency band. $G_{ss}(\bar{f}_i)$ is auto spectral density of the acceleration measured at the human-seat interface. $G_{ff}(\bar{f}_i)$ is the auto spectral density of the base acceleration and df is the discrete frequency band. By definition:

$$\int_{f_l}^{f_u} G_{ss}(\bar{f}_j) df = a_s^2(\bar{f}_j) \quad \text{and} \quad \int_{f_l}^{f_u} G_{ff}(\bar{f}_j) df = a_f^2(\bar{f}_j) \tag{2.9}$$

where $a_s^2(\bar{f}_j)$ and $a_f^2(\bar{f}_j)$ are the mean squared accelerations of the seat and floor vibration, respectively, corresponding to the center frequency $\bar{f}_j$. Equation (2.8) can thus be simplified to:

$$\text{S.E.A.T.}=\left[\frac{\sum_{j=1}^{n} a_s^2(\bar{f}_j)W_b^2(\bar{f}_j)}{\sum_{j=1}^{n} a_f^2(\bar{f}_j)W_b^2(\bar{f}_j)}\right]^{1/2} \tag{2.10}$$

Since the weighting factors in most standards ISO-2631 (1985) [14], ISO-2631 (1994) [17] and BS6841 [16], are conveniently defined in the 1/3-octave frequency bands, the above estimation can be effectively used to derive S.E.A.T. values using 1/3-octave band rms acceleration. The S.E.A.T. values may be also derived based upon unweighted acceleration, as:

$$\text{S.E.A.T.}_{\text{unweighted}}=\left[\frac{\sum_{j=1}^{n} a_s^2(\bar{f}_j)}{\sum_{j=1}^{n} a_f^2(\bar{f}_j)}\right]^{1/2} \tag{2.11}$$

The synthesized vibration spectra for different seats, however, may exhibit significant differences in their magnitudes and frequency contents. The analysis of different seats may thus pose difficulties in assessing the performance characteristics in terms of their S.E.A.T. values, when different excitation spectra are employed. The relative performance characteristics of the seats are thus effectively analyzed under identical swept harmonic excitations in the 0.625-10 Hz frequency range. The measured response and excitation data are then analyzed to determine the acceleration transmissibility characteristics of the seats and to determine the range of variations attributable to the subject's weight. The acceleration transmissibility characteristics for seats 'A' and 'B' show considerable variations among the measurements performed with different subjects. Furthermore, an envelope of the vibration transmissibility and mean transmissibility curve is derived for each seat, as illustrated in Figures 2.18 and 2.19. The

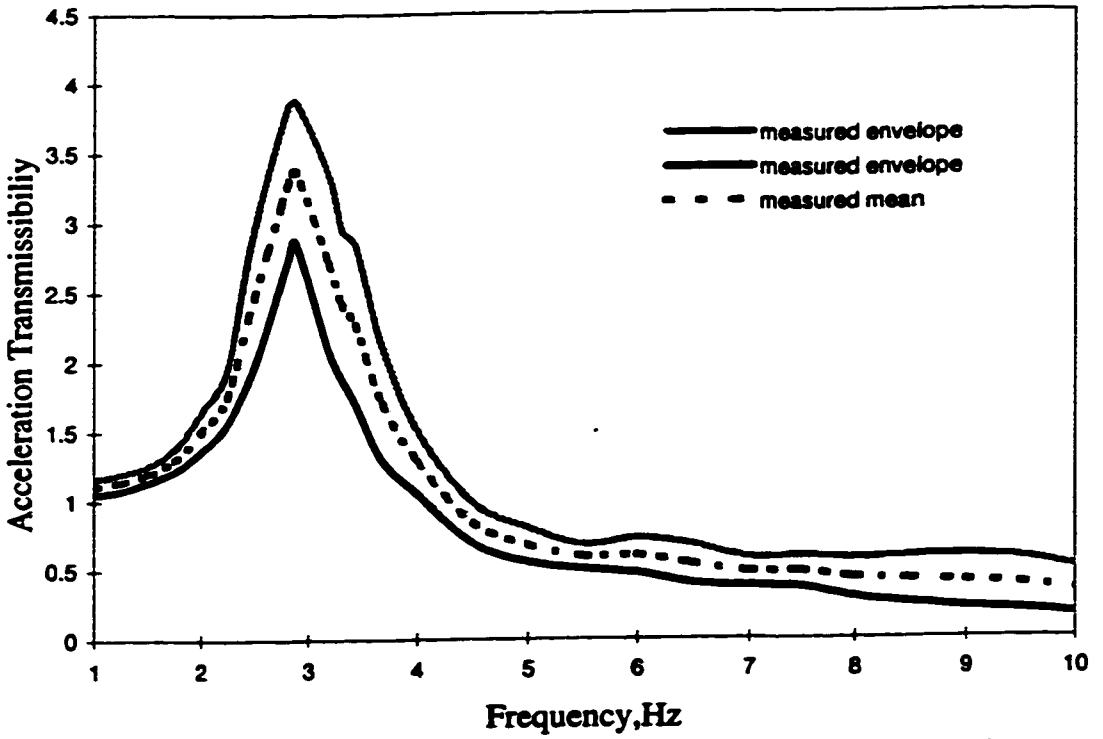

Figure 2.18: The Envelope and Mean of Measured Acceleration Transmissibility for Seat 'A'.

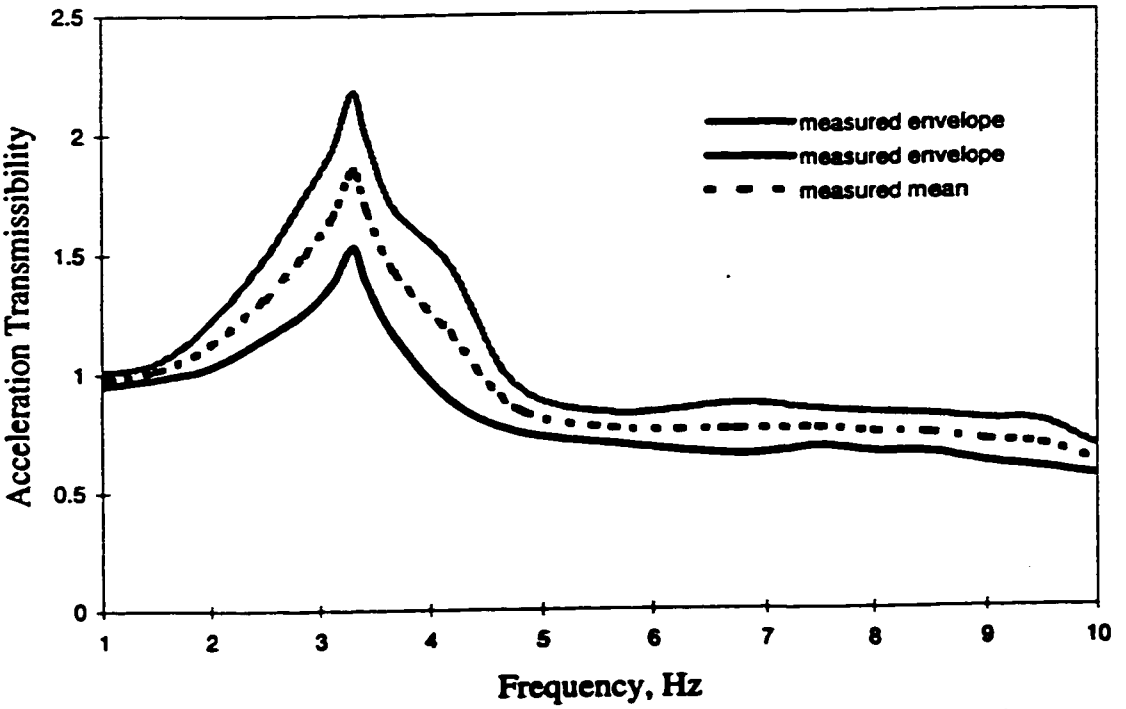

Figure 2.19: The Envelope and Mean of Measured Acceleration Transmissibility for seat 'B'.

mean transmissibility curve for seat 'A' reveals seat–subject system natural frequency near 2.9 Hz, with peak transmissibility of the order of 3.3. The mean curve for seat 'B' indicates a natural frequency near 3.3 Hz with peak transmissibility of 1.7. A comparison of Figures 2.18 and 2.19 clearly indicates relatively light damping and superior vibration isolation of the seat 'A', when compared with that obtained for the seat 'B'.

2.6 Analysis of Seat-Human Body Models

The vibration comfort performance of a seat-human system necessitates appropriate consideration of the human body frequency weighting filter proposed in different standards or guidelines [14,16,17]. The comfort performance of the seat is assessed in terms of frequency-weighted rms acceleration and/or the Seat Effective Amplitude Transmissibility (S.E.A.T.). The use of frequency-domain analysis technique is thus desirable to assess the seat-human system performance. This technique is specifically employed for determination of random response and parametric sensitivity analysis, where many repetitive simulations need to be performed. The frequency-domain analysis technique, however, can only be applied to either linear or linearized system models. The nonlinear stiffness and damping characteristics due to seats are thus expressed by their linear equivalents to derive linearized occupant-seat model.

2.6.1 Development of Linear Equivalent Seat-Human Body Models

While the biodynamic response characteristics of the seated human body can be derived using linear analytical models reported in the literature, the seat cushion exhibits nonlinear stiffness and damping characteristics. The measured force-deflection

characteristics, presented in section 2.4, clearly reveal that stiffness and damping characteristics are strongly dependent upon excitation frequency and amplitude. The resulting nonlinear properties of the seats are expressed by their linear equivalents in order to apply the weighting filter in the convenient frequency domain. The usual approach is to replace the nonlinear element by an equivalent linear element, such that the response behavior of the equivalent system does not deviate considerably from that of the nonlinear system. A number of such approximation techniques have been developed to analyze nonlinear systems [65,66]. The assumption of linear spring and damping elements, however, may be considered adequate only for system operating in linear range (small disturbance). The nonlinear seat-human body systems do not operate in the linear range and thus can not be accurately analyzed through such linear analytical tools.

Alternatively, nonlinear analytical tools such as equivalent linearization techniques have been widely used to determine the response of stochastically excited nonlinear dynamic systems. These techniques have been reviewed by various researchers [53,65,67,68] to date, with regard to their applicability to specific problems, computational efficiency and degree of accuracy to represent the dynamic quantities of interest. Equivalent linearization techniques invariably compute equivalent values of viscous damping and stiffness coefficients as functions of response characteristics and type of nonlinearity, such that the response behavior of the linear system does not deviate significantly from that of the original nonlinear system. The nonlinear spring and damping mechanisms are represented by an array of local equivalent coefficients, where each local constant is determined as a function of local excitation frequency, excitation amplitude and properties of the nonlinearity. Each local constant is considered valid in a

narrow frequency band centered around a selected (local) excitation frequency [53,67,68].

The local equivalent linearization technique, however, is based on the principle of energy similarity and can be developed only for nonlinear elements with well-defined force-displacement and force-velocity relations [21]. The experimentally established dynamic force-deflection characteristics of seats 'A' and 'B', presented in section 2.4.3, do not exhibit such well defined relations due to extreme dependency on frequency, magnitude of excitation and preload. Therefore a look up table is formulated for the dynamic stiffness and damping coefficients. These tables represent the cushion behavior in 0-10 Hz frequency range, 2.6-13 mm excitation amplitude and preload of 480 N (48.75 kg). The nonlinearities within the seat-human body models are thus expressed by an array of linear equivalent models as functions of discrete excitation frequency, excitation amplitude, response amplitude and the type of nonlinearity. Determination of local equivalent constants, however, requires prior knowledge of relative displacement response across the nonlinear elements corresponding to a selected excitation frequency. A local equivalent iterative algorithm is thus developed to compute the local coefficients for both deterministic and random excitations. The description and application of this algorithm are described in the following sections.

2.7 Verification of Analytical Models

The nonlinear and linearized analytical models of the driver-seat systems are solved for both sinusoidal and random excitations. The acceleration response at the driver-seat interface is analyzed to derive the acceleration transmissibility under

sinusoidal excitations and PSD of interface acceleration under random vibration. The response characteristics of the seats with a rigid representation of a driver, single-, two- and four-DOF human body models are compared with the mean measured response to verify the validity of the models. The relative performance characteristics of the models are further discussed in an attempt to identify a suitable human body model.

2.7.1 Response under Sinusoidal Excitations

The second order differential equations of motion for seat-human body models, developed in section 2.3, represent a seat model combined with four different representations of a driver: rigid mass, single-, two- and four-DOF human body models. The resulting nonlinear equations of motion can be expressed as follows:

Seat model with a rigid mass:

$$M\ddot{X}_1 + F_{CUSH} = 0 \tag{2.12}$$

Seat model with a single-DOF human body model:

$$\begin{aligned} &M_2\ddot{X}_2 + C_B(\dot{X}_2 - \dot{X}_1) + K_B(X_2 - X_1) = 0 \\ &M_1\ddot{X}_1 + C_B(\dot{X}_1 - \dot{X}_2) + K_B(X_1 - X_2) + F_{CUSH} = 0 \end{aligned} \tag{2.13}$$

Seat model with a two-DOF human body model:

$$\begin{aligned} &M_0\ddot{X}_0 + F_{CUSH} + K_1(X_0 - X_1) + C_1(\dot{X}_0 - \dot{X}_1) \\ &+ K_2(X_0 - X_2) + C_2(\dot{X}_0 - \dot{X}_2) = 0 \\ &M_1\ddot{X}_1 + K_1(X_1 - X_0) + C_1(\dot{X}_1 - \dot{X}_0) = 0 \\ &M_2\ddot{X}_2 + K_2(X_2 - X_0) + C_2(\dot{X}_2 - \dot{X}_0) = 0 \end{aligned} \tag{2.14}$$

Seat model with a four-DOF human body model:

$$
\begin{aligned}
&M_4\ddot{X}_4 + F_{CUSH} + K_3(X_4 - X_3) + C_3(\dot{X}_4 - \dot{X}_3) = 0 \\
&M_3\ddot{X}_3 + K_3(X_3 - X_4) + C_3(\dot{X}_3 - \dot{X}_4) + K_2(X_3 - X_2) + C_2(\dot{X}_3 - \dot{X}_2) = 0 \\
&M_2\ddot{X}_2 + K_2(X_2 - X_3) + C_2(\dot{X}_2 - \dot{X}_3) + K_1(X_2 - X_1) + C_1(\dot{X}_2 - \dot{X}_1) = 0 \\
&M_1\ddot{X}_1 + K_1(X_1 - X_2) + C_1(\dot{X}_1 - \dot{X}_2) = 0
\end{aligned}
\tag{2.15}
$$

where F_{CUSH} is the nonlinear dynamic force due to cushion, which can be expressed as:

$$F_{CUSH} = K_{EQ}Z + C_{EQ}\dot{Z} \tag{2.16}$$

where Z and $\dot{Z}$ represent relative displacement and velocity across the cushion, and K_{CUSH} and C_{CUSH} are equivalent linear stiffness and damping coefficients that depend on excitation amplitude, frequency of excitation and preload.

The linearized second order differential equations of motion (2.12–2.15) describing the dynamics of the seat-human body can be presented in the following form:

$$[M]\{\ddot{Z}\} + [C(\omega, z)]\{\dot{Z}\} + [K(\omega, z)]\{Z\} = -[M]\{\ddot{X}_i\} \tag{2.17}$$

where $\{Z\}$ is the (n x 1) vector containing relative displacements

$Z_1 = X_1 - X_i$; and

$$Z_k = X_k - X_{k-1} \text{ for } k = 2, \ldots n \tag{2.18}$$

and $[M]$, $[K]$, $[C]$ are $(n \times n)$ mass, stiffness and damping matrices for the corresponding model. The order n is dependent upon the number of DOF for seat-occupant model, n = 2, 3 and 5 for single, two- and four-DOF occupant model. The matrices $[K]$ and $[C]$ contain values of local equivalent linear stiffness and damping constants due to nonlinear force-deflection and force-velocity properties of the cushion.

At each specified excitation frequency, the dynamic force due to the cushion can be expressed as:

$$F_{CUSH}(Z_1,\dot{Z}_1) = K_{EQ}(X_1 - X) + C_{EQ}(\dot{X}_1 - \dot{X}_i) \qquad (2.19)$$

where K_{EQ} and C_{EQ} are local constants which are considered valid for certain narrow frequency band centered around the local excitation frequency, specified range of excitation amplitude and preload. An iterative algorithm is developed to compute the local coefficients under sinusoidal excitations. This algorithm is summarized as follows:

- The equivalent viscous damping and equivalent stiffness coefficients of the cushion $C_{EQ}(\omega,Z_1)$ and $K_{EQ}(\omega,Z_1)$ are initially assumed as $C^0{}_{EQ}$ and $K^0{}_{EQ}$ at a discrete excitation frequency ω.
- The linearized equations of motion are then formulated and solved to determine relative displacement response vector [Z] corresponding to the selected frequency ω, such that:

$$[Z(j\omega)] = \left[[K(\omega,z)] - \omega^2[M] + j\omega[C(\omega,\dot{z}]\right]^{-1}[M]\{\ddot{X}_i(j\omega)\} \qquad (2.20)$$

- The equivalent viscous damping, C_{EQ}, and stiffness, K_{EQ}, coefficients corresponding to the computed value of $Z_1(w)$ are then determined from the look up tables, formulated in section 2.4.3. The magnitudes of errors between the assumed and computed values of the coefficients are then evaluated as:

$$\varepsilon_K = \left|K_{EQ} - K_{EQ}{}^0\right|$$
$$\varepsilon_C = \left|C_{EQ} - C_{EQ}{}^0\right| \qquad (2.21)$$

If the maximum of ε_K or ε_C exceeds a specified tolerance, the assumed values of local coefficients are updated and the iterative procedure is repeated until convergence is achieved.

The coupled differential equations of motion for the nonlinear seat-human body systems are solved in the time domain using the fourth-order Runge-Kutta method. Under sinusoidal excitations, the equations are solved at selected discrete frequencies of excitation to evaluate the seat-to-base transmissibility in the 1-10 Hz frequency range. The analytical acceleration transmissibilities are then compared with those obtained from the laboratory measurements in order to validate the analytical model. Since measured acceleration transmissibility characteristics of the seats 'A' and 'B' show considerable variations for different human subjects belonging to 50th percentile male category, the model response characteristics are compared with the envelope and mean of the measured acceleration transmissibility.

SEAT 'A'.

The verification is initially performed for a seat 'A' loaded with a rigid mass to establish the validity of a seat model. The nonlinear differential equation (2.12) is solved for sinusoidal excitations in the frequency range of 1-10 Hz, using numerical integration. The iterative algorithm is used to compute the local stiffness and damping coefficients for seat cushion under different excitation frequencies. Figure 2.20 presents a comparison of the analytical and experimental vibration transmission characteristics of seat 'A' loaded with a rigid mass. The analytical vibration transmissibility characteristics are in good agreement with those established via laboratory experiments only in 1-5 Hz frequency range. The considerable discrepancies exist at frequencies above 5 Hz, which can be

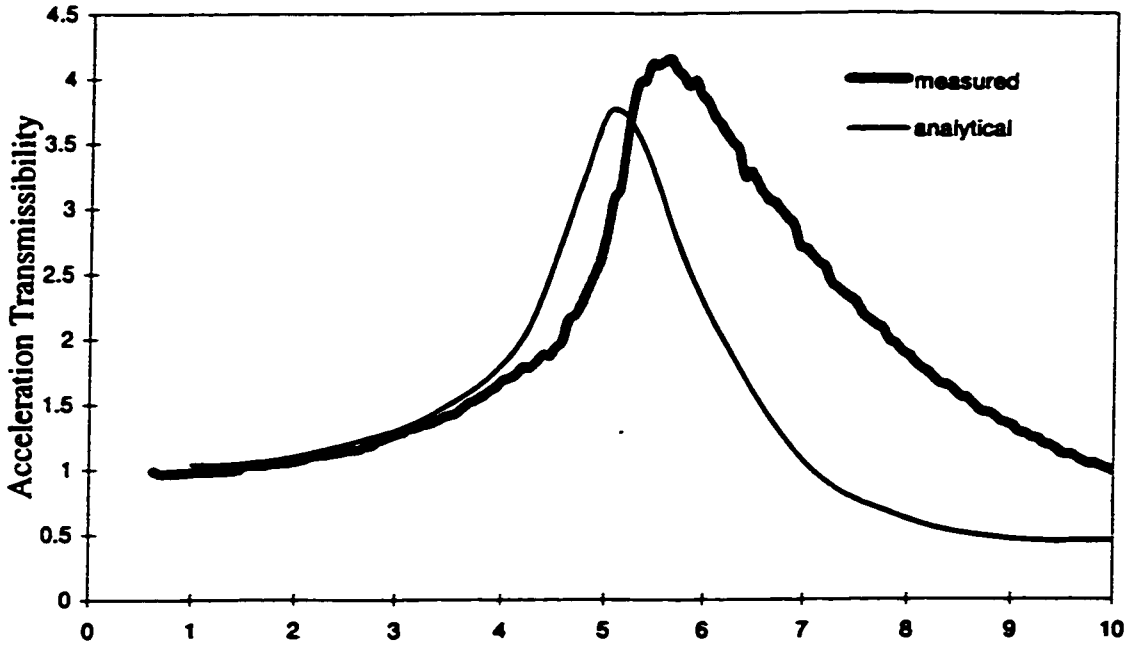

Figure 2.20: A Comparison of Analytical and Measured Vibration Transmission Characteristics for Seat 'A' Loaded with Rigid Mass.

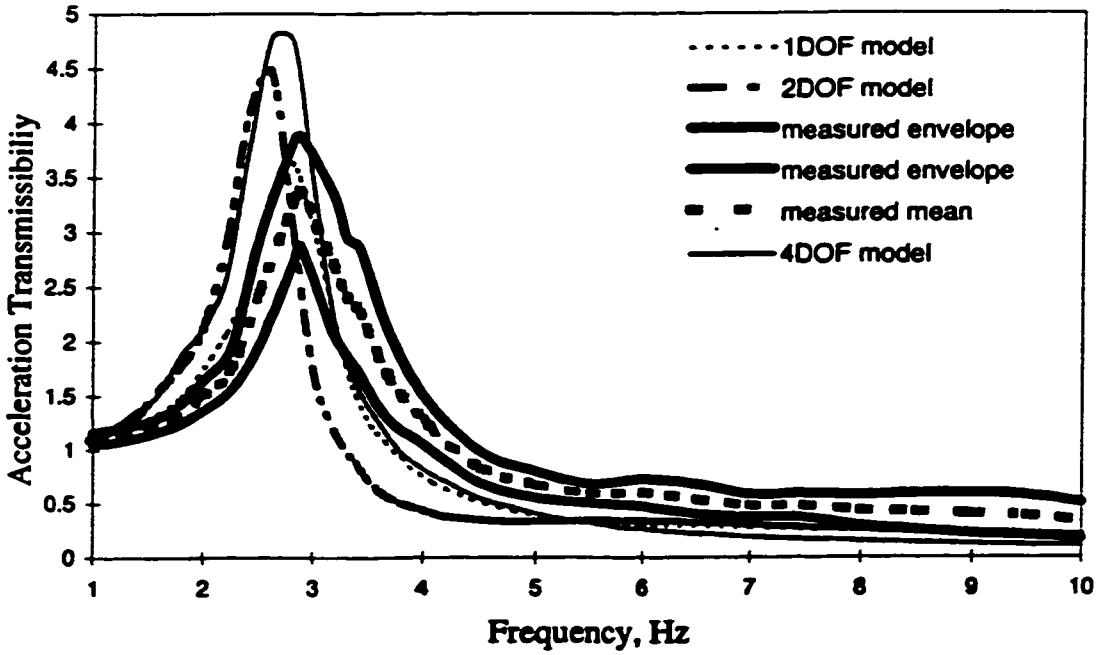

Figure 2.21: Comparison of Measured and Simulated Acceleration Transmissibility Characteristics for Seat 'A Loaded with Human Subjects.

attributed to significant hopping effect of the rigid mass, which was observed under resonant and higher excitation frequencies.

The acceleration transmissibility characteristics of seat 'A' employing three different human body models are illustrated in Figure 2.21, together with mean and envelope curves of the measured data. The analytical response clearly reveals the significant influence of the human body model. The mean acceleration transmissibility obtained from the experimental data reveal peak transmissibility in the order of 3.3 near 2.9 Hz. The envelope curves show considerable variations in the peak transmissibility ranging from 2.7 to 3.9.

The single-DOF model, proposed by Griffin [39] yields relatively good agreement between the measured and computed acceleration transmissibility. In the 1-3.3 Hz frequency range, the analytical response curve for the single-DOF human body model lies within the envelope formed by the measured data, although its resonant frequency is observed to be slightly lower (~2.7 Hz). The peak acceleration transmissibility is in the order of 3.6, which is slightly higher than the mean of measured values. At excitation frequencies higher than 3.3 Hz, the single-DOF model underestimates the measured transmissibility by as much as 50%.

The response characteristics of the seat-occupant model employing two- and four-DOF human body models result in transmissibility curves which differ considerably from the measured response in the entire frequency range. At lower excitation frequencies (~1-3 Hz), both models grossly overestimate the acceleration transmissibility, while the peak transmissibility at resonant frequency approach values of 4.6 and 4.9, respectively, for the two- and four-DOF models. In the 5-10 Hz frequency range, however, all three models

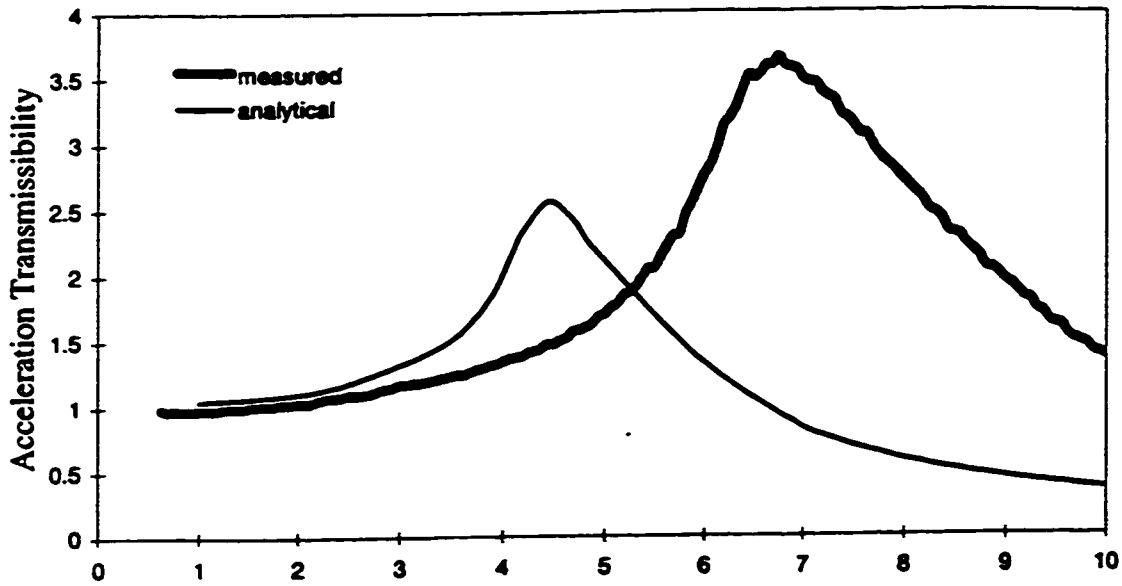

Figure 2.22: A Comparison of Analytical and Measured Vibration Transmission Characteristics for Seat 'B' Loaded with a Rigid Mass.

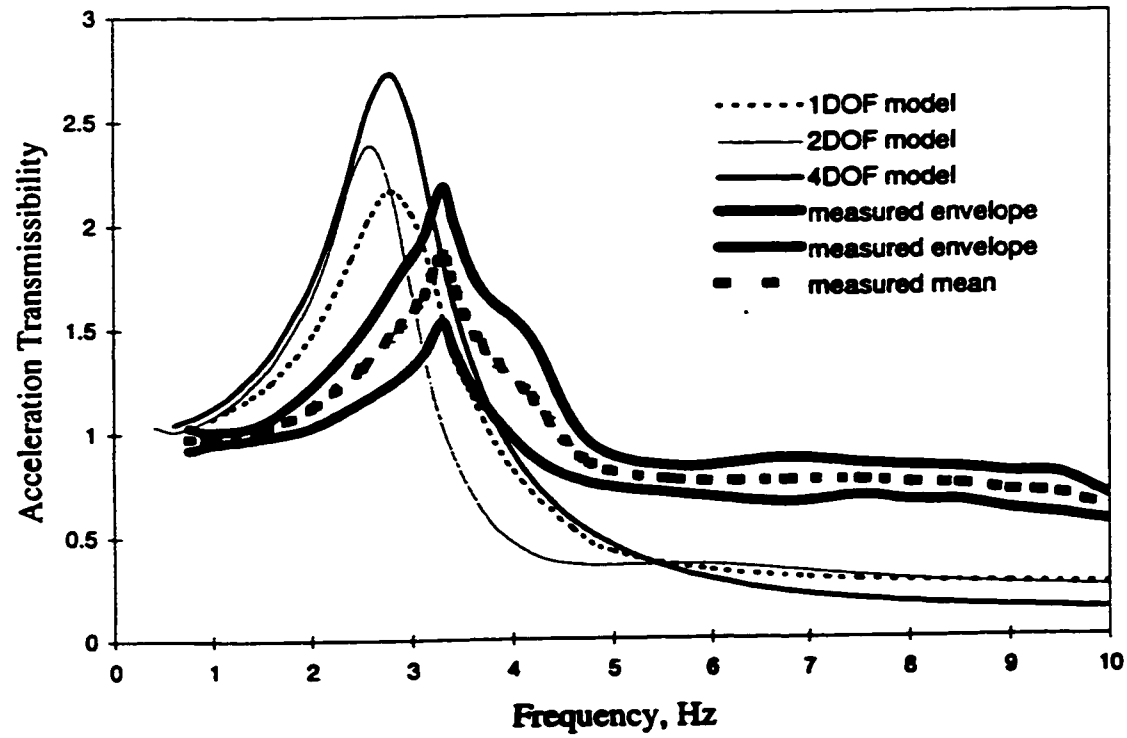

Figure 2.23: Comparison of Measured and Simulated Acceleration Transmissibility Characteristics for Seat 'B' Loaded with Human Subjects.

exhibit the same behavior, underestimating the measured response by approximately 50%.

SEAT 'B'.

Equation (2.12) was used to derive the analytical acceleration transmissibility characteristics for seat 'B' loaded with a rigid mass representation of a driver. Figure 2.22 presents a comparison of the analytical and experimental vibration transmission characteristics of seat 'B' loaded with a rigid mass. The analytical response correlates with measured data only in the 1-3 Hz frequency range. The significant discrepancies at higher frequencies are attributed to the inability of the analytical model to simulate the hopping motion of the rigid mass, which was observed to be considerable during the tests.

Figure 2.23 presents a comparison of the analytical and experimental vibration transmissibility characteristics for seat 'B' employing three different occupant models. It should be noted that the acceleration response characteristics of seat 'B' differ significantly from that of seat 'A'. The mean transmissibility curve for seat 'B' reveals considerably lower peak value of 1.75 corresponding to a resonant frequency of 3.3 Hz. The resonant frequency of seat 'B' tends to be larger than that of seat 'A' (2.9 Hz), due to its relatively higher stiffness. The high equivalent damping of seat 'B' yields considerably lower peak transmissibility than that of seat 'A' (3.3). The acceleration transmissibility at higher excitation frequencies, however, is larger than that of seat 'A', which is attributed to higher damping properties of the seat 'B' cushion.

From Figures 2.21 and 2.23, it is apparent that the higher order models yield poor correlation with the measured data. While the single-DOF human body model may be

considered appropriate for estimating the response behavior of seat 'A', it yields poor correlation with the measured data for seat 'B'. It can thus be concluded that biodynamic behavior of the occupant is strongly dependent upon the visco-elastic properties of the seat. The model derived from the apparent mass or seat-to-head acceleration transmissibility measured for the subjects seated on a rigid seat cannot be generally applied to elastic seats. The envelope curves derived from the measured data for seat 'B' also show relatively less variations between the maximum and minimum limits in comparison with seat 'A', the peak variation in the acceleration transmissibilities is approximately 0.7. The result further show that acceleration transmissibility characteristics differ considerably from the measured data, irrespective of the occupant model employed. All the three occupant models yield considerably lower resonant frequency and higher resonant values, while the acceleration transmissibility at higher frequencies is considerably lower than the measured values. From the results, it may be concluded that all the three occupant models, considered in this study, are inappropriate for estimating the response behavior of seat 'B'.

2.7.2 Verification of a Linearized Model under Harmonic Excitations

Since the frequency contents of the ride vibration are often of greater interest than the time history, the frequency-domain methods have long been used to analyze linear systems. In the frequency-domain analysis the time dependent variables are Fourier transformed to frequency dependent variables. The linear or linearized equations of motion for the seat-human body models, in general, can be expressed in the matrix form:

$$[M]\{\ddot{X}\}+[C]\{\dot{X}\}+[K]\{X\}=[K_F]\{X_i\}+[C_F]\{\dot{X}_i\} \qquad (2.22)$$

where [M], [K], [C] are (n x n) mass, stiffness and damping matrices, respectively. $[K_F]$ and $[C_F]$ are (n x n) forcing damping and stiffness matrices. $\{X\}$ and X_i are (n x 1) vectors containing excitation and response variables. Equation (2.22) is Fourier transformed to yield:

$$\{X(j\omega\}=[H(j\omega]\{X_i(j\omega)\} \tag{2.23}$$

where $[H(j\omega)]$ is the complex matrix representing the frequency response function to the seat-human body model, given by:

$$[H(j\omega)]=\left[-\omega^2[M]+j\omega[C]+[K]\right]^{-1}[[K_F]+j\omega[C_F]] \tag{2.24}$$

Linear analytical models of dynamic systems are conveniently expressed by their frequency response function in order to carry out random response analysis. Nonlinear analytical models of dynamic systems, however, are described by the frequency response functions of their linear equivalent models such that convenient linear analytical tools may be applied to evaluate their response. Discrete harmonic linearization technique can be applied to express the nonlinear model by an array of local equivalent linear models, where each linear model describes the nonlinear model's behavior in the vicinity of a discrete frequency [53, 68]. Complex frequency response of the local equivalent model can thus be generated to be used as the transfer function operating on the random excitations. Determination of local equivalent constants, however, requires prior knowledge of relative displacement response across the nonlinear elements corresponding to a selected excitation frequency (as discussed in section 2.6.1). Since the relative displacement response is dependent upon the excitation amplitude, the random excitation at a seat base is represented by an equivalent deterministic excitation to estimate the excitation amplitude. The iterative algorithm, presented in section 2.7.1 is

then used to compute the relative displacement response and thus the local equivalent coefficients.

The nonlinear seat-human body models for seats 'A' and 'B' are locally linearized using the linearization technique described in section 2.6.1 and the response characteristics are evaluated for sinusoidal base excitations. The response characteristics of the linearized seat-driver models are presented in terms of acceleration transmissibilities and compared with those established via numerical integration. The seat-human body models with only single-DOF representation of the driver are analyzed using the model parameters, derived from static and dynamic tests performed in the laboratory. Figures 2.24 and 2.25 illustrate a comparison of acceleration transmissibility characteristics of the locally linearized seat-single-DOF human body models for seats 'A' and 'B' with those of the nonlinear suspension models. These figures clearly demonstrate the effectiveness of local equivalent linearization technique for constant amplitude harmonic excitations. The comparison reveals errors of small magnitudes only at higher excitation frequencies.

2.7.3. Random Response

The iterative methodology, which is described in a previous section, initially assumes the values of local equivalent constants to formulate an initial linear model at a pre-selected excitation frequency. The random vibration spectrum at the seat base is descretized to yield the excitation amplitude corresponding to the selected excitation frequency. An excitation amplitude vector is estimated from the power spectral density of the vibration at the seat base, in the following manner:

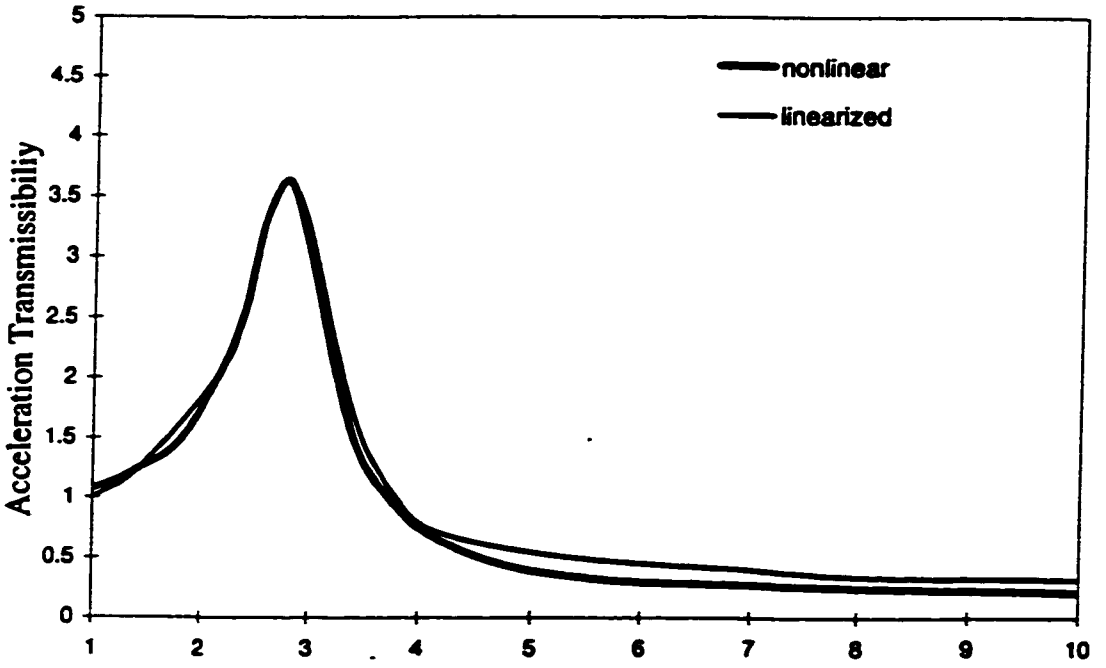

Figure 2.24: Comparison of Response Characteristics fo Linearized Model with those of the Nonlinear Model for Seat 'A'.

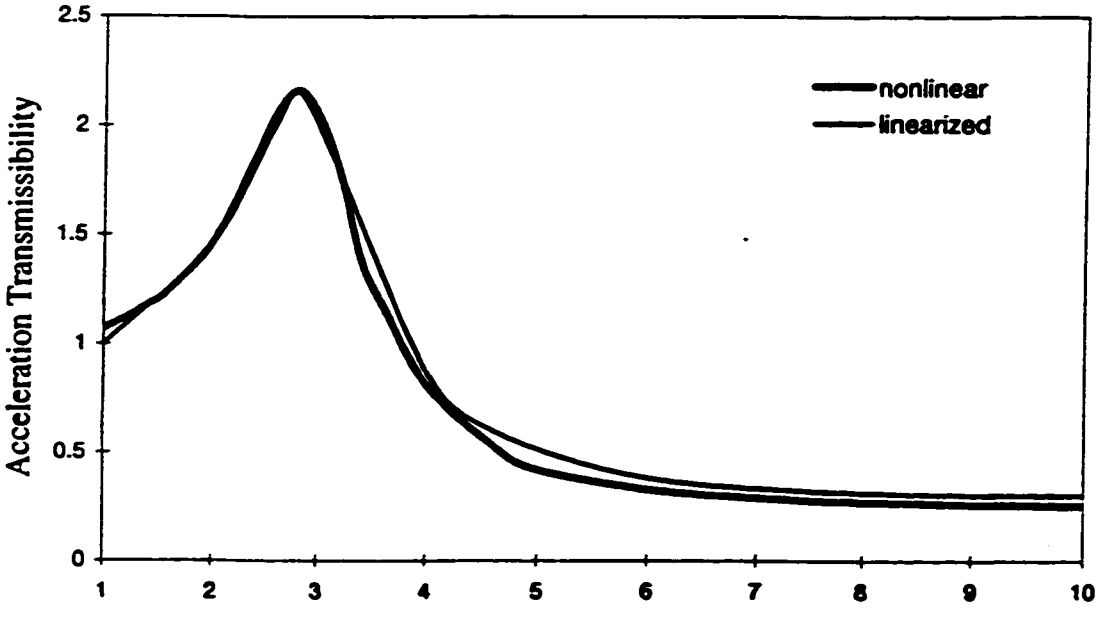

Figure 2.25: Comparison of Response Characteristics of Linearized Model with those of the Nonlinear Model for Seat 'B'.

$$\ddot{X}_i(\omega) = \alpha \left[\int_{\omega-\Delta\omega/2}^{\omega+\Delta\omega/2} S_I(\omega) d\omega \right]^{1/2} \tag{2.25}$$

where $\ddot{X}_i(\omega)$ is the amplitude of acceleration excitation corresponding to discrete excitation frequency ω , $S_I(\omega)$ is the PSD of acceleration at the seat base, $\Delta\omega$ is a small frequency band around the center frequency ω, and $\alpha = \sqrt{2}$ is a constant. A displacement time history can thus be synthesized then using sine series approximation:

$$X_{input}(t) = \sum_{D=1}^{N} X(\omega) \sin(\omega t + \phi) \tag{2.26}$$

where N is total number of discretized excitation frequencies considered, ϕ is the randomly distributed phase angle and $X_i(w)$ is the displacement amplitude corresponding to a selected excitation frequency w. The linear system of equations is then solved to compute the relative displacement response using the estimated excitation amplitude, $X(\omega)$. The iterative algorithm, developed in section 2.7.1, is then used to determine the local equivalent damping and stiffness constants corresponding to discrete excitation frequency , ω, using the look-up tables. The spectral density of response acceleration is then computed in the following manner:

$$S_0(\omega) = \left| H(\omega, X_i(\omega)) \right|^2 S_I(\omega) \tag{2.27}$$

where $H(\omega, X_i(\omega))$ is the complex frequency response function corresponding to discrete excitation frequency ω and amplitude excitation $X(\omega)$; $S_0(\omega)$ is the response acceleration PSD and $S_I(\omega_D)$ is the input acceleration PSD (at the seat base).

Random response characteristics of different seat-human body models are evaluated using Equation 2.27 in conjunction with local equivalent linearization

algorithm described in section 2.7.1. The description of the input random excitations is given in section 2.5.3. The vibration response characteristics of seat-human body models for seats 'A' and 'B' are compared with those derived from the laboratory tests performed using the WBVVS, in order to demonstrate the validity of different analytical models.

SEAT 'A'.

Figure 2.26 presents the comparison of PSD of acceleration response of the seat 'A' coupled with three different occupant models with the mean measured response under identical random excitations. The response acceleration PSD derived using the single-, two-, and four-DOF human body models are observed to be considerably different. In low frequency range (1-2 Hz), all the three models demonstrate good agreement with the measured response, while the single-DOF model yields excellent correlation with the measured data in this frequency range, the two- and four-DOF models exhibit only small discrepancies. The excellent correlation in this low frequency range can be mostly attributed to negligible contributions of the human body dynamics at lower frequencies. It has been reported that seated human subjects behave similar to a rigid mass at excitation frequencies below 2 Hz [3]. In the 2-5 Hz frequency range, the single-DOF model demonstrates the best performance among all the three models considered, although none of them yields reasonable correlation with the measured response in the vacinity of the resonant frequency of the seat-human body system (around 3 Hz) and in 3.5-4 Hz band. In above mentioned frequency bands, all the occupants models yield extremely poor correlation with the measured response. The relative response characteristics of the occupant models are similar to those observed under

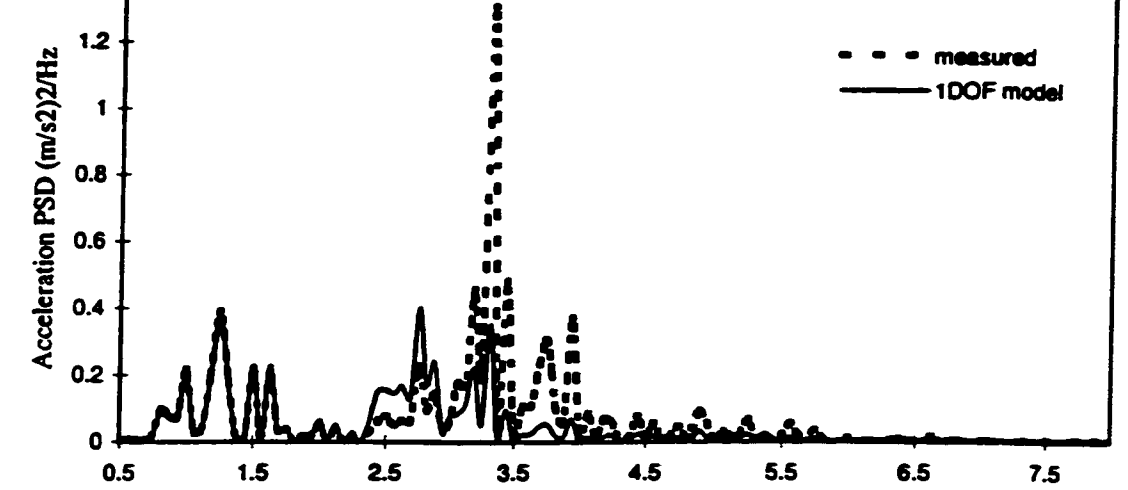

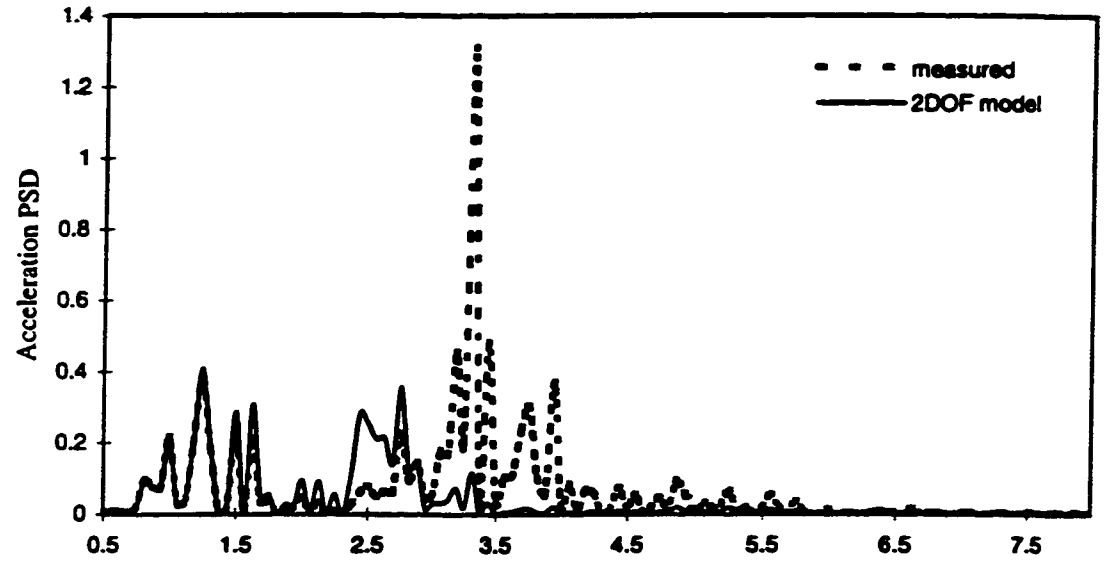

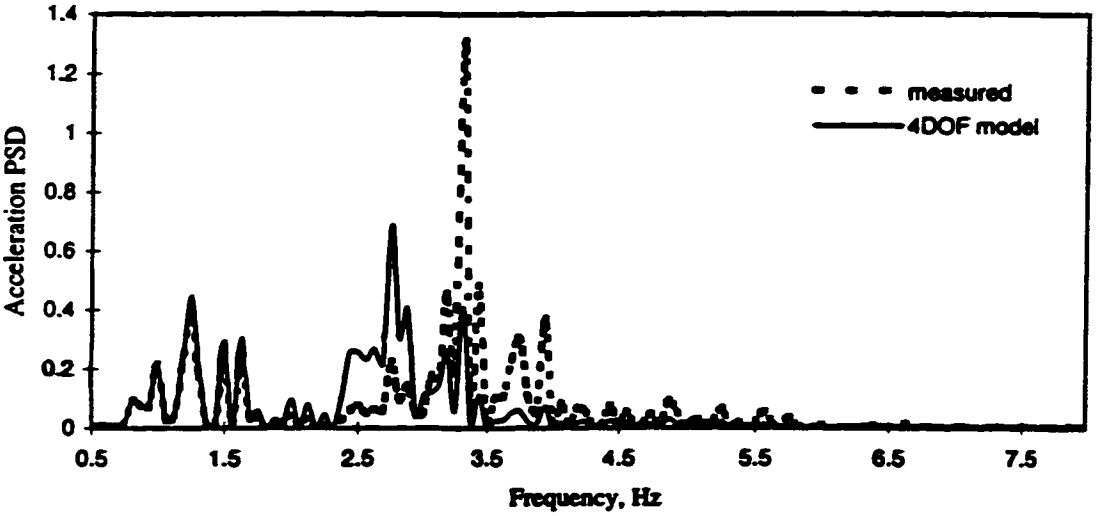

Figure 2.26: Comparison of Mean Measured and Computed Seat-Human Body System Response under Random Excitations for Seat 'A'.

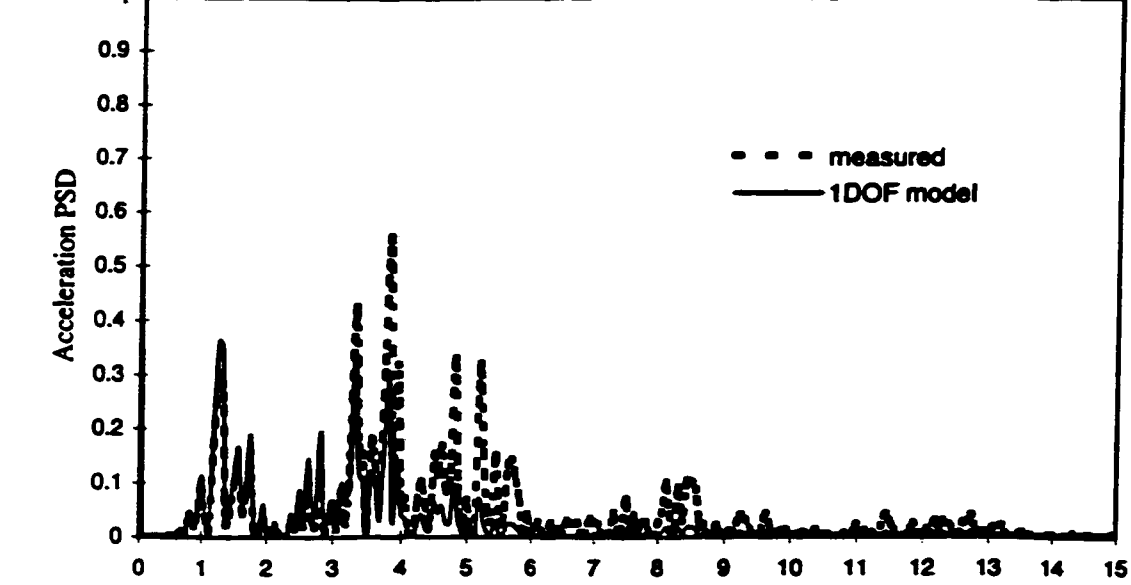

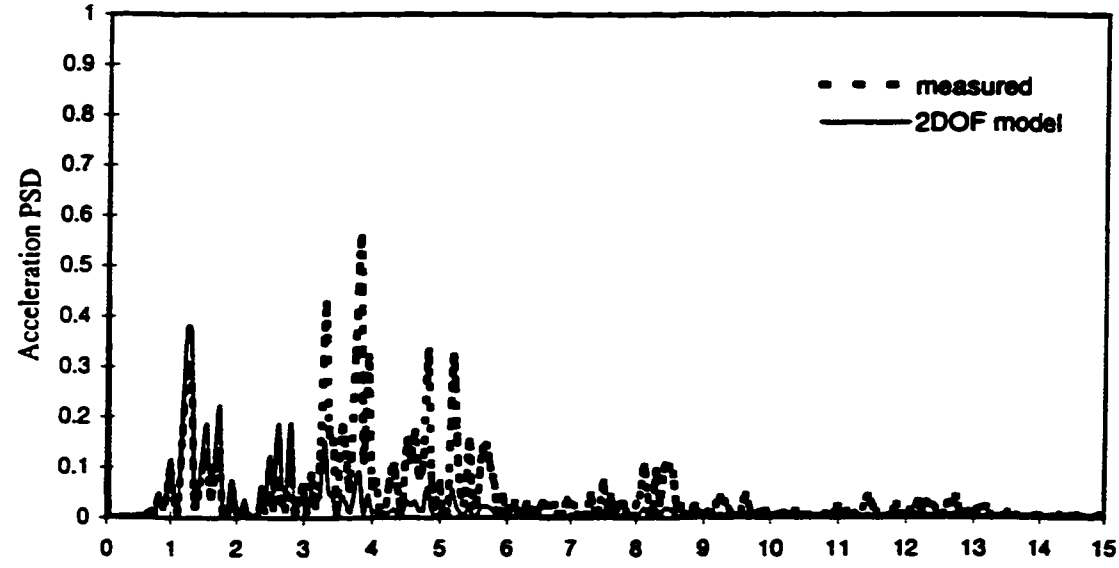

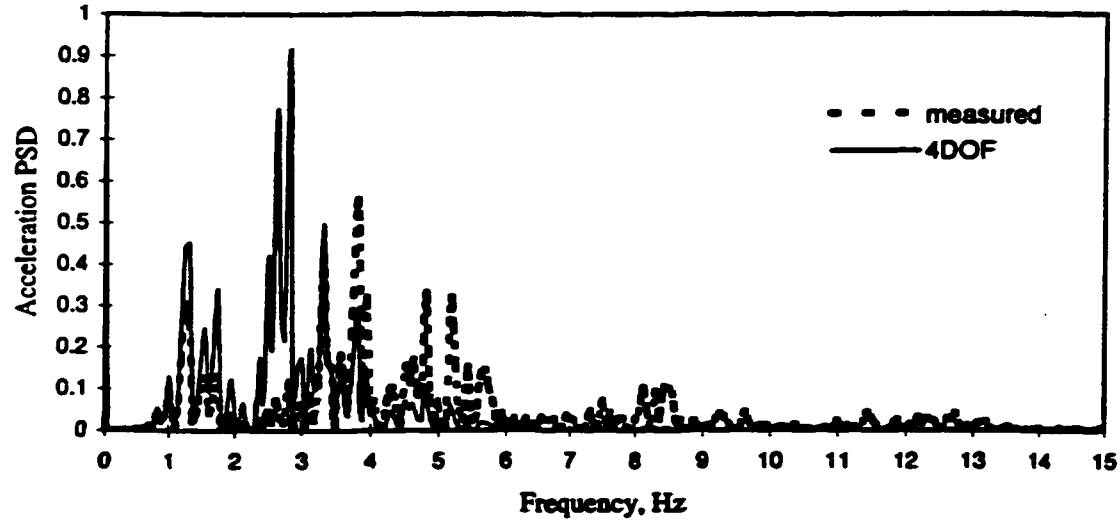

Figure 2.27: Comparison of Mean Measured and Computed Seat-Human Body System Response under Random Excitations for Seat 'B'.

sinusoidal excitations. The single-DOF model, which resulted in reasonable correlation with the measured data under sinusoidal excitations, also yields poor resonant behavior under random excitations.

SEAT 'B'.

Figure 2.27 presents a comparison of measured and analytical acceleration PSD response of seat 'B' employing the three human body models under random excitations. While the response characteristics of the seat with three different occupant models are considerably different, the single-DOF model yields reasonable correlation with the mean measured response. A comparison of the resonance behavior under sinusoidal and random excitations further dictates that the effectiveness of the occupant model is not only dependent upon the properties of the seat, but also on the nature of vibration excitations. The single-DOF model resulted in acceptable correlation for seat 'A' with the measured data under sinusoidal excitations, but somewhat poor agreement under random excitations. The seat 'B' coupled with the single-DOF occupant model revealed poor correlation with the measured data under sinusoidal excitations, but reasonably good agreement under random excitations. These findings clearly emphasize the complexities associated with the biodynamic representation of the seated occupant coupled with static seats, which are known to exhibit considerable variations in their visco-elastic properties.

2.8 Selection of an Appropriate Human Body Model

In previous section, the ride response characteristics of different seat-occupant systems incorporating single-, two- and four-DOF human body models are evaluated to

illustrate the influence of human body dynamics on the total ride performance. Following observations may be deduced from the results presented in Figures 2.21 to 2.27:

- All the three human body models employed in this study, in general, provide a very conservative estimate of the ride response for both seats.
- The two- and four-DOF occupant models yield considerably higher resonant transmissibility, and lower resonant frequencies.
- Under deterministic excitations the acceleration response derived using single-DOF human body model is in close agreement with measured data only for seat 'A'. For seat 'B' the model incorporating single-DOF human yields poor correlation with the measured response. The two- and four-DOF human body models exhibit extremely unsatisfactory results and thus cannot be considered for the purpose of simulating the seat-occupant system. It can thus be noted that with the increasing complexity in human body models, the differences between computed and measured data become more pronounced.
- Under random excitations, a relatively good agreement between measured and computed response is observed only when single-DOF human body model is employed. The resulting seat-human body model, however, grossly underestimates the measured response in vicinity of the resonant frequency (~3 Hz) of seat 'A'. The system models incorporating two- and four-DOF human body models result in considerable errors between the measured and computed response.

In view of the above observations, it can be concluded that among the three human body models selected for the study, the single-DOF model can be considered as the most appropriate one for assessment of the seat-occupant system subject to different types of excitations. Considerable magnitudes of errors in the vicinity of the resonant frequency and at higher excitation frequencies, however, can be expected.

2.9 Summary

In this chapter, the seat-occupant system is analytically modeled by incorporating three different human body models to the seat model. The laboratory methods and results of identifying the static and dynamic properties of seats cushion are described. The test

apparatus and methodology for experimental characterization of human-seat system are also presented. A local equivalent linearization algorithm is employed to express nonlinear stiffness and damping properties of seat cushion by an array of local equivalent spring and damping constants. The response characteristics of selected seat-human body models are discussed under different types of excitations in order to assess the relative performance of the human body models and the most appropriate human body model is selected. It is concluded that the proposed occupant models yield considerable errors in the estimated response. An alternate methodology to assess the vibration comfort performance of the static seat coupled with the occupant is thus proposed in the following chapter.

CHAPTER 3
ESTIMATION OF VIBRATION TRANSMISSION CHARACTERISTICS OF STATIC SEATS

3.1 General

The vibration transmitted to the occupant through the seat forms an important factor related to the overall perception of the comfort of the automotive seats. The assessment of vibration transmission performance of the seat under representative excitations arising from the tire-road interactions is thus highly vital to achieve the design objective of enhancing the occupant comfort. The comfort characteristics of automotive seats are frequently assessed through objective ride performance tests. Such objective tests provide important quantitative information related to design, seat-human interactions, the role of body weight and size, the role of back-rest and foot-support position, etc. The objective assessments may be performed either in the field or in the laboratory under representative road conditions.

A relative assessment of vibration performance of automotive seats can be effectively carried out in the laboratory by loading the seat with a rigid load or a dummy. The dummy in such tests needs to be designed without the legs, since the relative displacement of the seat with respect to the base can cause repetitive impacts of the dummy's feet against the floor. Such an approach, however, does not provide an assessment of the seat-human interactions. It has been well established that the occupant dynamics contributes considerably to the overall comfort performance of the seat [21,22,26]. While the contributions of the human occupant dynamics to the performance of low frequency suspension seats are known to be relatively small [69], the human body dynamics affects the performance of relatively high frequency automotive seats

considerably [23]. The probable variations in the response characteristics of the seat with human subject and a passive load, thus, need to be established to study the overall performance of the seat. These variations can be further utilized to construct an adequate dummy for assessing the vibration isolation of the seats. The objective assessment methods based upon the use of a test dummy offer considerable advantages over use of human subjects, namely:

(i) The potential safety risks to human subjects caused by exposure to vibration can be eliminated.

(ii) The ethical concerns and potential liability arising from vibration testing of human subjects can be avoided.

(iii) The need to perform the repetitive measurements with a large number of subjects can be eliminated.

(iv) The repeatability of measurements performed with dummy can be enhanced, which is not affected by variability of the human subjects.

(v) The relative ride and comfort performance of various seats can be carried out in a highly efficient cost-effective manner using an adequate dummy.

A test dummy for such vibration tests may be designed using various human body models, presented in section 1.4. Majority of the proposed models, however, have been derived from the seat-to-head vibration transmissibility and/or driving-point mechanical impedance characteristics measured under excitations and conditions, which are not at all representative of automobile driving. The validity of these models for applications in automotive environment is thus questionable. Furthermore, the biodynamic response characteristics reported in terms of seat-to-head transmissibility or apparent mass or driving point mechanical impedance are known to vary with many factors, such as frequency and magnitude of excitation, human sensitivity to vibration, body weight,

posture, hands and feet position, and height [20,70,39]. The dependency of hysteresis and the natural frequency of the polymer foam seats on the preload, amplitude and frequency of excitation further contribute to the formidable task of deriving a satisfactory model for the design of the dummy.

Although adequately designed passive loads may provide an effective and reliable method to carry out relative performance characteristics of the seats, the dynamic contributions due to visco-elastic properties of the human body cannot be incorporated. The influence of human body dynamics on the vibration attenuation performance of a seat under sinusoidal excitations can be demonstrated by comparing the measured response characteristics of the seat-human system with those obtained using a rigid load. The measurements were performed with seat 'A' using the WBVVS driven by the synthesized sinusoidal signal defined in section 2.5.3. The tests were performed with a seated subject, feet resting flat on the WBVVS platform and hands in contact with steering wheel. The test data was acquired with subject #2, identified in Table 2.2, with mass supported by the seat equal to 63 kg, which is slightly lower than the mass of 63.6 kg used as a rigid load. Fig 3.1 illustrates a comparison of the vertical seat acceleration transmissibility characteristics measured under sinusoidal excitations with a rigid mass and with a human subject. The human body response differs considerably from that of the rigid mass both in resonant frequency and resonant amplitude. However, as it was indicated above, the assessment methods using human subjects pose many ethical and safety risks. Alternatively, the assessment methods based upon the passive load offer considerable advantages in eliminating the ethical concerns, safety risks and the need to perform repetitive measurements with human subjects.

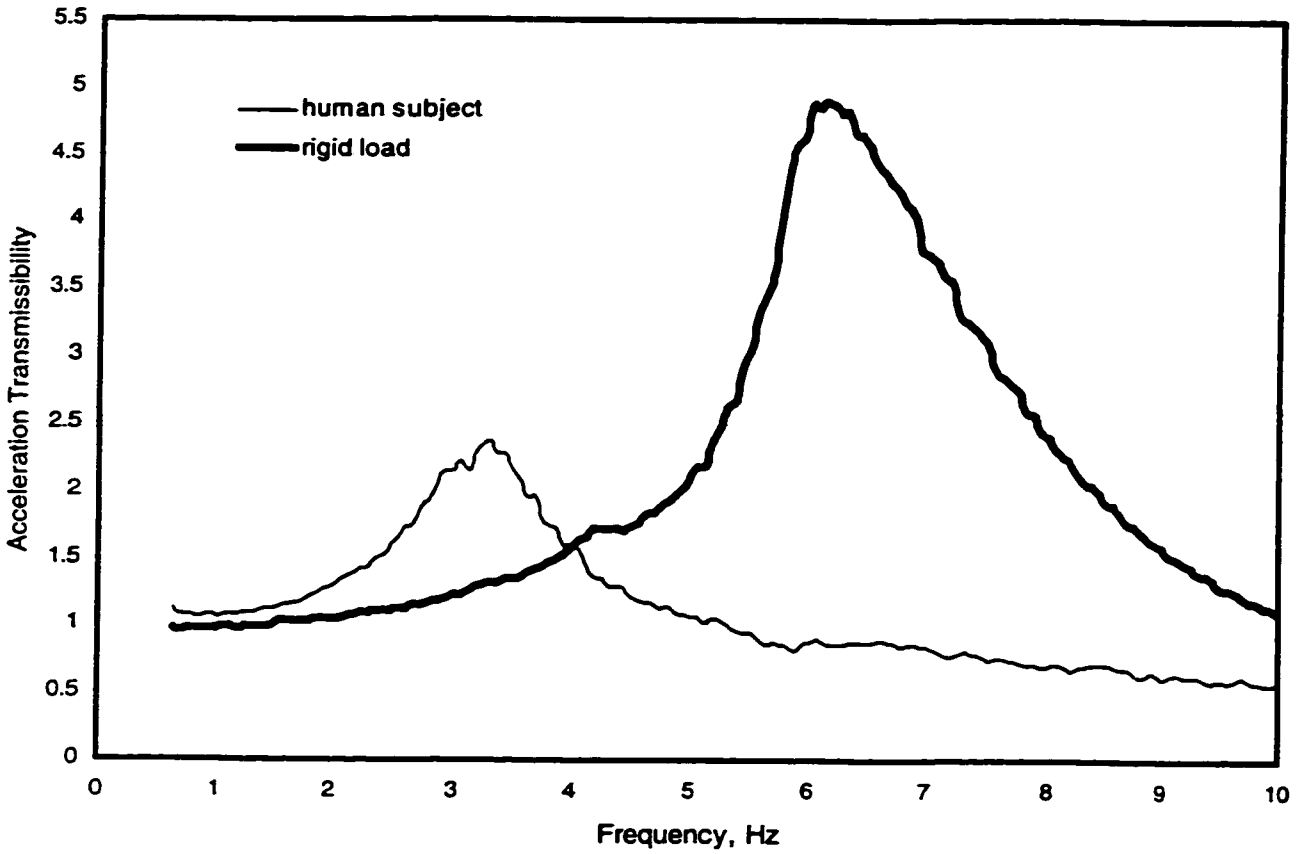

Figure 3.1: Comparison of Acceleration Transmissibility of Seat 'A' Loaded with Human Subject and Rigid Load.

It is thus highly desirable to derive a Human Response Function that can characterize the contributions of the human body, such that the overall comfort performance of the seat-human body system can be evaluated upon integrating the Human Response Function into the dynamic response behavior of the seat-load system, as illustrated in Figure 3.2. This function may be identified through a thorough examination of the vibration response behavior of the seat-human and seat-load systems. The Human Response Function can then serve as a very important tool to assess the overall performance of the seats, while eliminating the complex testing involving human subjects.

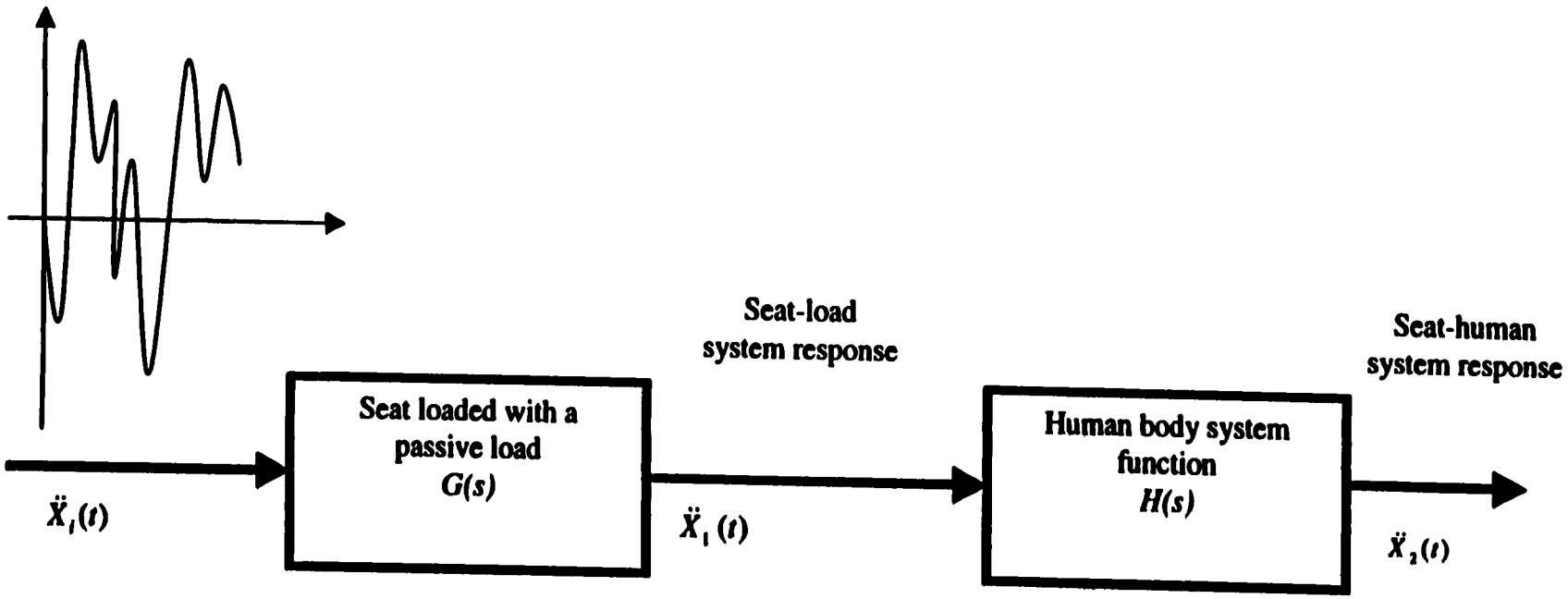

Figure 3.2. The concept of human body describing function for evaluating the seat-human system response.

In this chapter, the vibration transmission performance of seats 'A' and 'B' obtained with 6 different subjects representing 50th percentile male population, are compared with those obtained with a passive load. The results of the comparative study are discussed to highlight the nonlinear dependency of the seat performance characteristics on the nature of excitation and the contributions of the human body. The data is analyzed to derive a human response function representing the occupant contribution that may be utilized to estimate the seat-human system performance from the measured seat-passive load performance characteristics.

3.2 Vibration Transmission Characteristics of the Seats Loaded with Passive Load and Human Subjects

The vibration behavior of the seat-load system is strongly influenced by the load and its distribution. A passive seat load, comprising two sand bags characterizing lower and upper body weights, was configured in the laboratory to reduce the magnitude of possible relative movements between the load and the seat. One sandbag, weighing 33.2 kg was placed on the seat cushion, while the second bag weighing 22.7 kg was placed against the back rest. The two sand bags were contained in a single bag to provide a flexible hinge between the two bags, as shown in Figure 3.3. The sand bag thus permitted relative rotations of the bags about the hinge-point under pitch oscillations of the back-rest. The sand bag representing the back rest load was secured to the backrest of the seat by using a seat belt.

The seats 'A' and 'B' loaded with the sand bag and the human subjects were evaluated under both harmonic and field measured random excitations described in section 2.5.3. The harmonic excitations, however, were synthesized to yield three

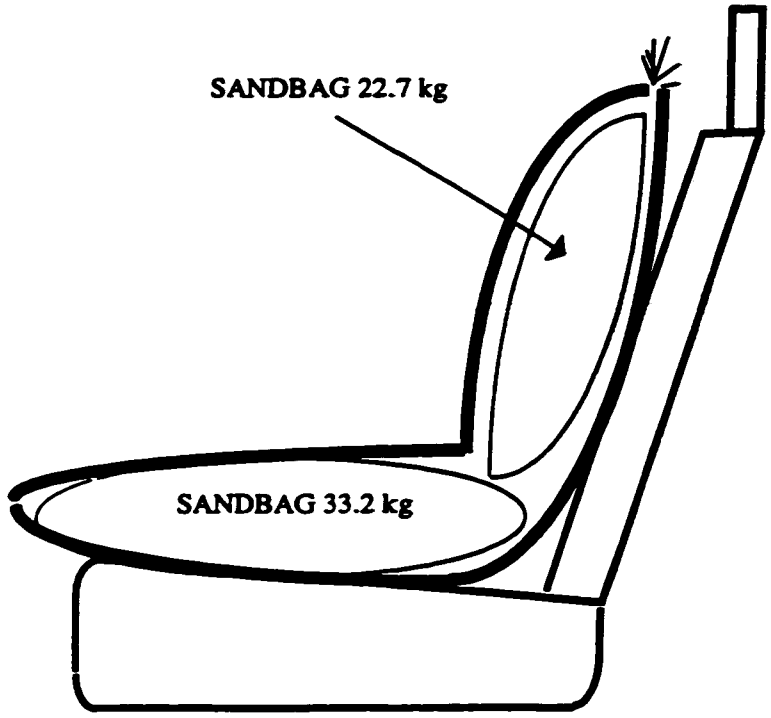

Figure 3.3. Schematic of the Passive Seat Load Realized Using Two Sandbags.

different peak displacement amplitudes: 6.35 mm, 9.5 mm and 12.7 mm in the low frequency range (0.625-2 Hz) and constant amplitude acceleration at frequencies above 2 Hz. Table 3.1 summarizes the nature of harmonic excitations used in the study.

TABLE 3.1: Summary of Harmonic Excitations Used in the Study.

Excitation	Seats with Human Subjects	Seats with Passive Load
Sinusoidal	(i) 6.35 mm peak displacement: 0.625-2 Hz frequency range	(i) 6.35 mm, 9.5 mm, 12.7 mm peak displacement in 0.625-2 Hz frequency range
	(ii) 0.1 g peak acceleration in 2-10 Hz frequency range	(ii) 0.1 g, 0.15 g, 0.2 g peak acceleration in the 2-10 Hz frequency range

The vibration tests were performed with seats 'A' and 'B' loaded with sand bags under sinusoidal excitations of different amplitudes. The test data was analyzed to determine the acceleration transmissibility and influence of excitation level on the frequency response characteristics. The test results revealed that the acceleration transmissibility of the seat-load system is strongly influenced by the magnitude of excitation. This may be partly attributed to the nonlinear visco-elastic properties of the seat and different kinds of sliding motions of the sand bag with respect to the seat.

The acceleration transmissibility characteristics of the seat 'A' loaded with the sand bags, derived in the 0-40 Hz frequency range as a function of the excitation

amplitude, are shown in Figure 3.4. The results show a single distinct peak in the 5.5 to 6.2 Hz frequency range, which corresponds to the fundamental resonance of the seat-load system. Both the natural frequency and the peak acceleration transmissibility decrease with increase in the excitation amplitude. The fundamental frequency is observed to be near 6.2 Hz under 6.35 mm peak displacement excitation, which decreases to 5.5 Hz under 9.5 mm peak excitation. Figure 3.5 presents a comparison of acceleration transmissibility of seat 'A' loaded with sand bags with the mean values obtained using the human subjects. The comparison is presented for 6.35 mm peak excitation in the 0.625 to 10 Hz frequency range. The magnitudes of peak acceleration transmissibility obtained with the sand bags are considerably larger than those obtained with human subjects. It is apparent that the human body contributes considerably in reducing the fundamental frequency, peak acceleration transmissibility and the vibration transmission in the isolation frequency range.

The acceleration transmissibility characteristics of the seat 'B' loaded with the sandbag and subject to three different amplitudes of excitations are illustrated in Figure 3.6. The results are quite similar to those obtained for seat 'A'. The seat 'B', however, exhibits resonance at relatively higher frequencies, in the 6.2 to 7.5 Hz range, due to its higher effective stiffness. A comparison with the mean acceleration transmissibility of the seat 'B' loaded with human subjects, presented in Figure 3.7 reveals considerable contributions due to dynamics of the human subjects. The natural frequency, peak acceleration transmissibility and vibration transmission in the isolation range of the seat loaded with human subjects is considerably lower when compared to those obtained with the sand bags.

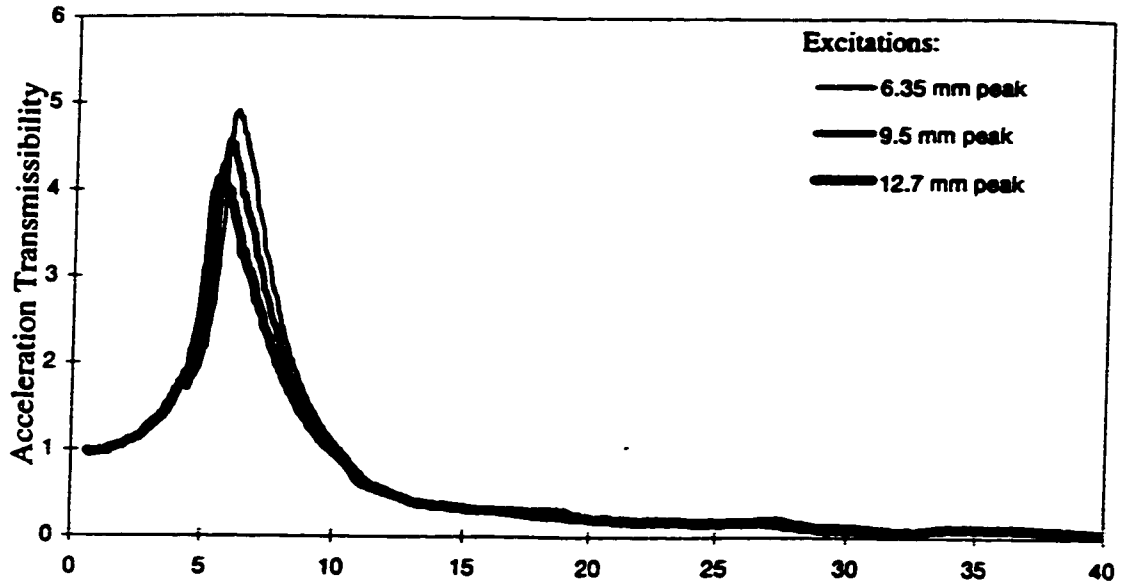

Figure 3.4: Influence of Amplitude of Excitation on the Acceleration Transmissibility Characteristics of the Seat 'A Loaded with Sandbags.

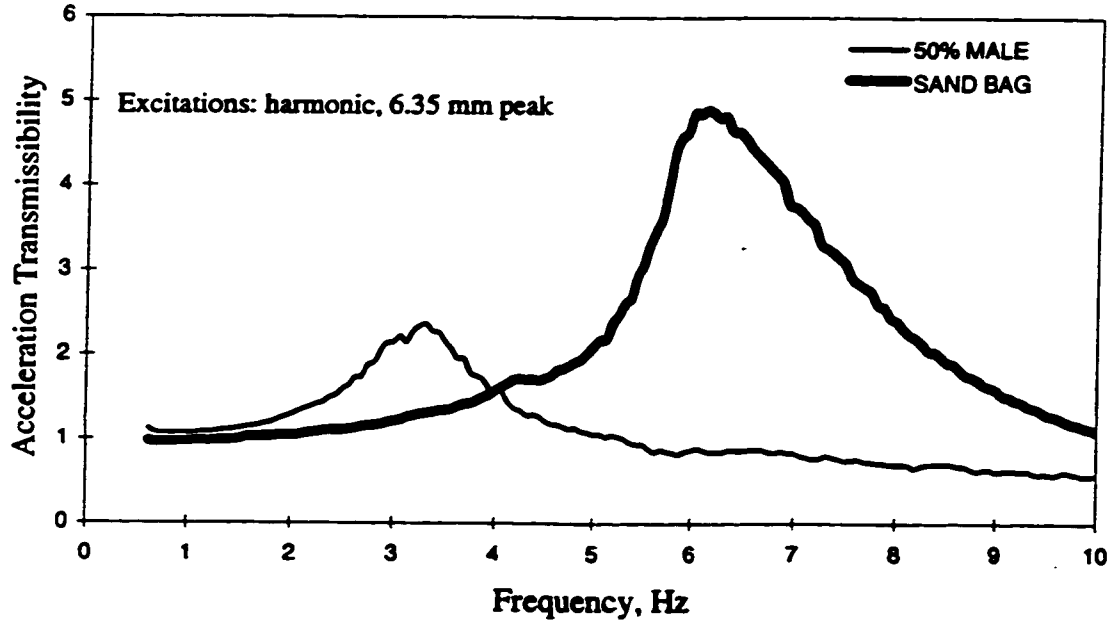

Figure 3.5: Comparison of Acceleration Transmissibility of the Seat 'A' Loaded with Human Subjects and the Sandbags.

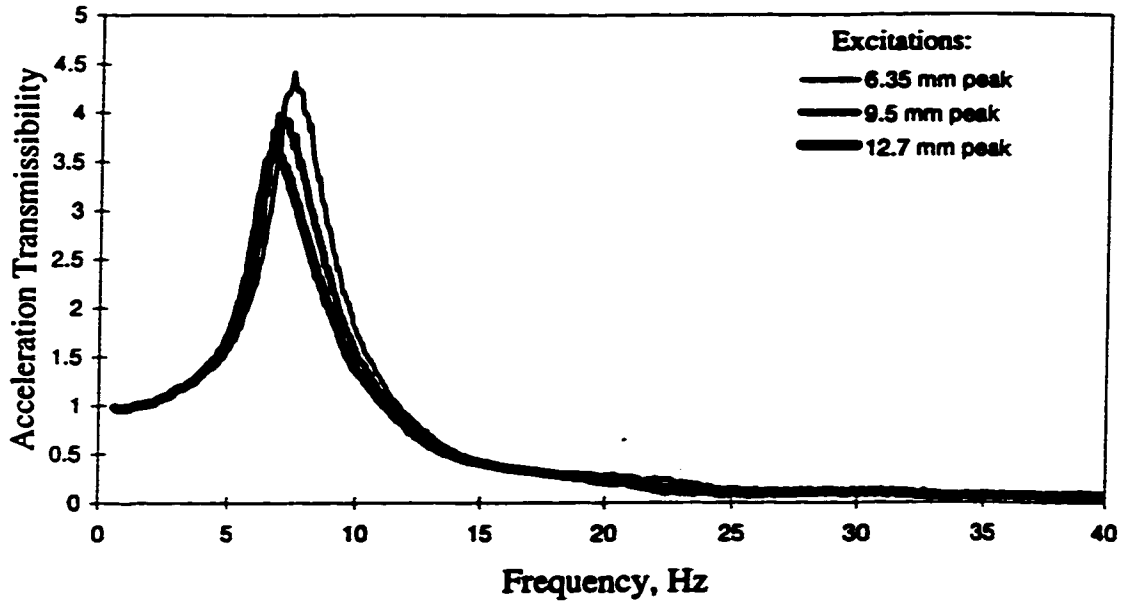

Figure 3.6: Influence of Amplitude of Excitation on the Acceleration Transmissibility Characteristics of the Seat 'B Loaded with Sandbags.

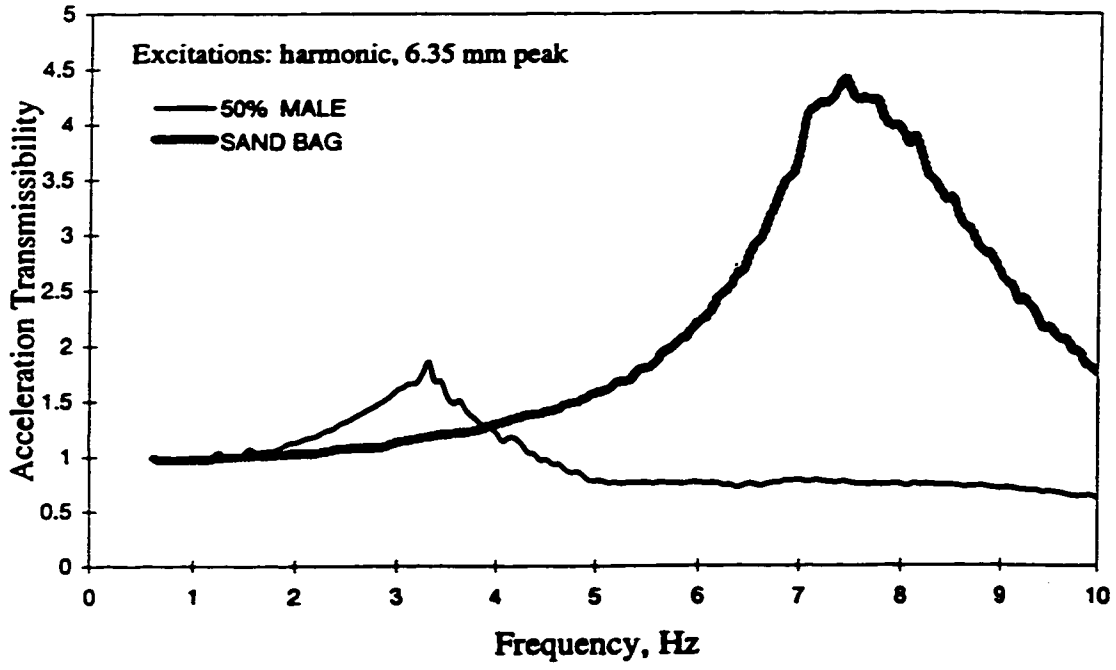

Figure 3.7: Comparison of Acceleration Transmissibility of the Seat 'B' Loaded with Human Subjects and the Sandbags.

Figures 3.4 to 3.7 clearly illustrate the important contributions of the human subjects. The biodynamic visco-elastic properties of the human body result in considerably lower values for both natural frequency and peak acceleration transmissibility of the coupled seat-human system than those of the seat-load system. While the human body contributes to high degree of vibration attenuation at frequencies greater then 5 Hz, the seat-load system exhibits mostly vibration amplification in the entire frequency range of 1-10 Hz.

3.3 Development of a Human Response Function

The acceleration transmissibility characteristics of the seats 'A' and 'B' obtained under sinusoidal excitations were evaluated in relation to the mean values obtained for the seats loaded with 50th percentile male subjects. Since the sand bag weight correlated closely with the 50th percentile male subjects, the analysis was limited to only 50th percentile male subject data. This approach was taken to eliminate the nonlinear dependency of the vibration transmissibility on the seated weight. The frequency response characteristics of the seat-load system obtained under 6.35 mm peak displacement excitations were compared with the mean acceleration transmissibility characteristics established for 50th percentile male subjects in order to identify the human response function:

$$H(s) = \left| \frac{\ddot{X}_2(s)}{\ddot{X}_1(s)} \right| \qquad (3.1)$$

where $H(s)$ is the system function formulated to describe the contributions of the seated human subject. $\ddot{X}_1(s)$ and $\ddot{X}_2(s)$ are the magnitudes of acceleration transmissibility

of the seat-load and seat-human systems, respectively. Equation (3.1) is solved using the measured data obtained for both seats 'A' and 'B' under harmonic excitations in the 0.625-10 Hz. The analysis of the data obtained with seats 'A' and 'B' resulted in somewhat comparable frequency response characteristics of the Human Response Function for both seats. Figures 3.8 and 3.9 illustrate the frequency response of the Human body Response Functions under different amplitudes of excitations and the mean frequency response functions for seats 'A' and 'B', respectively. Although the Human Response Function is derived using the data obtained with human subjects under 6.35 mm peak displacement excitations, the results show relatively insignificant influence of the excitation amplitude for seats 'A' and 'B'. The system gains obtained for both seats are observed to be quite comparable in the 0.625-10 Hz frequency range.

The frequency response characteristics of the Human Response Functions for seats 'A' and 'B' reveal fundamental resonance near 3.5 Hz, which corresponds to the resonant frequency of the coupled seat-human system. The frequency response characteristics further reveal that a secondary peak may be expected to occur at frequencies above 10 Hz. The frequency response behavior can thus be considered to characterize the dynamic response of a two-DOF dynamical system. The frequency response characteristics further show almost unity gain at frequencies below 2 Hz, which implies the dynamic contributions of the seated subject are insignificant at low frequencies. This observation conforms with the various reported studies on the biodynamic behavior of the seated human body [3,21,22]. The Human Response Functions further reveal considerable attenuation in the 5-7 Hz frequency range, which corresponds to the resonance range of the seat-load system for both seats.

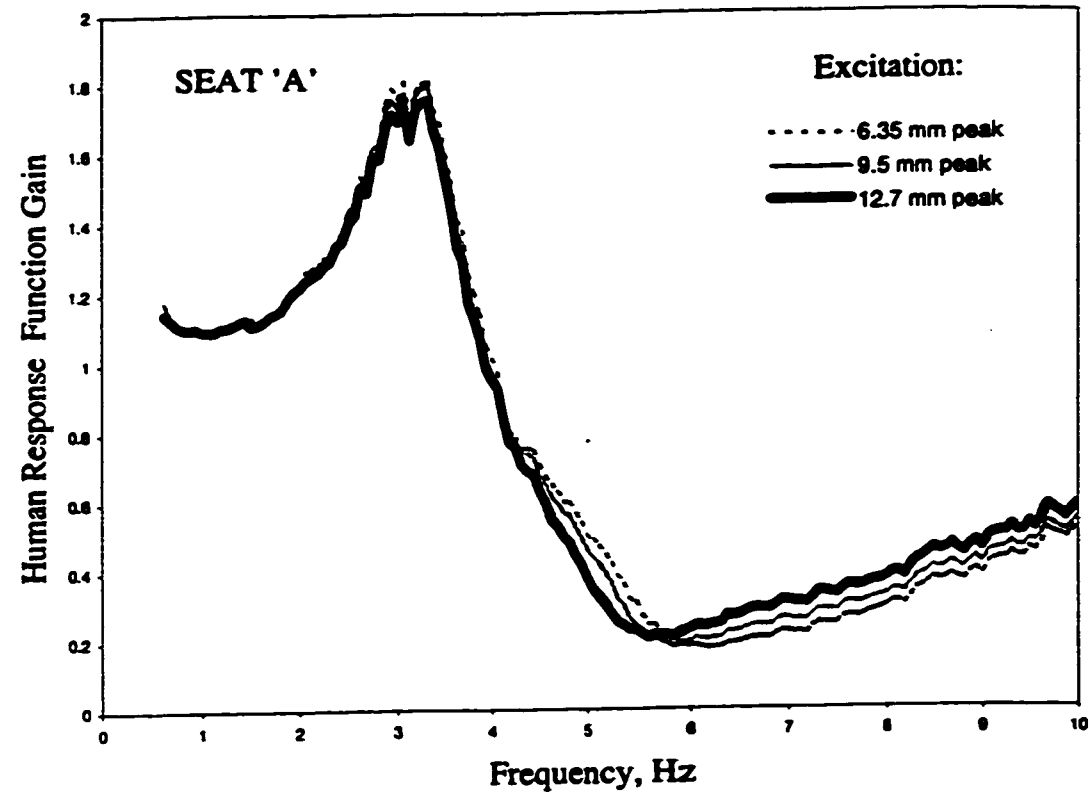

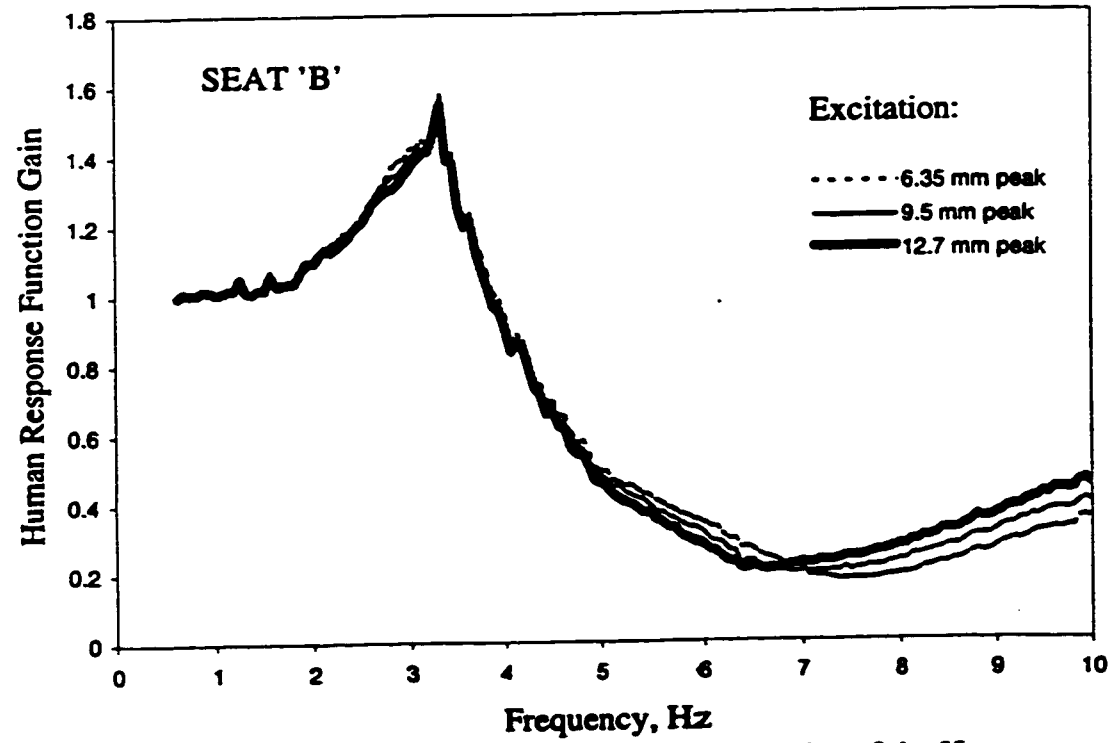

Figure 3.8: Frequency Response Characteristics of the Human Body Response Function.

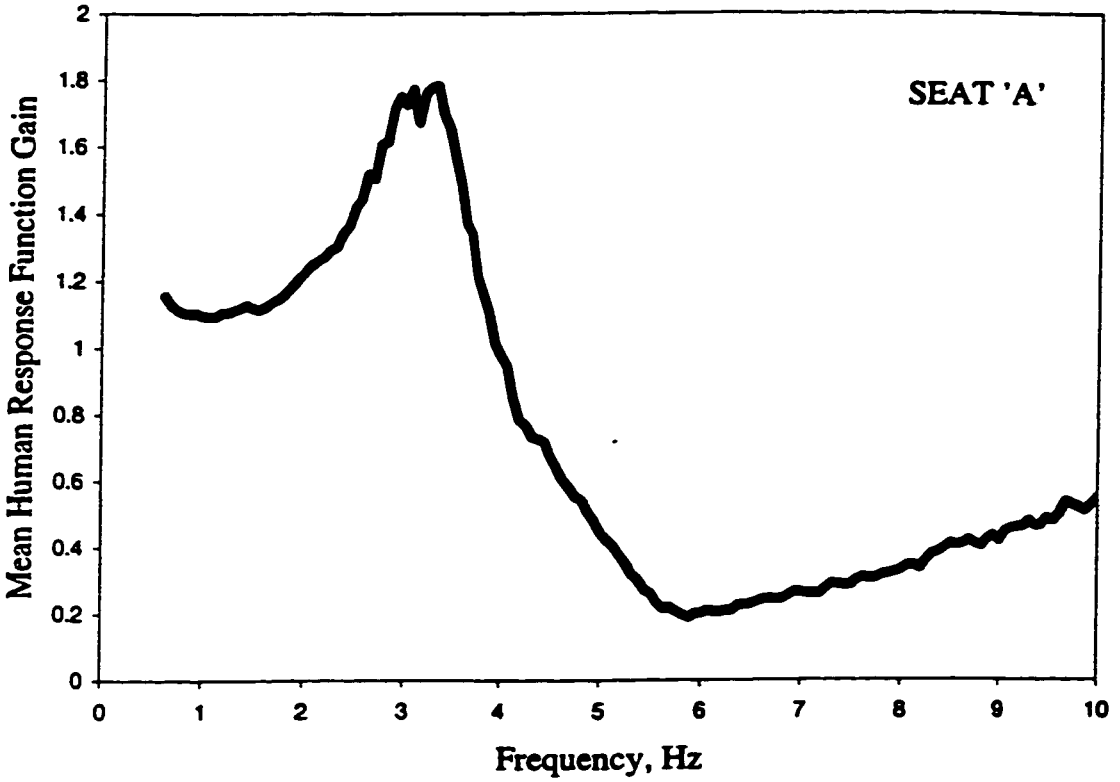

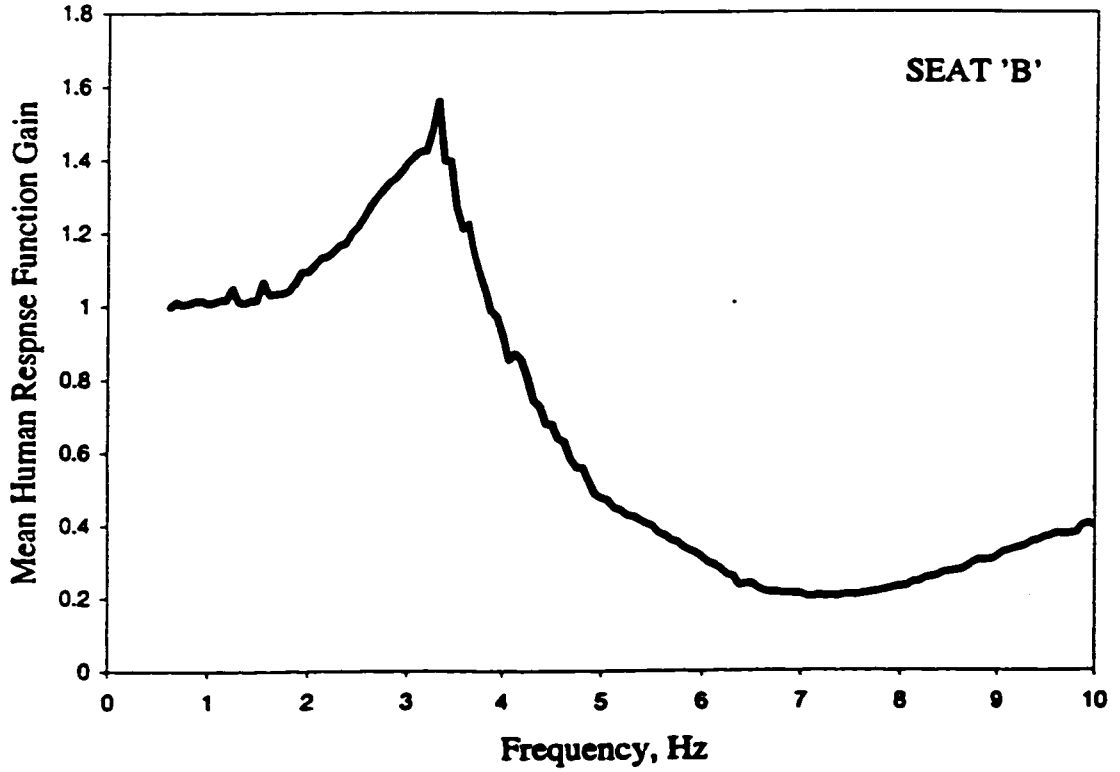

Figure 3.9: Mean Frequency Response Characteristics of the Human Body Response Function.

3.4 Analytical Model Representation of the Human Response Functions

The frequency response characteristics of a Human Response Function for both seats reveal fundamental resonance near 3.5 Hz with a secondary resonant peak at frequencies above 10 Hz. The frequency response behavior of a Human Response Function can thus be represented by a two-DOF dynamic system, illustrated in Figure 3.10.

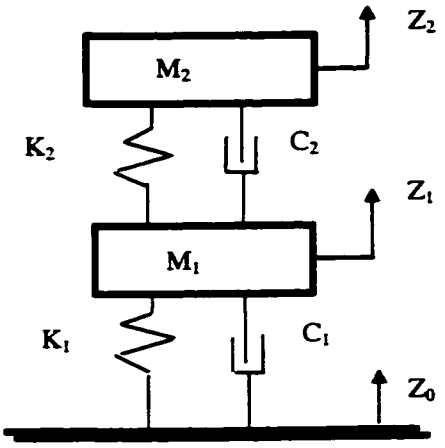

Figure 3.10. Two-DOF system.

The equations of motion for this model can be expressed in the following manner:

$$\begin{aligned} m_1\ddot{z}_1 + k_1(z_1 - z_0) + c_1(\dot{z}_1 - \dot{z}_0) + k_2(z_1 - z_2) + c_2(\dot{z}_1 - \dot{z}_2) &= 0 \\ m_2\ddot{z}_2 + k_2(z_2 - z_1) + c_2(\dot{z}_2 - \dot{z}_1) &= 0 \end{aligned} \tag{3.2}$$

where k_1, k_2, c_1, c_2 are linear stiffness and damping coefficients; z_1 and z_2 are vertical displacement coordinates of masses m_1 and m_2; z_0 is the vertical input displacement. Assuming harmonic solution, the system function, $H(s)$, may be expressed as:

$$H(s) = \left| \frac{\ddot{X}_2(s)}{\ddot{X}_1(s)} \right| = \frac{Z_2(s)}{Z_0(s)} = \frac{A_1 + A_2 s + A_3 s^2}{A_4 + A_5 s + A_6 s^2 + A_7 s^3 + s^4} \quad (3.3)$$

The coefficients A_1 through A_7 are estimated using the MATLAB Identification Toolbox, which can be directly related to the system parameters in the following manner:

$A_1 = k_1k_2/m_1m_2$; $A_2 = (k_2c_1 + k_1c_2)/m_1m_2$; $A_3 = c_1c_2/m_1m_2$; $A_4 = k_1k_2/m_1m_2$;

$A_5 = (k_1c_2 + k_2c_1) / m_1m_2$; $A_6 = A_3 + k_2/m_1 + k_1/m_1 + k_2/m_1$; $A_7 = c_2/m_2 + c_1/m_1 + c_2/m_1$.

TABLE 3.2. Values of Identified Constants A_1-A_7 for Seats 'A' and 'B'.

Describing function of:	A_1	A_2	A_3	A_4	A_5	A_6	A_7
Seat 'A'	1424.0	39.4	46.8	1472.3	220.2	139.8	5.8
Seat 'B'	1406.7	73.3	26.1	1563.0	196.0	136.5	0.0
Mean	1364.3	77.7	34.8	1500.5	224.7	142	4.5

The coefficients of the system functions, derived for seats 'A' and 'B' are listed in Table 3.2. Equation (3.3) is solved to determine the frequency response of the estimated system function in the 0-40 Hz frequency range. Figure 3.11 illustrates the magnitude of the system function derived for seats 'A' and 'B' in the 1.0-40 Hz frequency range. The frequency response of the function for seat 'A' reveals resonances near 3.5 Hz and 10.5 Hz, respectively, while that for seat 'B' exhibits peaks near 3.5 Hz and 11 Hz, respectively. The magnitudes of the two resonant peaks for the both seats are quite comparable. The frequency response characteristics are further compared with the mean response obtained from the experimental data in the 0.625-10 Hz range, as shown in Figure 3.12. The figure shows reasonably good correlation between the estimated and

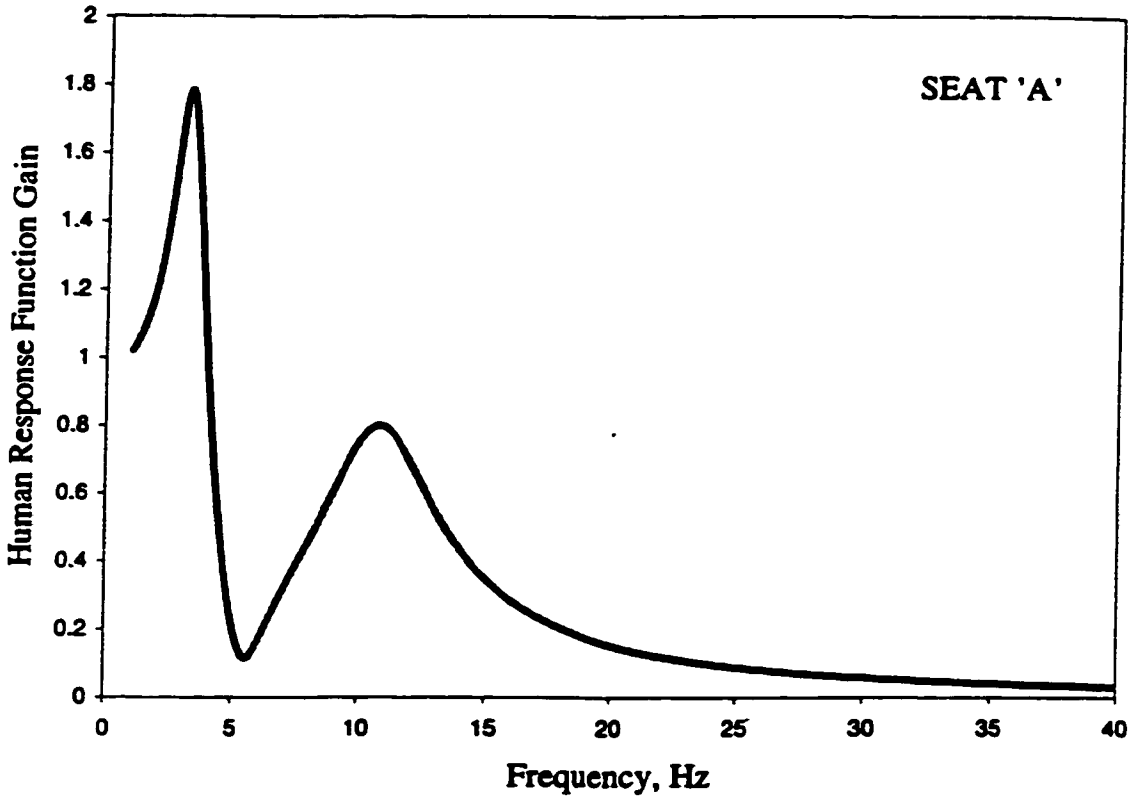

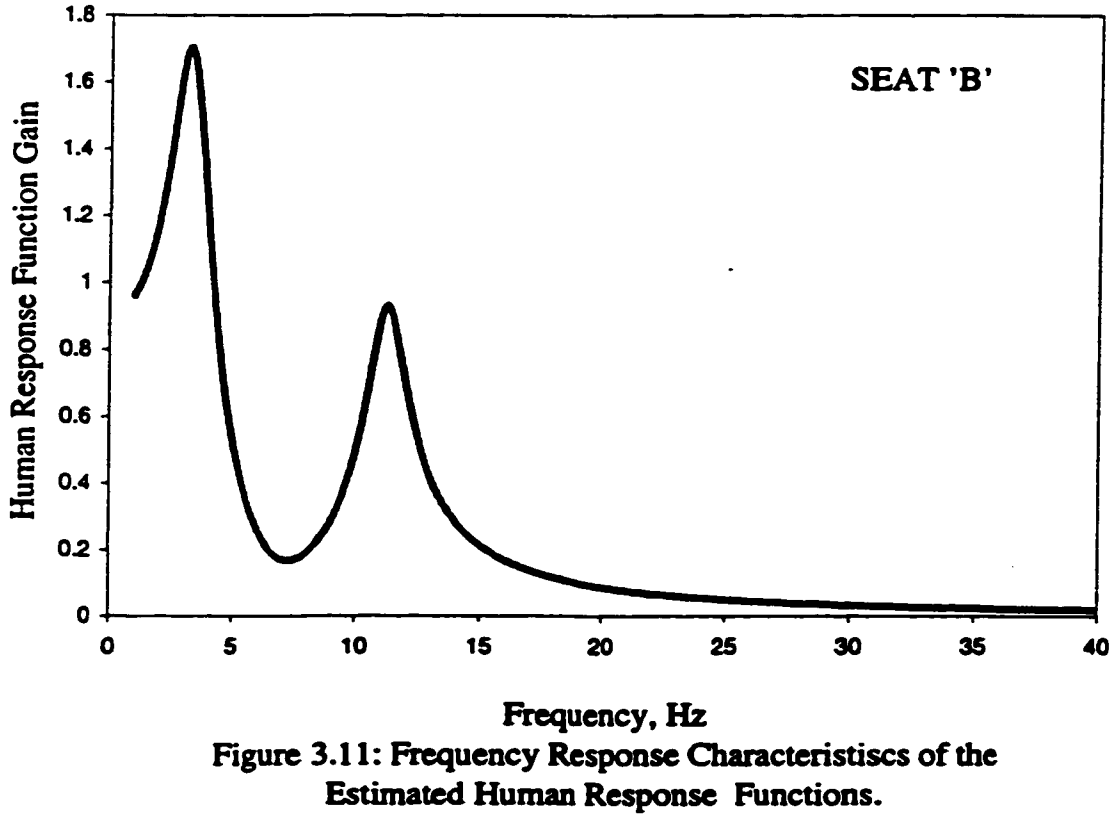

Figure 3.11: Frequency Response Characteristiscs of the Estimated Human Response Functions.

measured response for seat 'A' in the entire frequency range. The estimated function response for seat 'B', however, shows certain error in the vicinity of fundamental resonant frequency.

The measured data for both seats is further analyzed to derive mean of the Human Response Function in an attempt to establish a generally applicable response function, which may be used to assess vibration performance of the seat-human system. Figures 3.13 present the mean of the mean frequency response characteristics of the human response function based on the measured data together with the mean response for seats 'A' and 'B'. The mean of the mean frequency response is referred to as the mean hereafter.

The mean of the estimated functions for seats 'A' and 'B' is also derived in the 1-40 Hz range, as shown in Figure 3.14. The validity of the mean estimated function is examined by comparing its frequency response with the mean measured data in the 0.625-10 Hz frequency range, as shown in Figure 3.15. The results show reasonably good correlation between the mean estimated and measured response, with only slight errors in the vicinity of the fundamental resonant frequency and at higher frequencies. The peak deviation between the response based upon the estimated function and measured data is obtained well below 6% in the vicinity of the resonant frequency. The mean response function is thus considered as the target function to represent the contributions due to human subject to the overall comfort performance of the seat.

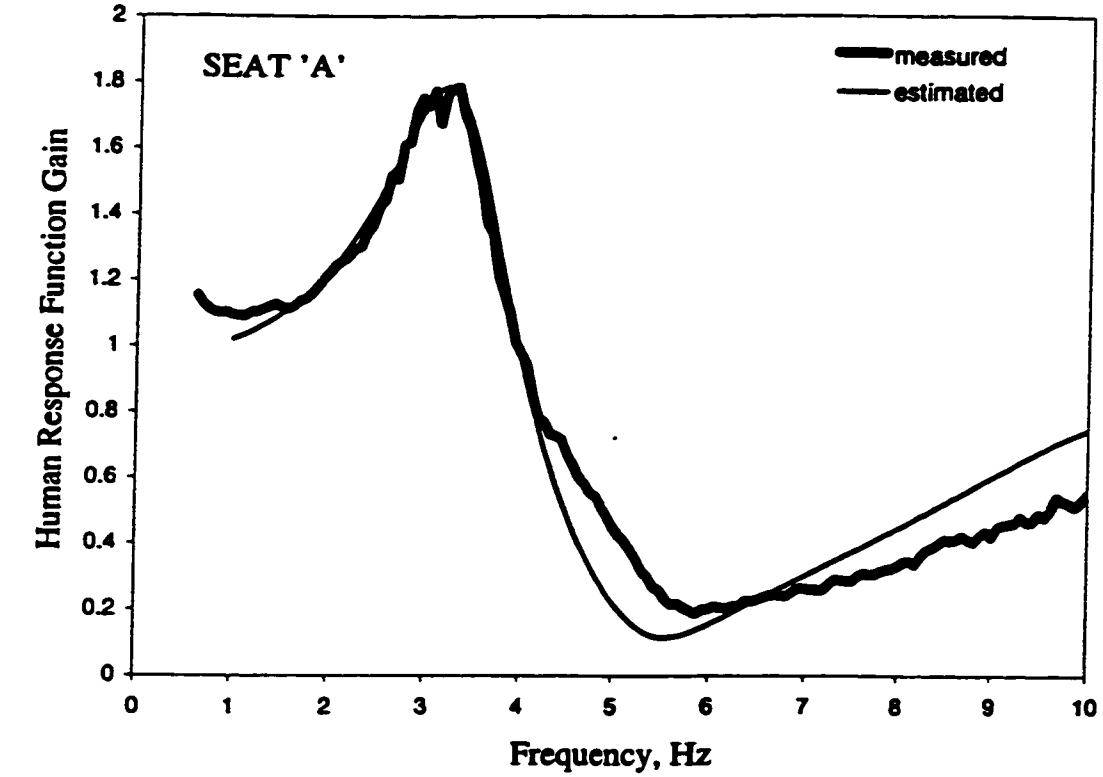

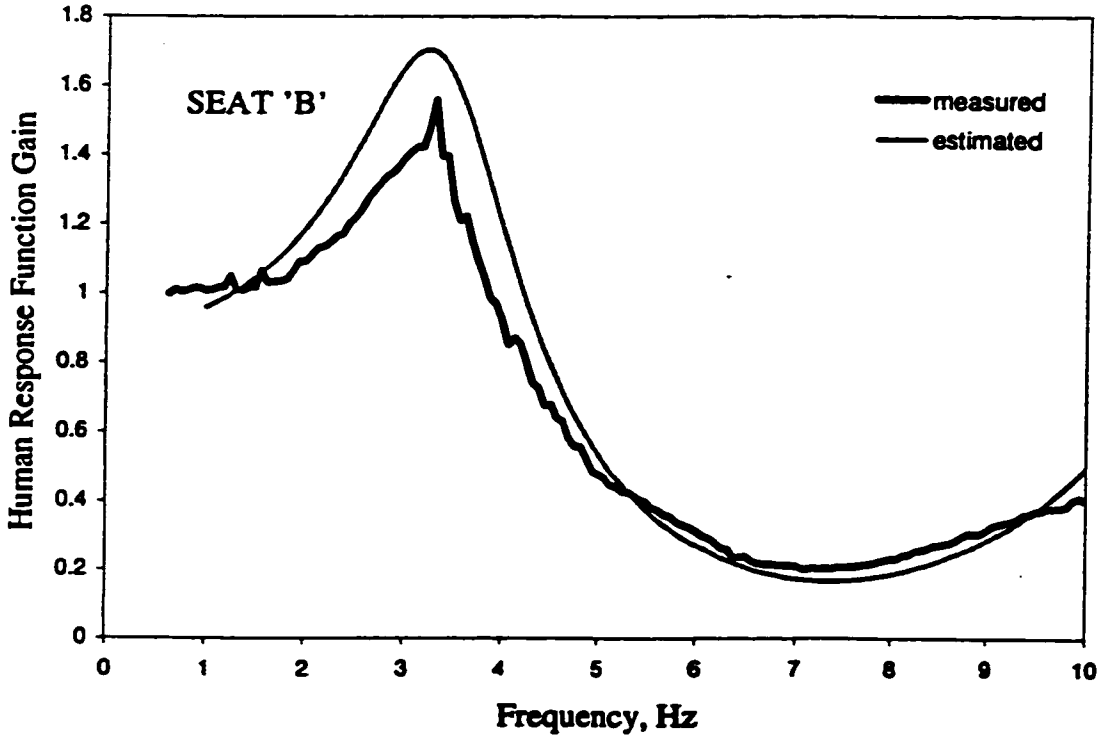

Figure 3.12: Comparison of Frequency Response Characteristics of the Estimated and Measured Human Response Functions.

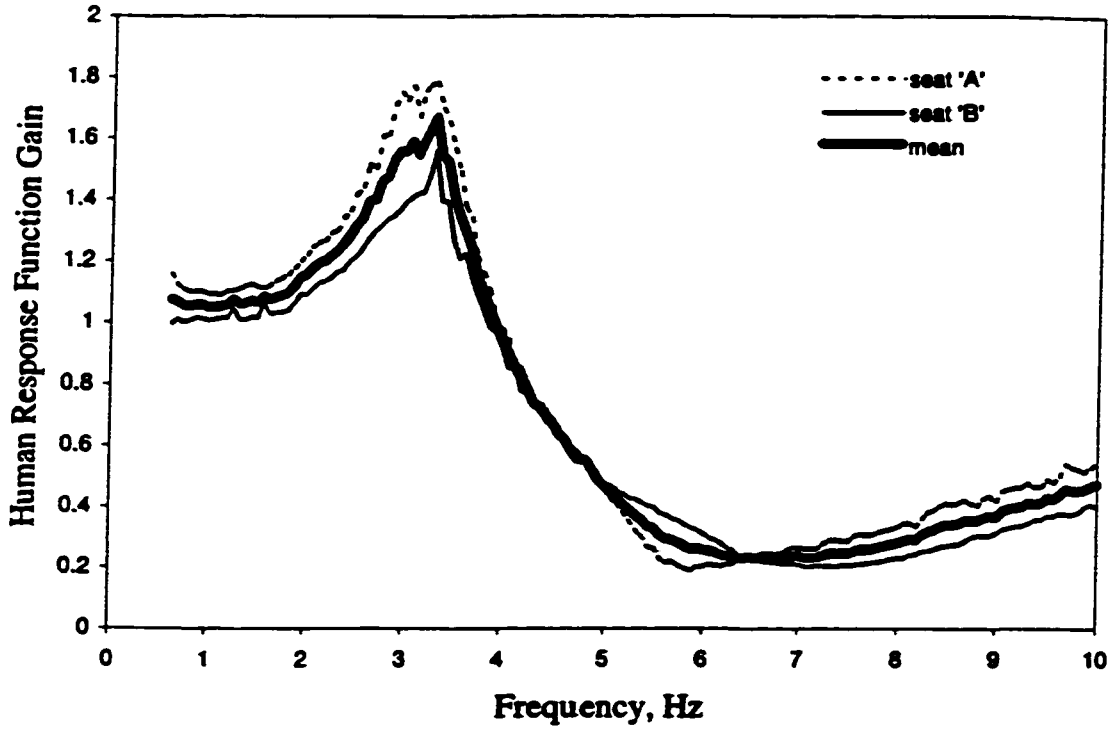

Figure 3.13: Comparison of Mean Frequency Response Characteristics of the Measured Human Response Functions for Seats 'A' and 'B', with the Mean of Mean.

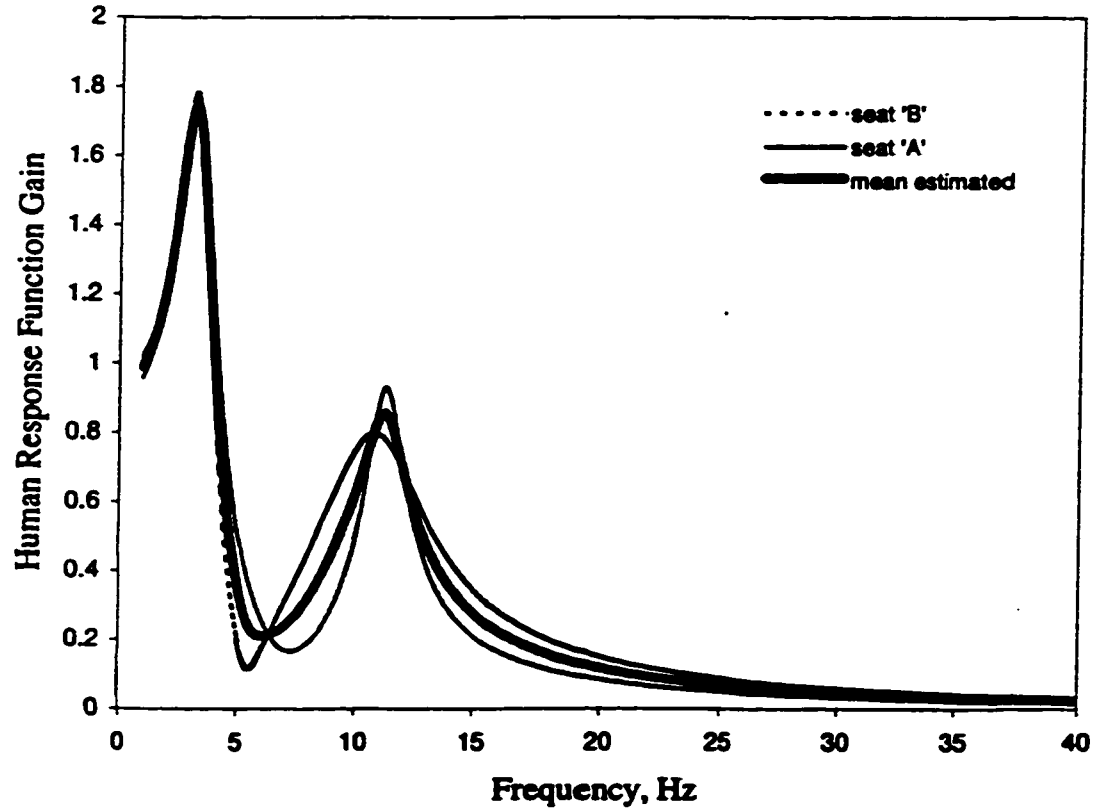

Figure 3.14: Comparison of Estimated Human Response Function Response for Seats 'A' and 'B' and their Mean.

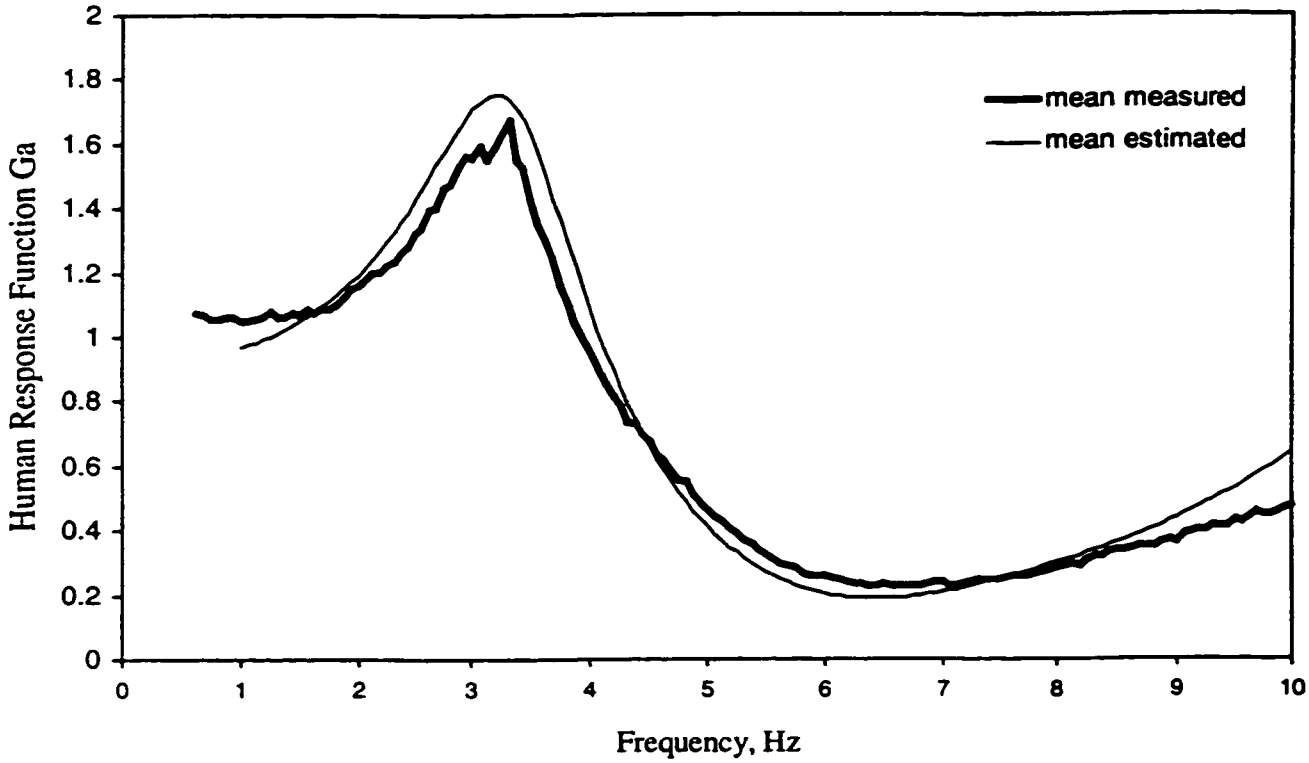

Figure 3.15: Comparison of Mean Measured with the Mean Estimated Response for Human Response Function.

The system identification toolbox is utilized to derive the coefficients of the mean human response function, which are summarized in Table 3.2.

3.5 Response Analysis of the Seat-Human System Using the Human Response Function

The response characteristics of the coupled seat-human system are derived using the methodology described in section 3.3. The measured acceleration response of the seat-load system is analyzed in conjunction with the mean describing or target function, derived in previous sections.

3.5.1 Sinusoidal Excitations.

The frequency response characteristics of the seat-human system in terms of acceleration transmissibility can be derived from:

$$\ddot{X}_2(s) = H(s)\ddot{X}_1(s) \tag{3.4}$$

where $H(s)$ is the target function. $\ddot{X}_1(s)$ is the acceleration transmissibility magnitude of the seat-load system measured in the laboratory under harmonic excitations and $\ddot{X}_2(s)$ is the estimated acceleration transmissibility of the seat-human system.

Each seat was loaded with a passive load equivalent to the 50th percentile male population and measurements were performed in the laboratory using sinusoidal excitation described in section 2.5.3. The measured acceleration response at the seat-load interface was analyzed to derive its acceleration transmissibility, $\ddot{X}_1(s)$. Equations (3.3) and (3.4) are then solved to derive the acceleration transmissibility $\ddot{X}_2(s)$ of the seat-human system. The estimated acceleration transmissibility characteristics are compared with those obtained from laboratory measurements performed with 50th percentile male subjects to examine the validity of the proposed methodology. Figures 3.16 presents a comparison of the measured acceleration transmissibility of the human-seat system with that estimated from the Human Response Function for seats 'A' and 'B'. The results show very good correlation between the measured and estimated response for seat 'A' in the entire frequency range. The estimated response for seat 'B' is slightly larger than the measured response in the vicinity of the resonant frequency. The peak deviation, however, is below 10%. From the results, it is apparent that the proposed methodology can be effectively employed to estimate the acceleration transmissibility characteristics of the seat-human system under sinusoidal excitations using the target function and the

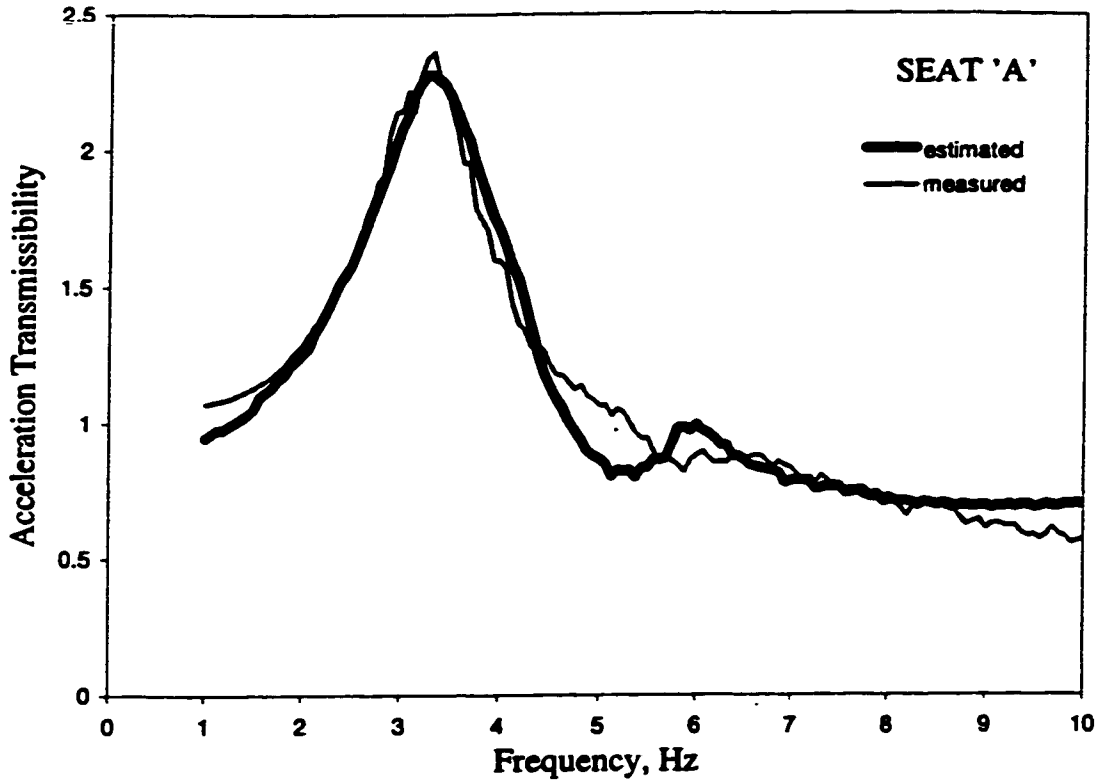

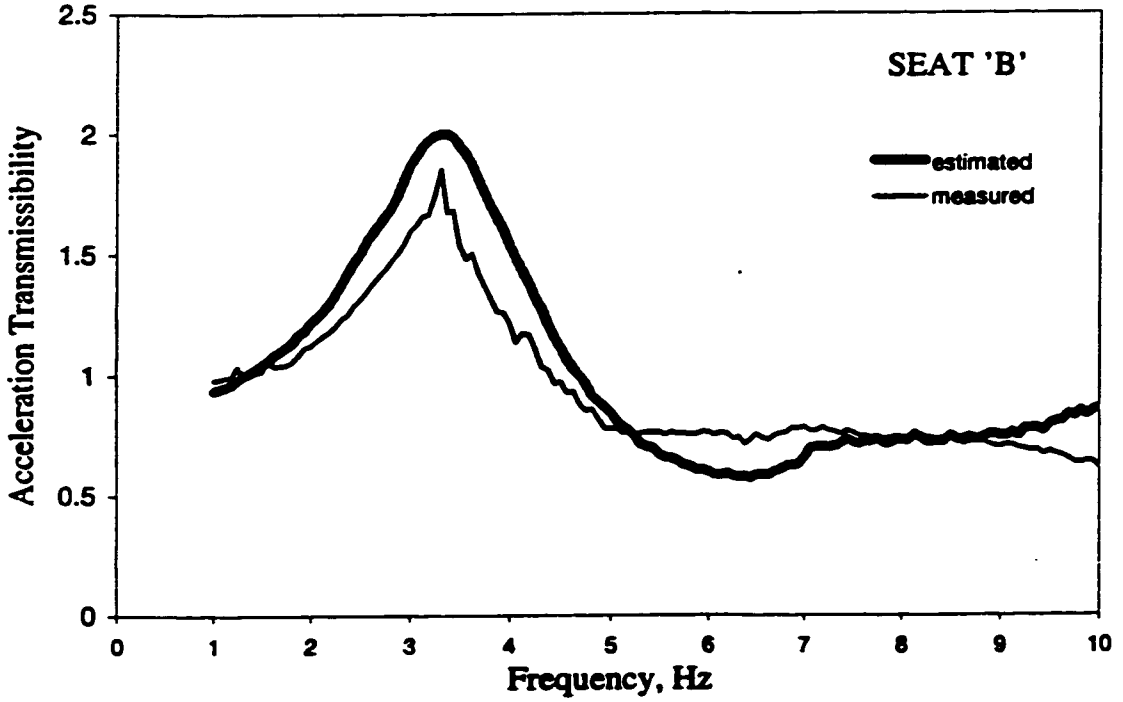

Figure 3.16: Comparison of Measured and Estimated Acceleration Transmissibility Characteristics of the Seat-Human System.

measured response of the seat-load system. The need to perform repetitive tests with human subjects can thus be eliminated using the proposed methodology.

3.5.2 Random Excitations

The response characteristics of the seat-human system subject to random excitations can be estimated from the measured response of the seat-load system and the target function:

$$S_{X_2}(\omega) = |H(\omega)|^2 S_{X_1}(\omega) \tag{3.5}$$

where $H(\omega)$ is the frequency response of the target function in the 0-40 Hz frequency range, $S_{X_1}(\omega)$ is the power spectral density (PSD) of acceleration response measured at the seat-load interface under random excitations and $S_{X_2}(\omega)$ is the estimated PSD of acceleration response at the seat-human interface.

The laboratory tests were performed on each seat loaded with a passive load under random excitations described in section 2.5.3. The PSD of acceleration response measured at the seat-load interface, $S_{X_1}(\omega)$, was derived using B&K signal analyzer. Equation (3.5) is then solved to derive the PSD of acceleration response at the seat-human interface, $S_{X_2}(\omega)$. The derived PSD of acceleration response is compared with the mean acceleration PSD response derived from the measurements performed with 6 male human subjects for both seats under synthesized random vibration spectra, as shown in Figure 3.17. The implementation of the general target function to the seat 'A'-load system yields very good correlation with the measured response of the human-seat system in the entire frequency range of 0-40. For seat 'B' the computed response also is

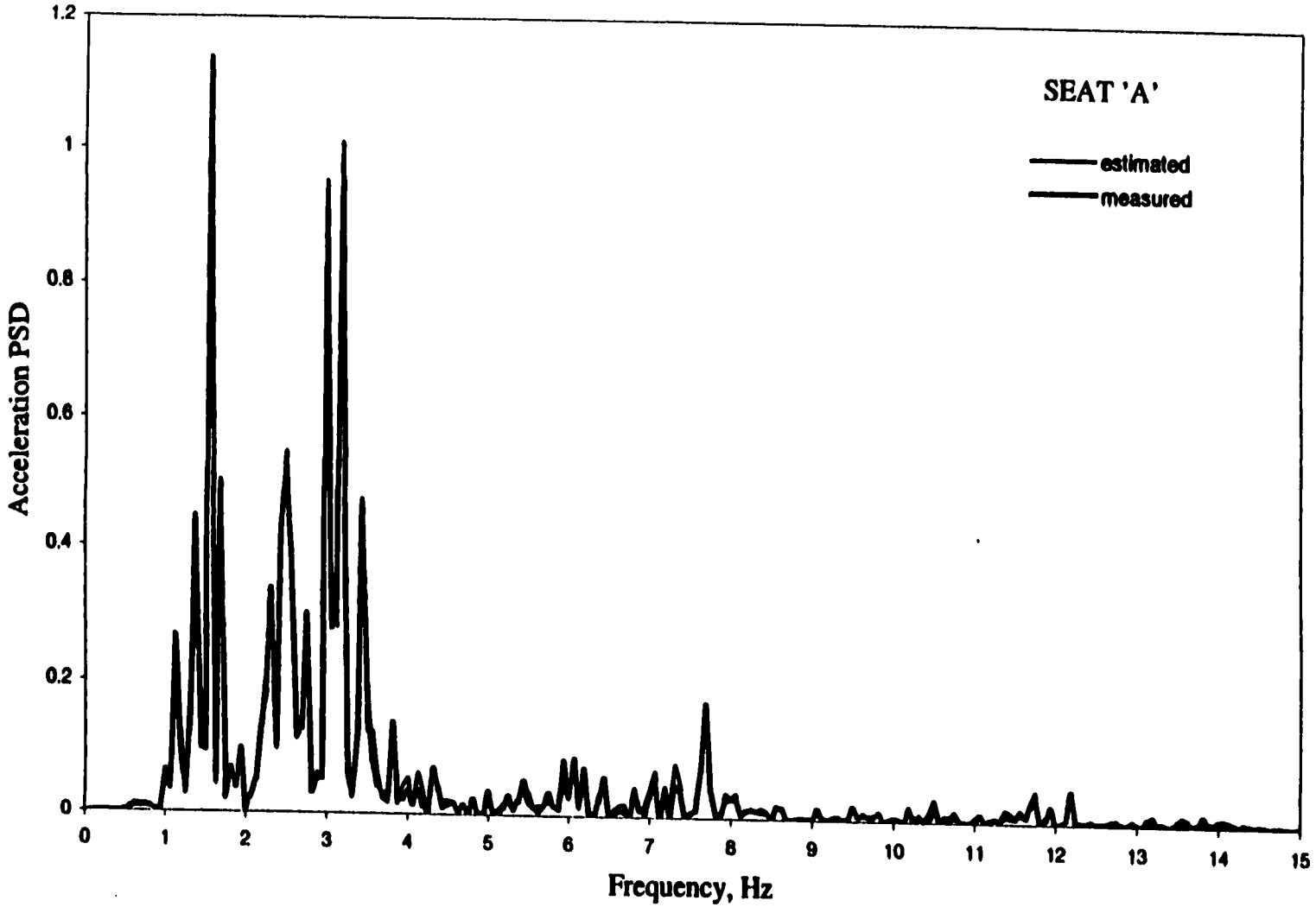

Figure 3.17 (a): Comparison of Estimated and Measured PSD of Acceleration at the Seat-Human Interface.

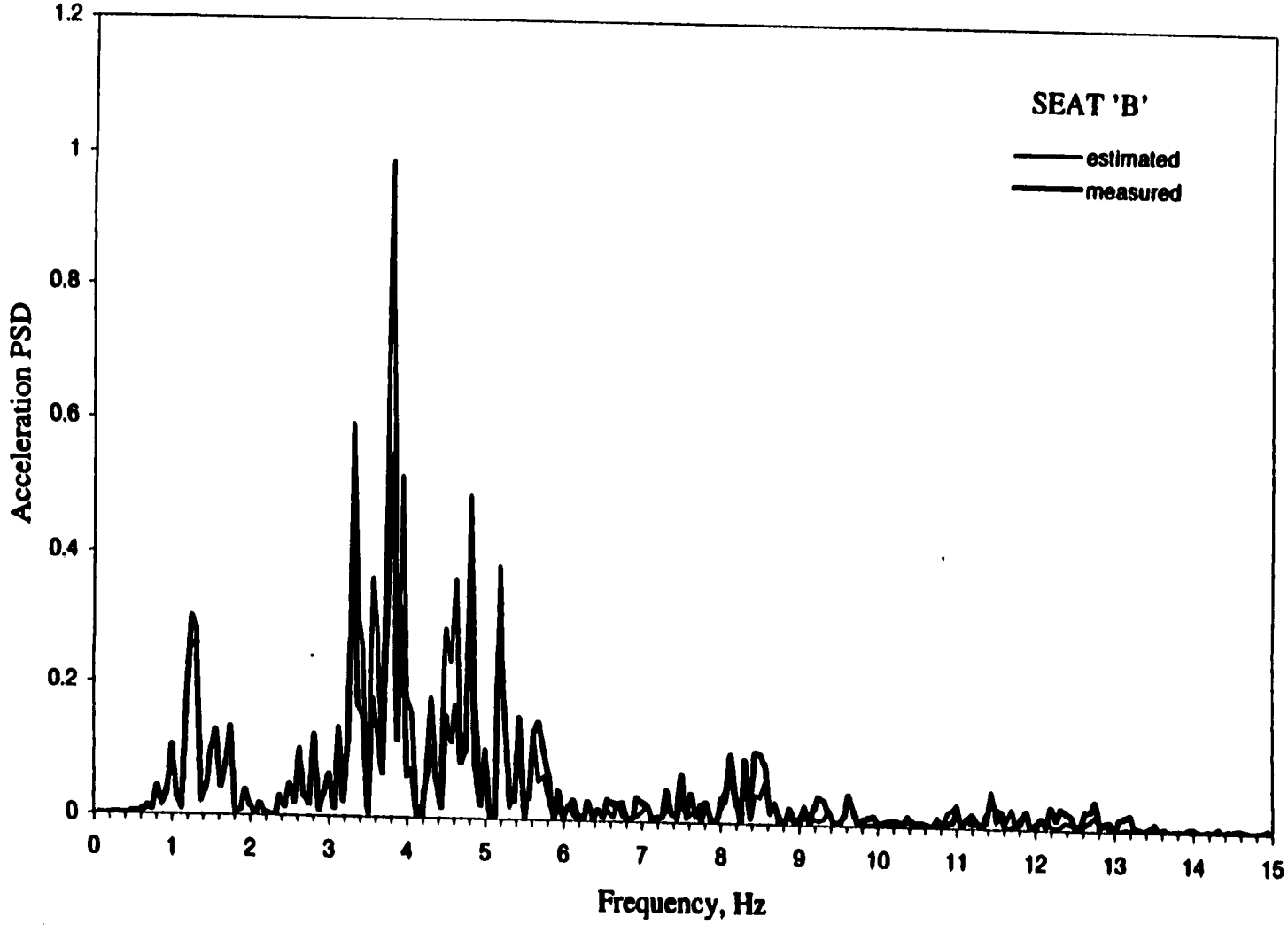

Figure 3.17 (b): Comparison of Estimated and Measured PSD of Acceleration at the Seat-Human Interface.

in close agreement with the measured response, except in the 3.5-4 Hz frequency range, where implementation of the Human Response Function overestimates the measured response. It should be noted that the response characteristics are presented only for 0-15 Hz frequency range, since the response in the higher frequency range is extremely low due to low levels of excitations.

The results presented in Figures 3.16 and 3.17 clearly illustrate the effectiveness of the derived target function for estimating the response characteristics for the seat-human system in important frequency bands under harmonic and random excitations. The errors associated with this approach may be considered within tolerable limits. The proposed target function and the methodology can thus serve as an effective tool to further study the response behavior of the seat-human system, the influence of the seat parameters on the vibration attenuation performance, and the optimal seat design to minimize the whole-body vibration exposure. The results further suggest that it is possible to derive a generally applicable Human Response Function using the proposed methodology. The development of a reliable Human Response Function, however, may necessitate the study of a large group of automotive seats and human subjects in conjunction with representative excitations.

3.6 Parametric Study

The effectiveness of an automobile seat in attenuating whole-body vibration is strongly dependent on the static and dynamic characteristics of the seat cushion. A parametric sensitivity analysis in which a single parameter is changed at a time may provide a basis for selecting design parameters that would yield near optimal ride

vibration performance at the human-seat interface. A parametric study is thus undertaken to establish the sensitivity of seat-occupant system performance to variations in seat parameters. Parametric sensitivity analysis and performance evaluations, however, necessitate the definition of an objective performance index. The performance index based on either the peak value of the steady-state response or the response spectra over a frequency range of interest may be selected. In this chapter, two performance indices are described to carry out parametric sensitivity analyses and the influence of cushion parameters on the vibration performance of a seat-human system. The parametric sensitivity analysis can then provide a guideline to select design parameters that would yield near optimal ride at the human body-seat interface.

3.6.1 Selection of Performance Indices

The primary objective of the parametric sensitivity analysis is to determine static seat parameters that would yield maximum driver or car occupant comfort. Although the car's occupant comfort is related to many subjective as well as objective design and operational factors, such as placement of controls, noise, temperature, vision, etc., the occupant's comfort related to vibration environment of the vehicle alone is considered in this study. The human comfort related to vibration environment of the vehicle, however, needs to be defined in a quantitative manner in terms of measurable performance indices. The performance indices for vertical seat-human system may be derived based on the consideration of human response to low frequency whole-body vibrations. Human body is known to be relatively more sensitive to vertical vibration in the vicinity of 5 Hz attributed to the primary resonance of the body [2,8,9]. It is thus desirable to assess the

performance of the seat-human system in terms of its frequency components. The two performance indices are thus selected to assess the static seat performance:

(i) Acceleration transmissibility characteristics of a seat-human system under harmonic excitations.

(ii) Seat effective acceleration transmissibility (S.E.A.T.) under random excitations.

3.6.2 Parametric Sensitivity Analyses of the Seat-Human System

Sensitivity of the seat performance indices to variations in a single parameters at a time is investigated in order to enhance an understanding of the influence of seat design parameters on the comfort performance. Specifically, the influences of cushion stiffness and damping on the dynamic performance of the seat-human system are investigated. The variations are performed about the nominal stiffness and damping values for the seat cushions, derived in section 2.4.3. Equations of motion for the seat-human model are solved using the local equivalent linearization technique described in Chapter 2, and the response characteristics are presented in terms of the selected performance criteria. The relative influence of cushion parameters on the overall comfort performance are evaluated using the single-DOF human body model in conjunction with the nonlinear seat model. The single-DOF human body model is chosen since it was concluded earlier (section 2.8) that this model can be considered as the most appropriate one for assessment of the seat-occupant system subject to different types of excitations. Seat 'A' incorporating a single-DOF human body model was considered to be the most appropriate to carry out the parametric sensitivity analyses because this system resulted in relatively better correlation with the measured data, as previously discussed in section 2.7.

Influence of cushion stiffness.

The equations of motion (2.1) are solved in the frequency domain at various discrete frequencies in the 0-10 Hz range. An iterative algorithm developed in section 2.7.1 is applied at each selected excitation frequency in order to compute the value of a local equivalent stiffness coefficient. The nonlinear cushion spring is then represented by an array $[K_{NOM}]$, which consists of nominal values of local equivalent constants where each local constant is considered valid in the vicinity of the selected discrete frequency. The influence of variations in the stiffness properties of the cushion on the performance index of the seat is examined by varying the stiffness values by $\pm 15\%$ and $\pm$ 30% of the nominal value for seat 'A'. The equivalent stiffness coefficients are thus further derived for $0.7[K_{NOM}]$, $0.85[K_{NOM}]$, $1.15[K_{NOM}]$ and $1.3[K_{NOM}]$. The Figure 3.18 illustrates the variations in the cushion stiffness coefficients in 0-10 Hz frequency range corresponding to $\pm 15\%$ and $\pm 30\%$ variations. The frequency response characteristics presented in Figure 3.19 illustrate the influence of cushion stiffness on the acceleration transmissibility of seat 'A'. The figure clearly reveals that a stiffer cushion tends to reduce the value of resonant acceleration transmissibility significantly. The peak transmissibility varies from 4.2 to 3.2 for considered variations in the cushion stiffness. Hard cushions also yield higher acceleration transmissibility in the attenuation frequency range. In view of the whole-body resonance near 5 Hz, the hard cushions yield relatively higher transmitted vibration at the occupant-seat interface. The overall comfort performance of hard seats is thus considered to be relatively inferior. Very stiff cushions further encourage slouched posture and thus result in occupant discomfort at the tuberosities [2,7]. On the other hand,

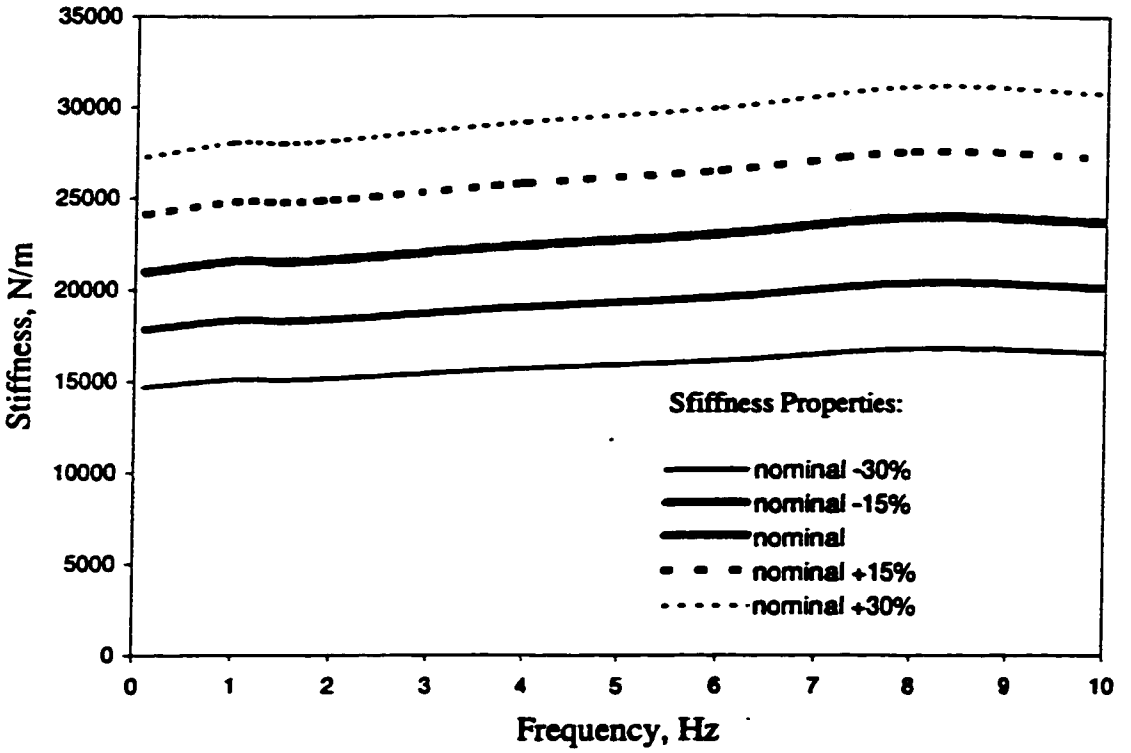

Figure 3.18: Variations in Cushion Stiffness Properties for Seat 'A'.

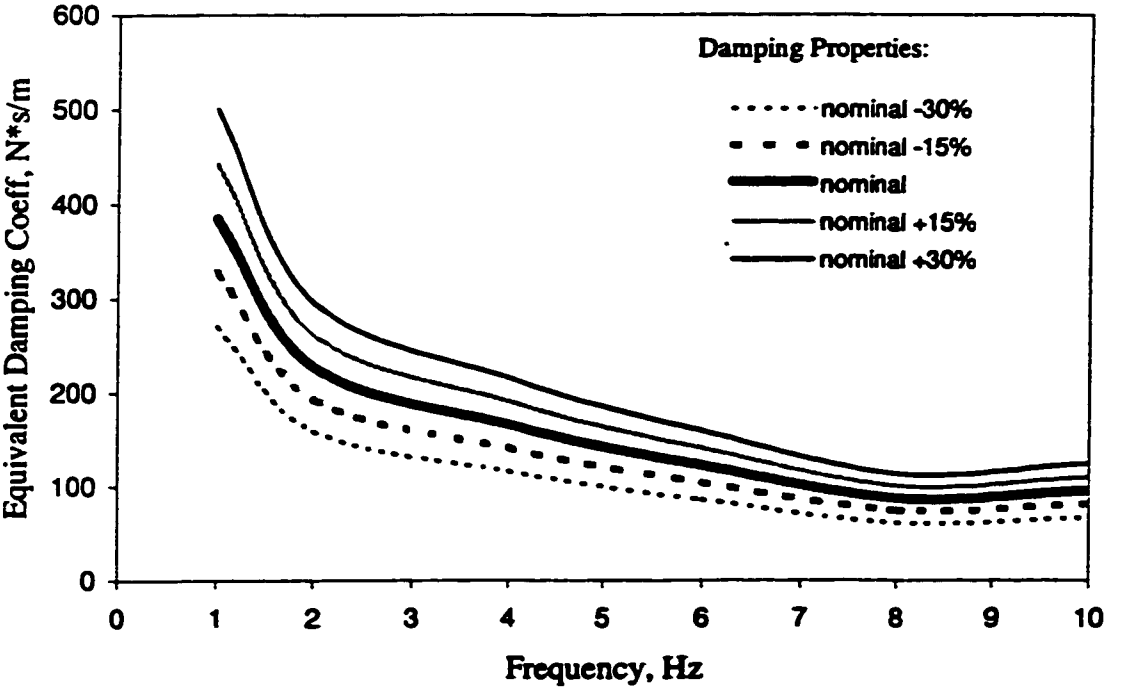

Figure 3.20: Variations in Cushion Damping Properties for Seat 'A'.

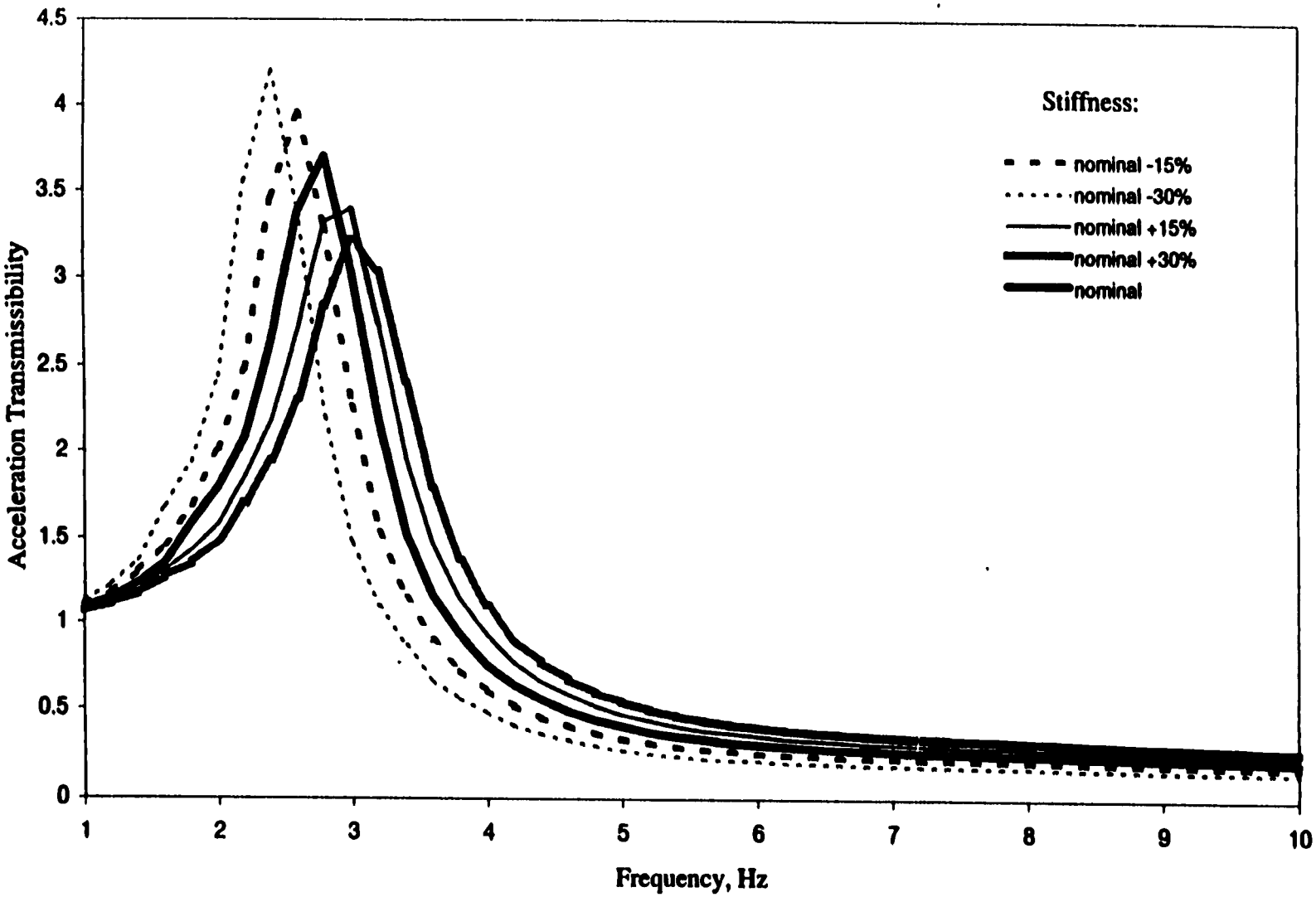

Figure 3.19: Influence of Variations in the Cushion Stiffness on the Acceleration Transmissibility of the Seat 'A'.

soft cushions lead to increased pressure and possibly pain and discomfort at the hip joint. Softer cushions also tend to reduce the resonant frequency of the seat-human system, from 3 Hz to 2.4 Hz, with a significant increase in the resonant acceleration transmissibility. The acceleration transmissibility in the vicinity of whole-body resonance and at higher frequencies, however, decreases. In view of the driver comfort and acceleration transmissibility, it is desirable to select a cushion that is neither too hard nor too soft.

Influence of cushion stiffness on the vibration attenuation performance of the static seat, subjected to random excitations, is investigated according to the methodology developed in section 2.7.2. The array of nominal local stiffness constants $[K_{NOM}]$ is varied within the identical to that described for deterministic excitations. The seat isolation efficiency is evaluated in terms of its S.E.A.T. values, which are derived based on the overall rms acceleration at the seat and the base, as described in section 1.2.3. While the S.E.A.T. values based upon unweighted acceleration response provide the effectiveness of the seat, the significance of frequency contents in relation to the human response to vibration is not truly described. A seat with predominant vibration occurring in the vicinity of the whole-body resonance can lead to poor comfort performance, while the S.E.A.T. value based upon overall rms acceleration may yield significantly different information. It is thus desirable to derive the S.E.A.T. values based on frequency weighted overall rms acceleration upon integrating the human body weighting filter. The recent versions of ISO-2631 [17] and British Standard 6841 [16] have proposed frequency weighting filters based upon human sensitivity to vertical vibration. The asymptotic values of the frequency weighting factors proposed in BS6841, which is quite

similar to the W_K filter proposed in ISO–2631 (1994), have been summarized previously in Table 1.1.

Table 3.3 summarizes the influence of variations in the cushion stiffness on the S.E.A.T. values of seat 'A' based upon unweighted and weighted acceleration response.

TABLE 3.3: Influence of cushion stiffness on S.E.A.T. values for seat 'A'.

K (cushion stiffness)	S.E.A.T. (unweighted)	S.E.A.T. (weighted)
Nominal -30%	0.86	0.8
Nominal -15%	0.90	0.9
NOMINAL	0.93	1.0
Nominal +15%	0.97	1.09
Nominal +30%	1.00	1.17

The seat evaluation method using S.E.A.T. values also takes into account the input vibration spectra, together with the seat and occupant response. The input acceleration PSD spectra for seat 'A' exhibit low level of vibration in the 2-3 Hz frequency band and relatively high levels of vibration in the 1-2 Hz and 3-6 Hz bands, as illustrated in Figure 2.16 (section 2.4.2). The seat cushion with stiffness equal to 70% of the nominal value yields good attenuation of vibration in the frequency bands where the vibration level are high. From the comparison of S.E.A.T. values derived from weighted and unweighted acceleration response, the following observations are made:

- S.E.A.T. values based upon overall true rms acceleration (unweighted) describe the variations in the seat effectiveness with variations in the cushion stiffness parameter.

- S.E.A.T. values based upon weighted acceleration response also provide a seat comfort performance information. When the frequency weighting for the human response to vibration is incorporated, the S.E.A.T. values increase when compared with the unweighted S.E.A.T. values. For a given particular vibration environment and nominal values of cushion stiffness, a S.E.A.T. value of 1.0 indicates that there is no overall improvement or degradation in vibration discomfort produced by a seat, although the seat may have amplified or attenuated vibration in certain bands. The results clearly illustrate that lower cushion stiffness yields lower value of S.E.A.T.

Influence of cushion damping.

An important factor in vibration isolation is the amount of damping present in the isolator and its influence on the vibration isolation performance. In this study, the damping due to a seat cushion is varied by $\pm$15% and $\pm$30% around nominal value to investigate its influence on the seat performance. At each selected discrete frequency, the equations of motions (2.1) are solved to determine nominal local damping corresponding to the nominal damping characteristics to formulate the array $[C_{NOM}]$. The arrays of nominal coefficients is scaled such as $0.7*[C_{NOM}]$, $0.85*[C_{NOM}]$, $1.15*[C_{NOM}]$ and $1.3*[C_{NOM}]$ represent the chosen variations in the cushion damping. Figure 3.20 illustrates the variations in the local equivalent damping constants in the 0-10 Hz frequency range. Figure 3.21 illustrates the influence of cushion damping on the acceleration transmissibility characteristics of the seat 'A'. An increase in cushion damping affects the resonant vibration transmission performance quite considerably, while the influence on the resonant frequency is insignificant. An increase in damping parameter from 0.7 to 1.3 of nominal causes peak transmissibility to decrease from 4.2 to 3.3, without affecting the transmission performance in the isolation frequency range.

The influence of variations in the cushion damping on the seat performance under random excitations is evaluated in terms of S.E.A.T. values for $\pm$15% and $\pm$30%

variations. Table 3.4 summarizes the S.E.A.T. values based upon unweighted and weighted rms accelerations as a function of the variations in the cushion damping. Table 3.4 illustrates that the changes in damping parameters also effect the S.E.A.T. values derived for a seat-human system. The S.E.A.T. values suggest that increase in damping parameter can improve the vibration isolation performance of a static seat. A +30% change in damping properties, however, reduces S.E.A.T. by only 5%.

TABLE 3.4: Influence of cushion damping on S.E.A.T. values for seat 'A'.

C (cushion damping)	S.E.A.T. (unweighted)	S.E.A.T. (weighted)
-30%	0.99	1.05
-15%	0.96	1.02
NOMINAL	0.93	1.00
+15%	0.91	0.97
+30%	0.89	0.95

3.7 Summary.

In this chapter, a comparative study between the vibration transmission characteristics of seats 'A' and 'B' loaded with human subjects and a passive load is performed. The data is analyzed to derive a Human Response Function, which is utilized to evaluate the seat-human system performance from the measured seat-passive load system performance characteristics. The effectiveness of the proposed Human Response

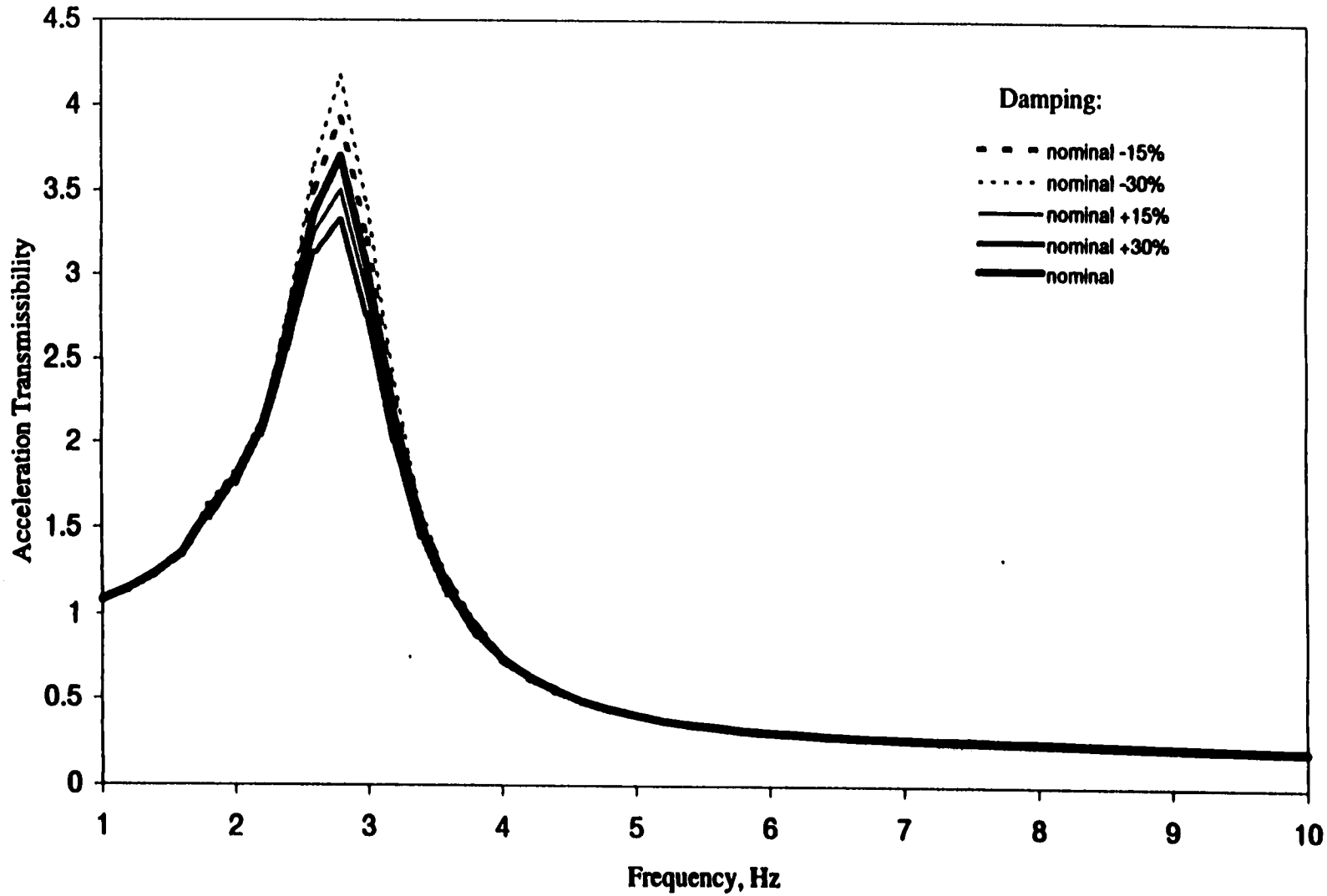

Figure 3.21: Influence of Variations in Cushion Damping on Acceleration Transmissibility of the Seat 'A'.

Function is investigated by comparing the seat-human system model response with that established from the laboratory tests. The comparison demonstrated a high degree of correlation between the analytical and experimental data. Two performance indices based on deterministic and random response characteristics are defined to investigate the influence of variations in the seat parameters on the ride performance of the seat-human model. The results of the parametric sensitivity analyses revealed that the comfort performance of a seat can be enhanced by decreasing its stiffness and increasing its damping characteristics.

CHAPTER 4

VIBRATION TRANSMISSION ANALYSIS OF DYNAMIC SEATS

4.1 General

The ride vibration of heavy vehicles, whether highway or off-highway, predominate in the frequency range of 0.5-5 Hz. The amplitudes of vibration encountered by the off-road vehicle drivers, however, are significantly larger than those encountered by the highway vehicle drivers. Although considerable research and development efforts have been made to improve off-road vehicle ride via suitable tires and primary-suspension, the need for further improvement in ride has been emphasized in view of three factors: large amplitude of ride vibrations, specifically in off-road vehicles; prolonged exposure time; and ride frequencies coinciding with the human body resonance in certain off-road vehicles [22,25]. In order to improve the off-road vehicle ride performance, the need for developing effective secondary (seat and cab) suspension has long been identified by the concerned industries. Suspension at the cab can provide for the drivers: a stable floor, isolation from forces introduced by implemented loads, and isolation from noise and chassis vibrations. However, the cabs in small size off-road vehicles are often welded to the chassis along with the Rollover Protection Structure (ROPS), and hence the suspension at the cab requires complex alterations. Suspension at the seat is perhaps the simplest option for ride improvement.

A dynamic or suspension seat comprises an energy restoring element, either pneumatic or mechanical, an energy dissipating element, motion limiting bump stops, and linkages to ensure nearly vertical motion. The performance characteristics of dynamic seats have been evaluated through laboratory and field measurements performed

using passive as well as human loads [21,22]. Analytical models have also been developed to derive effective designs of suspension components [21,22]. All the reported models, however, are based upon lumped parameters, where the kinematic and dynamic motions of the linkages are neglected assuming perfectly vertical motion [21]. Furthermore, majority of the models consider linear vertical stiffness and damping elements, while only few studies have considered symmetric nonlinear bump stops and damping properties [24,25,26]. In this study, an analytical model of a dynamic seat is developed incorporating kinematic and dynamic motions of the linkages, inclined damper and horizontal coil spring, nonlinear asymmetric damping and stiffness properties of the motion limiting bump stops. An analytical model of a selected under-the-seat-suspension system incorporating rigid load and human driver model is developed using ADAMS (Automated Dynamic Analysis of Mechanical Systems) software. The response characteristics derived under different types of excitations are compared with those obtained from the laboratory tests to validate the analytical model. The resulting model is then proposed as an efficient design tool to assess the suspension performance in view of its components and linkage design.

4.2 Description of Dynamic Seats

A number of seat-suspension systems with low natural frequency have been developed for highway as well as off-highway vehicles. The seats are designed with a range of adjustments, such as ride height, fore-aft, cushion angle, back-rest inclination, etc. Attenuation of terrain induced ride vibration is primarily achieved through suspension springs and shock absorber. Figure 4.1 illustrates the schematic of a

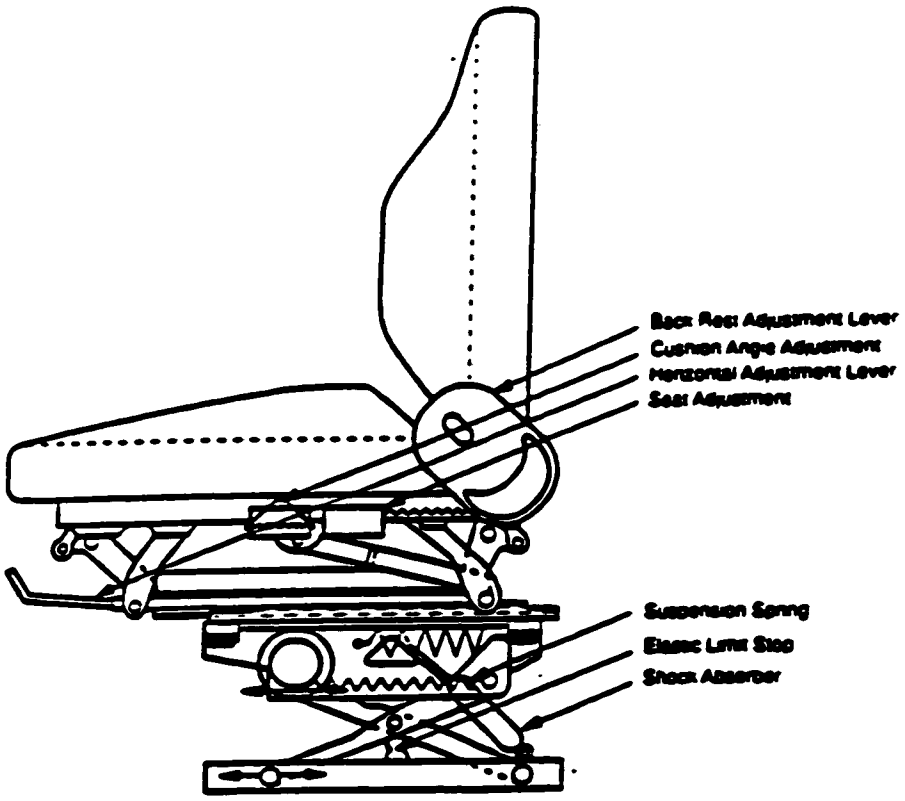

Figure 4.1. Schematic of under-the-seat mechanical seat-suspension.

mechanical under-the-seat suspension, which comprises a cross-linkage mechanism, an inclined shock absorber, horizontally mounted coil springs, and necessary adjustments. The suspension system comprises an elastic bump stop in the compression mode, and a relatively stiff stop in the extension mode. The suspension travel in the extension mode is limited by constraining the horizontal motion of guided rollers attached to the cross-links. The low natural frequency of the suspension seats yields high magnitudes of relative static and dynamic deflections under low frequency terrain-induced vehicular vibration. The drivers are then frequently exposed to shocks arising from impacts with the bump stops. The analysis of such shock motions necessitates the study of kinematic and dynamic motion of the cross-links and the guided rollers. The suspension seat consists of a horizontally mounted coil spring, which is attached to the cross-links. The suspension force developed by the spring is thus related to the angular motion of the cross-links. While all the analytical models reported in the literature consider only vertical springs, the suspension performance is influenced by the kinematic and dynamic motion of the cross-links.

4.2.1 Seat-suspension Components

The dynamic comfort offered by the seat is a function of design, construction, kinematics, easy of suspension adjustment, and vibration attenuation performance of the suspension system. Among these factors, the kinematics of the suspension linkage, stiffness, and the damping mechanism influence the vibration transmission characteristics of the seat-suspension.

Seat Compliance: The compliance in seat-suspension is invariably achieved through steel, rubber or air springs. Leaf springs have been extensively used in former rudimentary seats, but they are unable to meet the present stroke prerequisite. Torsion bars offer a convenient design, but the constraints on overall seat dimensions limit the use of plain conventional torsion bar. However, composite bars made of small wires and thin plates have been proposed. Rubber springs can be used only in conjunction with large leverage ratio to allow sufficient travel between the bump and the suspension. Pneumatic springs are frequently used in highway vehicle seat suspension since they provide the flexibility to adjust for driver's weight and low natural frequency.

Seat-Suspension Linkage: The linkage in a seat-suspension is designed to ensure parallel seat displacement nearly as vertical as possible along the suspension stroke, while providing the necessary height adjustment. The limiting factor is usually the available room. Linkage systems are grouped in two categories: under the seat linkage systems, as shown in Figure 4.1 and behind the seat linkage system. The primary considerations in linkage design include: (i) the ability to provide a wide range of height adjustment; (ii) to ensure almost vertical motion; (iii) to ensure minimum joint friction to minimize jerk; and (iv) compactness.

Damping Mechanism: The suspension seats invariably include a shock absorber to provide adequate damping. However, certain seats offer a mechanism to engage the shock absorber only when severe shock input is encountered. The role of damping in vibration attenuation performance is discussed in the following subsection and the typical dissipative properties of the shock absorbers employed in seat-suspension systems are described in details in section 5.3.2.

4.2.2 Vibration Attenuation Requirements

The human body is most sensitive to low frequency whole-body vibration and thus a suspension seat must be selected to minimize the transmission of these vibrations arising from wheel-terrain interactions and jolting. In order to provide the drivers with a controlled comfortable posture, the suspension seat should yield minimal relative displacement of the driver with respect to the controls, and minimize head snapping and back slap. Adjustabilities in view of seat height, seat-pedal distance, lumbar support, cushion angle, etc., must be available to ensure adequate vision and posture. The vibration environment and the enclosure design must be given appropriate consideration in selecting the seat-suspension for a specific vehicle.

The rms acceleration spectrum of a forestry vehicle, measured under typical operating conditions reveals that the ride vibration predominate in the low frequency, 2.2 to 2.6 Hz range [76], which is attributed to the resonant frequency of unsuspended wheeled off-road vehicles. This frequency range thus represents the range of excitation frequencies that should be attenuated through a properly tuned seat suspension. Consequently, the seat must be designed with a resonant frequency less than $1/\sqrt{2}$ times the forcing frequency, for the seat-to-floor transmissibility ratio to be less than 1.0 at the predominant frequency.

Since the seat's natural frequency, and thus its transmissibility characteristics, are likely to be influenced by the driver's weight, it is important that the seat-suspension be equipped with a control, whether manual or automatic, to permit suspension stiffness variations such that the natural frequency remains nearly constant regardless of the driver's weight. Most mechanical seat suspensions are equipped with a manual dial which

which permits adjustments for the driver's weight. In the case of pneumatic suspensions, automatic self-leveling mechanisms exist to automatically adjust the height according to the driver's weight on the seat. In any event, the weight compensation mechanism should be independent of the height adjustment for the seat to preserve its optimal vibration attenuation capabilities. Low natural frequency suspension yields excessive static and dynamic relative travel that affects the driver's interactions with the controls in an adverse manner. The suspension travel should thus be limited either by installing elastic limit stops, adequate suspension linkages, or both. A maximum travel of 100 mm is generally acceptable for off-road vehicles.

Finally, the damping coefficient associated with the suspension should be such that the amplification of the vibration at the seat's resonant frequency is not excessive. A transmissibility ratio ranging from 1.5 to 2.0 at the resonant frequency is generally considered to be a maximum acceptable value for the seat to be effective [21]. In addition, suspension damping must be sufficient to prevent occasional bottoming of the suspension in the case of shock loading or transient vibration.

4.2.3 Identification of Static and Dynamic Characteristics of the Seat-Suspension Systems

Development of an effective analytical system model necessitates a comprehensive knowledge of both static and dynamic characteristics of various subsystems. Seat-suspension systems, described in section 4.2, require quantitative description of the properties of the cushion, spring, shock absorber, etc. The parameters for the under-the-seat mechanical seat-suspension system have been identified from the static and dynamic tests performed in the laboratory [21] and summarized in Table 4.1.

The laboratory characterization study has reported equivalent linear stiffness and damping properties of the cushion, equivalent vertical spring rate of suspension, ideal friction force, and symmetric force-velocity characteristics of the suspension damper. The measured data was further analyzed to identify hysteretic damping due to cushion and asymmetric damping properties of the hydraulic shock absorber.

Table 4.1: Parameters of the ISRI-Mechanical Seat-Suspension System [21].

DESCRIPTION	VALUE
Driver mass, kg	56.2
Suspension mass, kg	10
Cushion stiffness, N/mm	70
Cushion damping coefficient, N*s/mm	0.15
Suspension Spring Stiffness, N/mm	4.9
Vertical distance between bump stops, mm	75
Shock absorber damping coefficients, N*s/mm - Low speed - High speed	$C_{1A} = 0.71$ $C_{1B} = 0.592$
Velocity at which transition from C_{1A} to C_{1B} occurs, mm/s	32
Coulomb friction force, N	20

SAE recommended test procedures, similar to those described in section 2.4.1, were used to measure the static characteristics of the seat cushion [68]. Figure 4.2 illustrates the static force-deflection characteristics of the cushion measured during loading and unloading. An examination of the measured force-deflection characteristics of the cushion reveals considerable hysteresis, as indicated by the difference between the

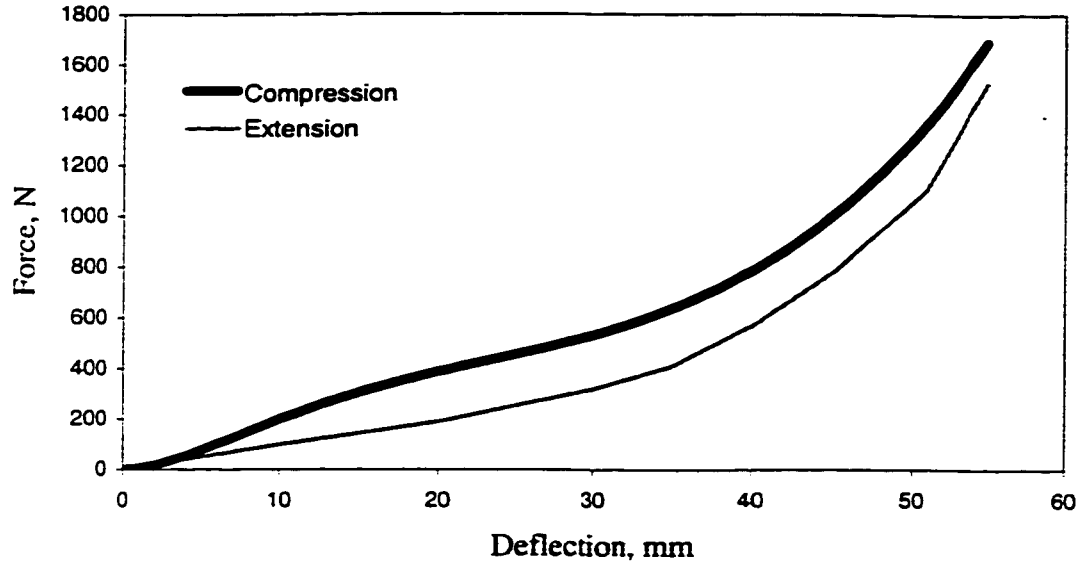

Figure 4.2: Static Force-Deflection Characteristics of Seat Cushion.

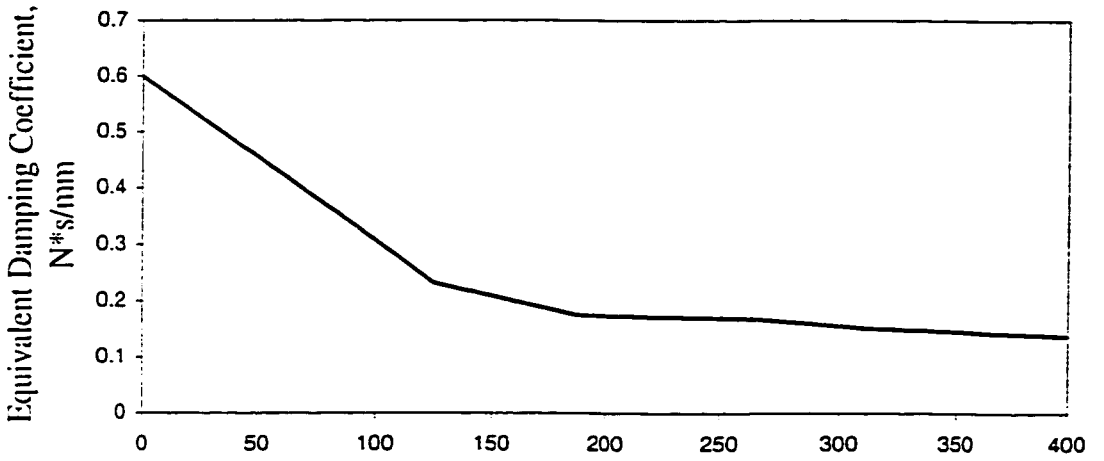

Figure 4.3: Damping Characteristics of the Seat Cushion.

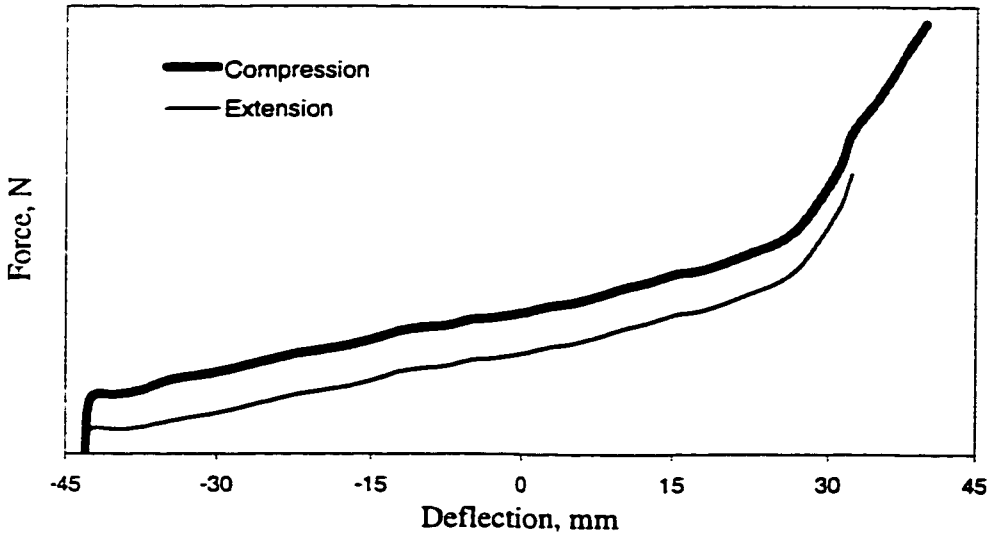

Figure 4.4: Static Force-Deflection Characteristics of the Seat-Suspension.

loading and unloading curves. The force-deflection characteristics exhibit certain nonlinearity, specifically under excessing load, which may be attributed to the deformation of the supporting structure.

The damping properties of seat cushion were evaluated via dynamic testing of the cushion. The seat cushion was tested under sinusoidal displacement excitations in the 1-8 Hz frequency range. The damping associated with the cushion was estimated by equating the energy dissipated per cycle of vibration by the cushion to that of a viscous damper. The equivalent damping coefficients of the seat cushion, evaluated as a function of the velocity, is presented in Figure 4.3. The seat cushion reveals high damping at low velocities or low frequencies and the damping coefficients decreases rapidly with increase in velocity or excitation frequency.

Static force-deflection characteristics of the ISRI seat-suspension system were also measured to determine the spring rate, hysteresis due to linkages, seat travel, and elastic properties of the travel limit stops. Figure 4.4 illustrates the static force-deflection properties of the seat suspension under 540 N preload. The force-displacement curves during loading and unloading revealed a steep slope at the extremities of the suspension travel, as shown in the figure. The slope of the curve around the extremities determines the spring rate of the bump stops in compression and rebound (extension).

Damping properties of the shock absorber were estimated from the force-velocity characteristics supplied by the manufacturer. The mean force-velocity characteristics of a typical shock absorber are presented in Figure 4.5. The mean force-velocity properties exhibit considerably higher damping force in rebound than that in compression. Furthermore, the damping coefficient corresponding to low velocities is considerably

larger than that at higher velocities. The force-velocity characteristics of the damper are thus represented by asymmetric piecewise linear function, as described further in section 4.3.2. Assuming asymmetric characteristics, the shock absorber parameters are deduced as: C_{1A}=280 N*s/m, C_{1B}=208 N*s/m, V_1 =0.032 m/s, C_{2A}=1120 N*s/m, C_{2B}=800 N*s/m, V_2 =0.06 m/s.

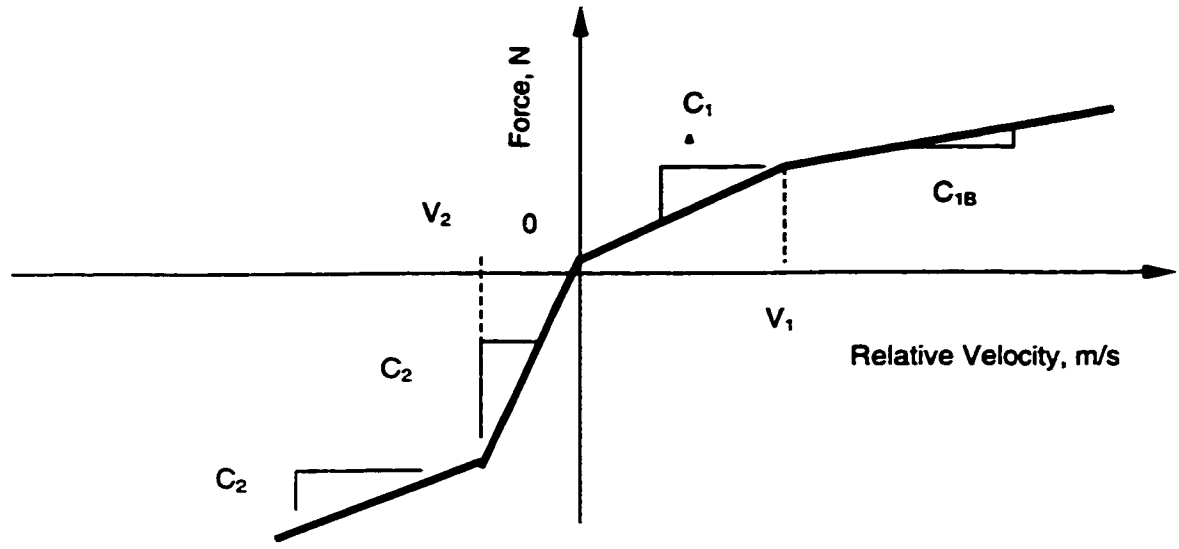

Figure 4.5: Typical Force-Velocity Characteristics of a Hydraulic Shock Absorber.

4.2.4 Description of Input Excitations

Mechanical suspension seats with limited travel are mostly used in off-road vehicles, such as these employed in forestry, construction and service sectors. The development of a design and analysis tools for suspension seat may thus incorporate representative of ride vibration environment of such vehicles. While the off-road vehicular vibration along the vertical axis predominate in the 0.5-5 Hz frequency range,

the human body exhibits higher sensitivity to vertical vibration in the 4-8 Hz frequency range. The frequency response behavior of suspension seats is thus frequently evaluated under sinusoidal vibration swept in the 0.5-10 Hz frequency range [21,22]. In this study, the proposed analytical model is evaluated under such harmonic excitations synthesized in the laboratory, as described earlier in section 2.5.3.

Sinusoidal excitations: The use of deterministic harmonic excitation offer the possibility of studying the behavior of the systems at selected frequencies, which otherwise would not be possible. The description of a synthesized swept sine signal, which was used for laboratory testing of an ISRI-mechanical seat-suspension system, is given in section 2.5.3.

Random excitations: Random vibrations, however, more closely represent the vibration environment of vehicles, in which the seat-suspension system must operate. Ride vibration data of various off-road vehicles have been reported in the literature [21,72]. The random data gathered during field measurements have been characterized by either acceleration PSD or rms acceleration. The consistency of the measured vibration data has lead to a rather standardized description of vertical vibration excitations for performance analyses of vertical seat-suspension systems. The ISO has proposed approximate expressions describing vertical acceleration PSD [72], which has been widely accepted for testing of vertical seat-suspension systems [53]. Based upon the ride vibration data of agricultural tractors measured on a simulated track, ISO 5007 [73] has proposed two vehicle classifications and their respective vertical accelerations in terms of PSD. The two vehicle classes, ISO1 and ISO2, are based upon vehicle loads, tire inflation pressure, and wheelbase. Figure 4.6 illustrates the acceleration PSD of the vertical

vibration characteristics of ISO1 and ISO2 classes. Alternatively, four classes of vibration are defined for different types of earthmoving machinery in ISO standard 7096 [74], of which Classes 1 and 2 have been compared with those of the forestry skidder vehicles [71]. The peak acceleration PSD measured at the seat location of Class 1 vehicles is 4.13 ($ms^{-2})^2$/Hz occurring at a frequency of 1.85 Hz, while the peak acceleration PSD of Class 2 vehicles is 2.4 $(ms^{-2})^2$/Hz occurring at 2.1 Hz. Figure 4.7 illustrates the acceleration PSD spectra of these two excitation classes.

Since WBVVS operates on the principle of position feedback, the proposed acceleration PSD function are analyzed to synthesize corresponding displacement-time histories. For this study, the ISO2 and Class 2 excitation classes were selected as input for the simulations and laboratory tests with WBVVS. The ISO2 and Class 2 input vibration signals were synthesized in the laboratory using DSP software and hardware. The resulting acceleration spectra are compared with those proposed in the standards, as shown in Figures 4.8 and 4.9. Although similar to the recommended PSD curves, the PSD of acceleration derived for synthesized motions corresponding to ISO2 spectrum yield peak values somewhat higher than the proposed values. The PSD of acceleration due to synthesized Class2 motion is observed to be lower than the recommended values, specifically in the 1-2.5 Hz range. The variations between the synthesized and recommended spectra are mostly attributed to excessive smoothing employed in deriving the proposed spectra. The spectrum of the synthesized signals is thus considered acceptable for the study of driver-suspension seat system, since they represent the most important spectral components.

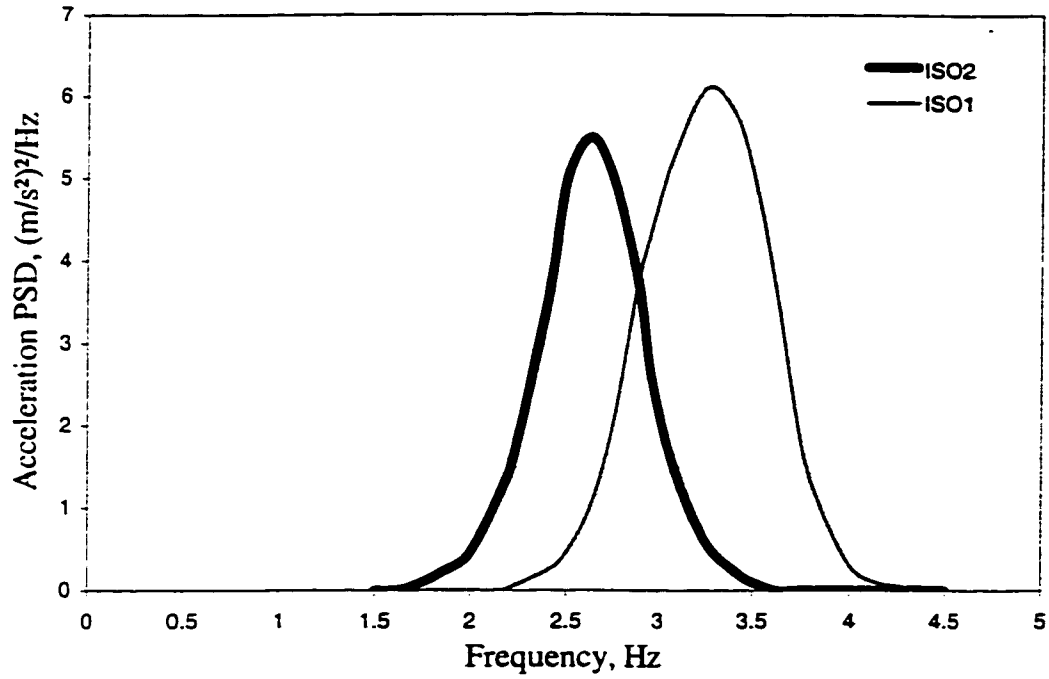

Figure 4.6: Acceleration PSD of the Vertical Vibration Characteristics of ISO1 and ISO2 Excitation Classes Defined in ISO 5007 [78].

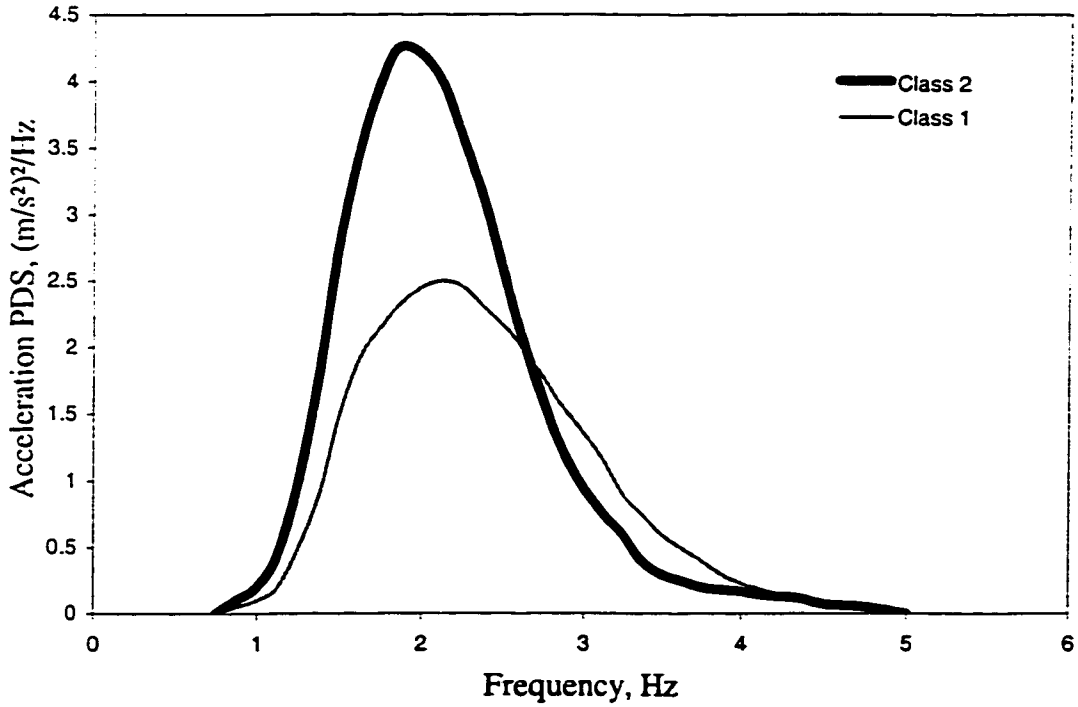

Figure 4.7: Acceleration PSD of the Vertical Vibration Characteristics of Class1 and Class2 Excitation Classes Defined in ISO7096 [79].

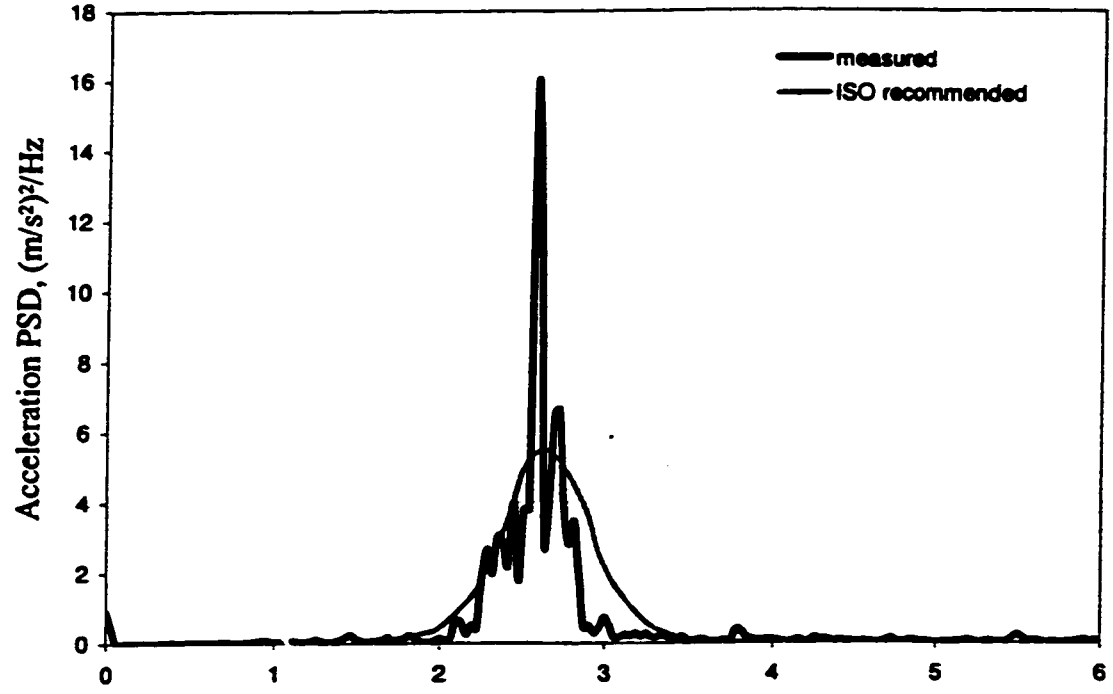

Figure 4.8: A Comparison of PSD of Measured Acceleration to that Recommended for ISO2 Vehicles.

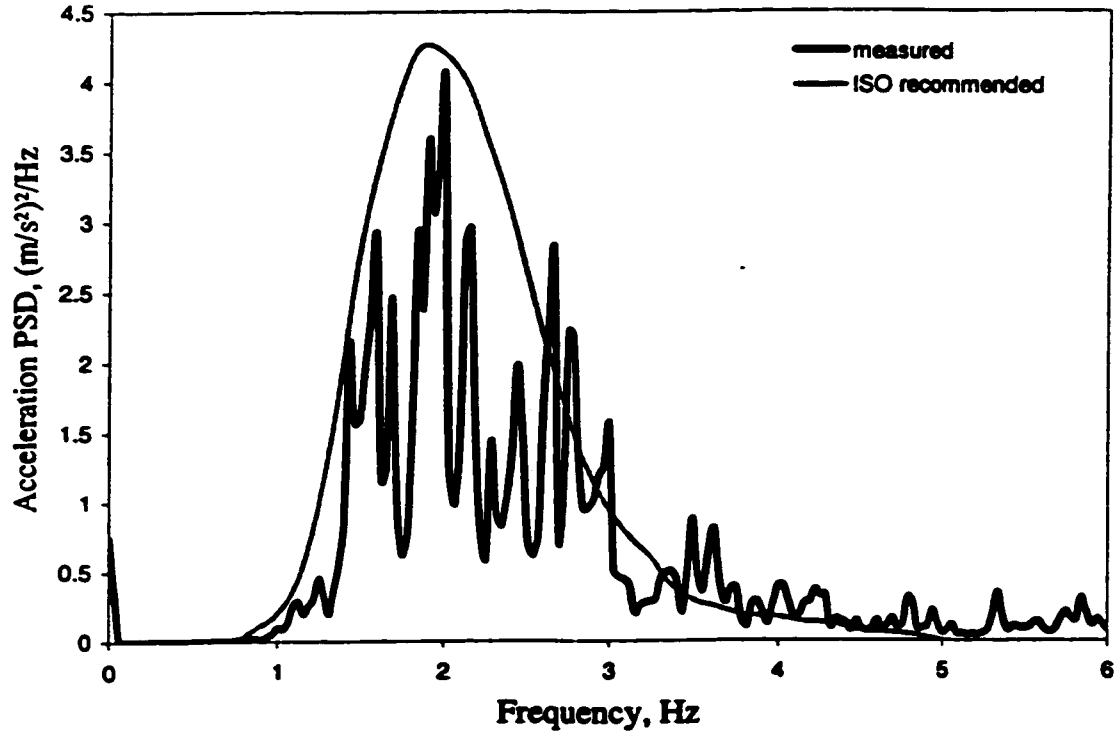

Figure 4.9: A Comparison of PSD of Measured Acceleration to that Recommended for Class2 Vehicles.

4.3 Development of Dynamic Seat and Occupant Model Using ADAMS Software

A number of analytical models of driver-seat suspension systems have been developed by different researches to derive the effective design of various suspension components. Different computer modeling techniques have been employed to investigate the effect of seat-suspension characteristics on a vehicle ride performance. The nonlinear effects were also included to better realize the quantitative and qualitative behavior of the seat-suspension system. The majority of the models, however, are based upon lumped parameters, neglecting linkage geometry, kinematics and dynamics of linkages. Only few studies have considered nonlinear spring, damping and bumpstops properties, and incorporated friction phenomena assuming ideal characteristics [21,22]. An ADAMS (Automated Dynamic Analysis of Mechanical Systems) software is a powerful tool that provides a user with the ability to develop and investigate the response of a mechanical system, which can incorporate about any of the existing nonlinearities with minimum assumption involved, kinematic and dynamic motion of linkages, joint friction phenomena, etc. A dynamic seat forms a mechanical system consisting of rigid and flexible components interconnected by different joints and constraint forces. The net reaction and applied forces determine the relative motions of the various components and thus the vibration characteristics of the seat. The kinematic and dynamic behavior of a mechanical system can be effectively analyzed using the Mechanical System Simulation (MSS) techniques, which is the study of motion of mechanical systems subjected to external forces and excitations. The MSS of a dynamic seat necessitates following considerations:

1) Identification of a physical system which undergoes large motion (i.e. the extent of the relative motion of the components can be on the order of the overall dimensions of the system);

2) Idealization of a system by identifying various parts, joints and forces;

3) Development of a computer model of the idealized system;

4) Formulation of equations governing the system motion;

5) Solution of equations of motion at each point in time;

6) Post-processing and interpretations of the numerical results, and animations.

The purpose of ADAMS simulation software is to automate the last four steps, which are known to be most complex and demanding on human resources. The dynamic analyses of systems based upon rigid and flexible multibody formalism necessitates following characterizations of the components:

(i) Mass, inertial properties and initial conditions of all bodies that move freely;

(ii) Kinematic and dynamic constraints imposed on the components; and

(iii) Description of the forces acting on the various system components.

The ADAMS simulation software utilizes the user input to formulate the equations of motion. The nonlinear force-motion relationships for the system components are further described by the user either in the form of analytical functions or look-up tables. The equations of motion are solved to yield the system response and the software provides a comprehensive description of the state of the system at user-specified time intervals as the output. Thus, the time histories of the response variables are saved in output files, which may include displacements, velocities, accelerations, reaction and applied forces, user-defined variables and functions, etc. A description of the mechanical

seat-suspension model developed within the ADAMS simulation program is presented in the following subsections.

4.3.1 Modeling of Linkages and Constraints

An ADAMS model consists of a number of rigid bodies representing different components within a system. These rigid bodies are the only model elements that are permitted to possess certain mass. Each rigid body is represented by a collection of geometric elements that act and move as a single unit and are described by its inertia, initial position, and initial velocity. The suspension mechanism is represented by five major components, or rigid parts, namely: the base, referred to as *lowplatform;* seat pan or cushion support, referred to as *upperplatform;* the cross-links, referred to as *link1;* sliding rollers, referred to as *link2;* and *rigid load*, as shown in Figure 4.10. Each of these rigid bodies is described by its geometry, inertia and coordinates with reference to a fixed axis system. The attachment or connectivity information for the bodies are described by the constraint functions and joints. Constrains define rigid connections between the bodies and the resulting degrees-of-freedom. Such constraints are modeled as idealized massless, frictionless and infinitely rigid joints. A joint is used to constrain the relative motion of a pair of rigid bodies by physically connecting them in a specific form. The motion of suspension components are described through the following constraints, which define relative movements between the different parts:

(i) A revolute joint (1): between the *lowplatform* and *link2*, to describe the motion of the guided rollers located at the suspension base.

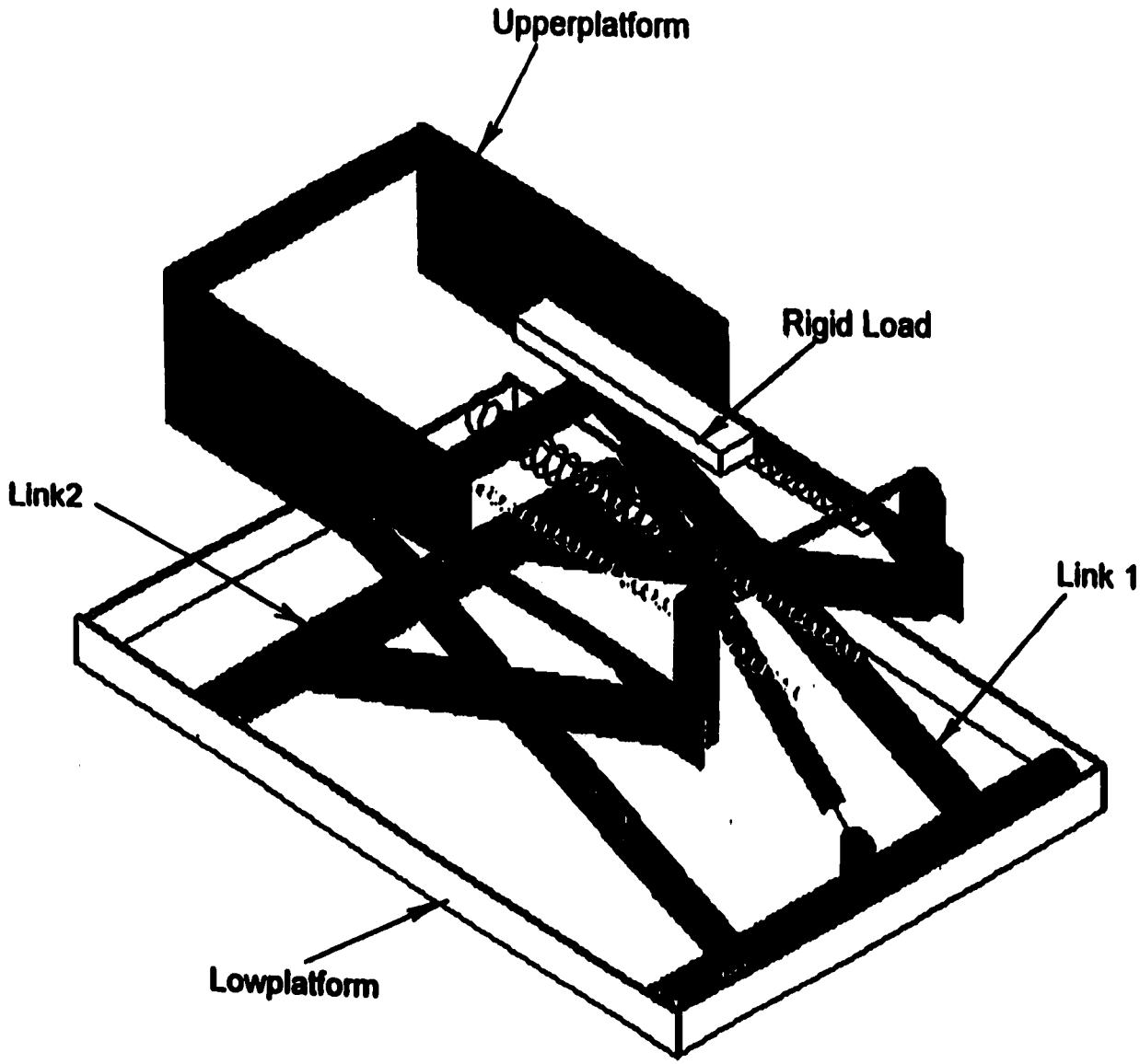

Figure 4.10 (a): An isometric view of a mechanical seat-suspension model coupled with a rigid load.

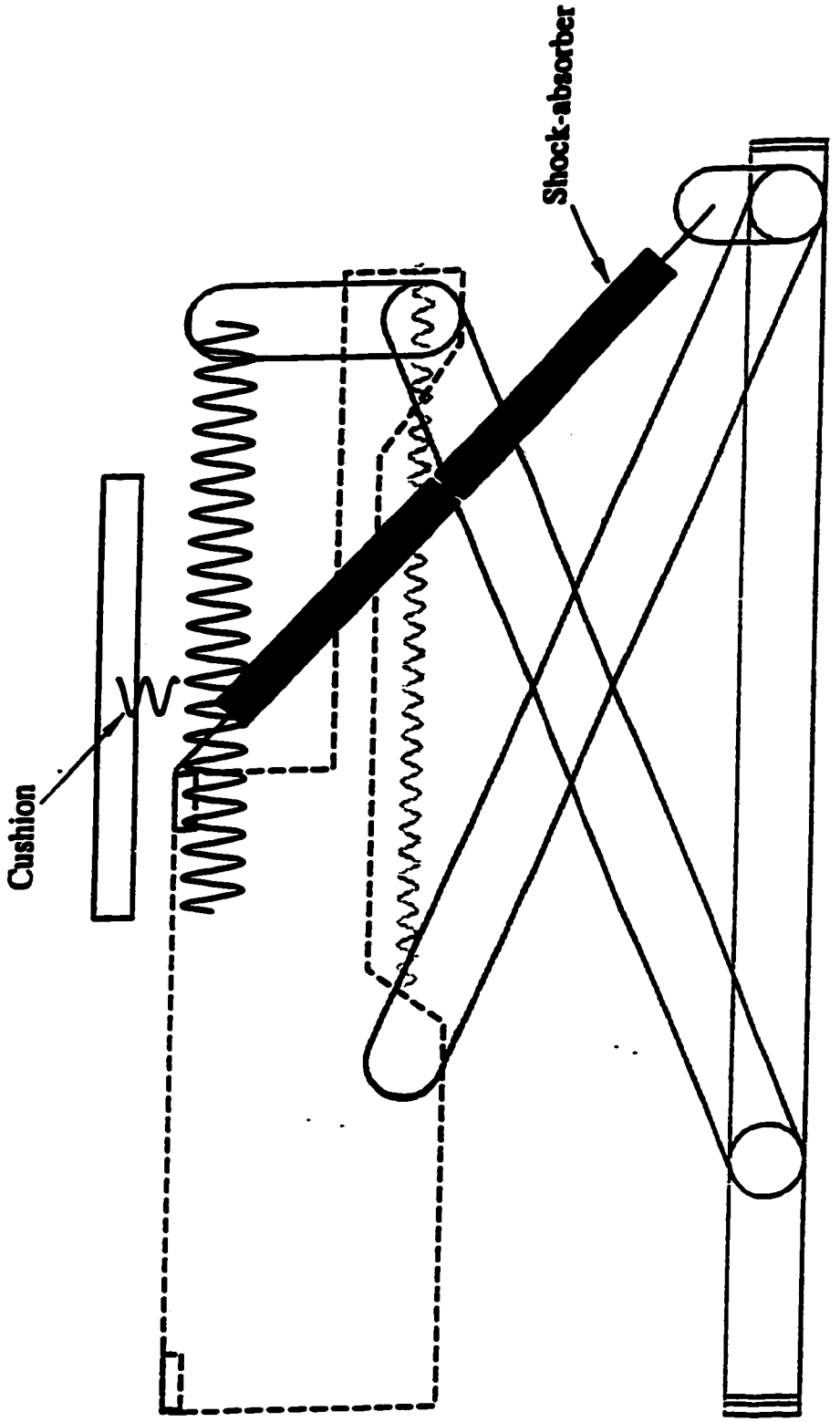

Figure 4.10 (b): Side view of the mechanical seat-suspension model coupled with a rigid load.

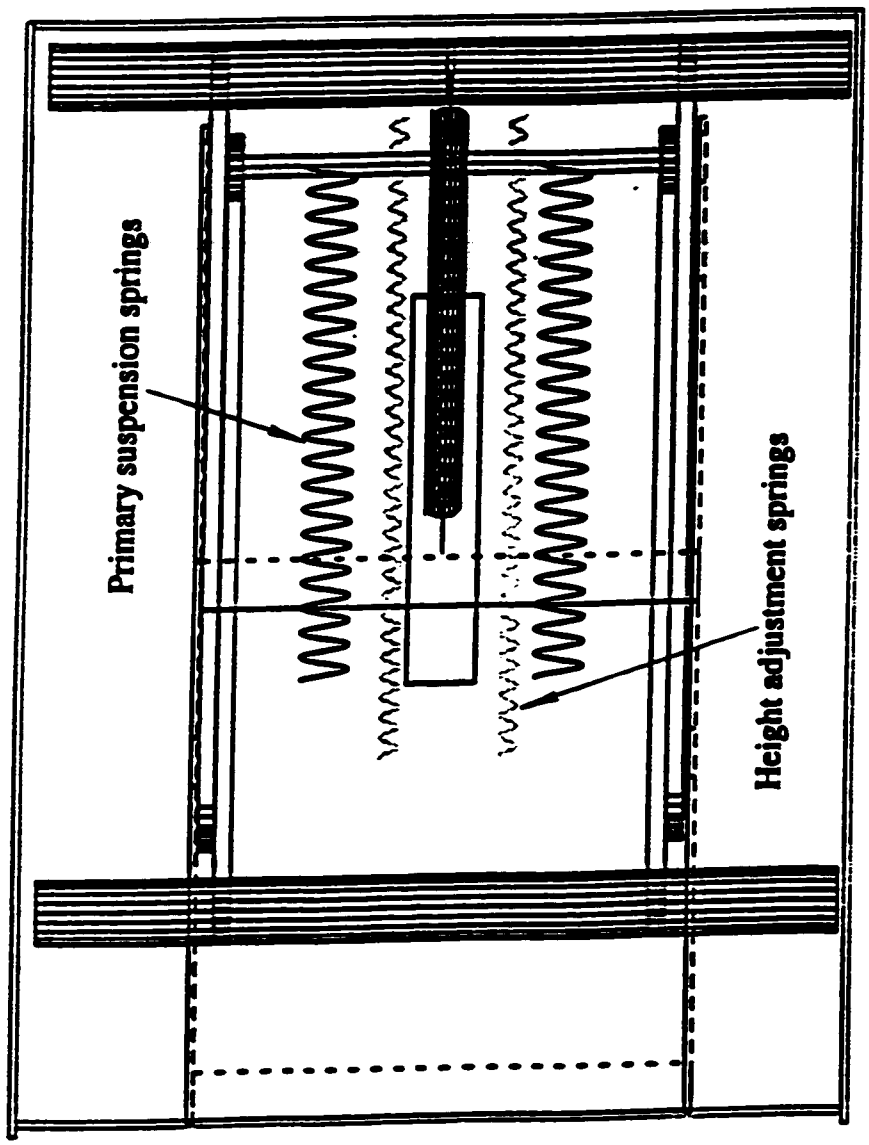

Figure 4.10 (c): Top view of the mechanical seat-suspension model coupled with a rigid load.

(ii) A revolute joint (2): between the *upperplatform* and *link1*, to describe the motion of upper guided rollers and thus the cross-links with respect to the seat pan or cushion support.

(iii) A revolute joint (3): between the *link1* and *link2*, to describe the relative kinematic motions of the cross-link about the bearing connection at the mid-section of the cross-links.

(iv) An inplane joint (1): between the *lowplatform* and *link2*, to describe the longitudinal motion of the rollers within the guides.

(v) An inplane joint (2): between the *upperplatform* and *link1*, to describe the longitudinal motion of the rollers within the guides.

(vi) A translational joint (1): between the *upperplatform* and *rigid load*, to describe the vertical motion of the seat load.

The revolute joint is a single-DOF joint that allows rotation of one part with respect to another about a common axis. Each of the revolute joint (1), (2) and (3) connects two different rigid parts and represents an existing physical analogue in a seat-suspension system, while the ADAMS inplane joints usually do not relate to physical analogy, they are employed to enforce the desired geometric constraints. An inplane joint indicates a five-DOF connection between two parts, which allows both transnational and rotational motion of one part with respect to another. The inplane joints (1) and (2) are used to describe the horizontal motion of the rollers attached to the links, within the lower and upper-platform guides. The guides impose one translational constraint that confines the relative vertical motion between the rollers and the platforms. Since in this study the vibration characteristics are derived for vertical direction only, a translational joint (1) is needed to ensure an appropriate motion for the part *rigid load* part that represents the seat load.

4.3.2 Modeling of Component Forces

The suspension components, such as springs and dampers, and the seat cushion are modeled as force generator, using their measured force-deflection and force-velocity characteristics. The component forces, thus defined, are applied as external forces to or between the rigid bodies in the ADAMS model. Such forces may be grouped into two broad classes:

- Specific (usually linear) force elements, such as beams and bushings, with predefined characteristics.
- General (nonlinear and user-specified) force elements for which there are no predefined characteristics, such as nonlinear springs, actuators, etc.

In the dynamic seat-suspension model, the force elements are defined to incorporate the restoring and dissipative forces due to cushion, forces due to suspension spring, bump stops, and hydraulic damper force in the model. The force elements corresponding to each of the component are described below.

Restoring Force due to Elastic Cushion: The nonlinear force-deflection characteristics of the seat cushion, illustrated in Figure 4.2 are incorporated in the ADAMS suspension-seat model using the SPLINE statement. The SPLINE statement utilizes discrete data points supplied by the user and performs interpolations using curve-fitting algorithms. The measured force-deflection properties of the seat cushion are thus used to formulate a look-up table in restoring force and deformation. The seat cushion is modeled as a translational single-component action-reaction force generating element, referred to as the "cush_spr". The force element is defined such that a translational force is applied along a vertical line connecting the *upperplatform* part and the *rigid load*, while the deformation is limited within the 0-55 mm range. This elastic range of

deformation is established from the measured force-deflection characteristics shown in Figure 4.2. The cushion exhibits bending deformation of the seat pan, when subject to further increase in the load. The bending of the seat pan, in general, yields higher vertical stiffness under deflection exceeding 55 mm. The restoring force due to cushion deformation beyond 55 mm is thus characterized by a second-stage spring, referred to as "cush-spr-endeffect". The restoring force developed by the seat cushion, represented by a two-stage stiffness element, is illustrated in Figure 4.11.

Cushion Damping Force: The hysteretic nature of the foam cushion is characterized by a damping force element. The damping force is developed as a function of the relative velocity between the *upper-platform* and *rigid load*. A translational damping force element, referred to as "cush_damp", is also defined on the basis of the SPLINE statement. The SPLINE function operates on a look-up table of discrete values of equivalent damping coefficients and relative velocity, derived from the data reported in Figure 4.3.

Restoring Force due to Suspension Spring: The measured static vertical force-deflection characteristics of the suspension, illustrated in Figure 4.4, exhibit effective restoring force due to horizontal spring suspension, hysteresis due to linkage and guided rollers, suspension travel and elastic properties of the travel limit stops. These suspension characteristics can be easily derived from the loading-unloading force-deflection curves presented in the figure. The results clearly show linear force-deflection characteristics in the 0-60 mm deflection range due to four horizontal steel springs. The restoring force developed by these springs is modeled using the VFORCE function in ADAMS, which

allows a representation of vertical force between *upperplatform* and *lowplatform* in the entire range of deflection.

Forces due to Bump Stops: Seat-suspension systems are invariably equipped with compression and extension bump-stops to limit the excessive travel of the suspension mass and the driver. The bump stops may be either rigid or compliant. Compliant bump stops, however, are highly desirable in view of excessive dynamic deflections of the low natural frequency suspension. Figure 4.11 illustrates the typical force-deflection characteristics of the suspension springs and the elastic bump stops, assuming symmetric properties in compression and rebound. The force-deflection characteristics reveal low stiffness coefficient (K_{1A}) due to the primary suspension springs, when the displacement amplitude is within the maximum permissible travel. The spring rate, however, increases considerably (K_{1B}) due to the elastic bump stops, when the suspension deflection exceeds the maximum permissible travel.

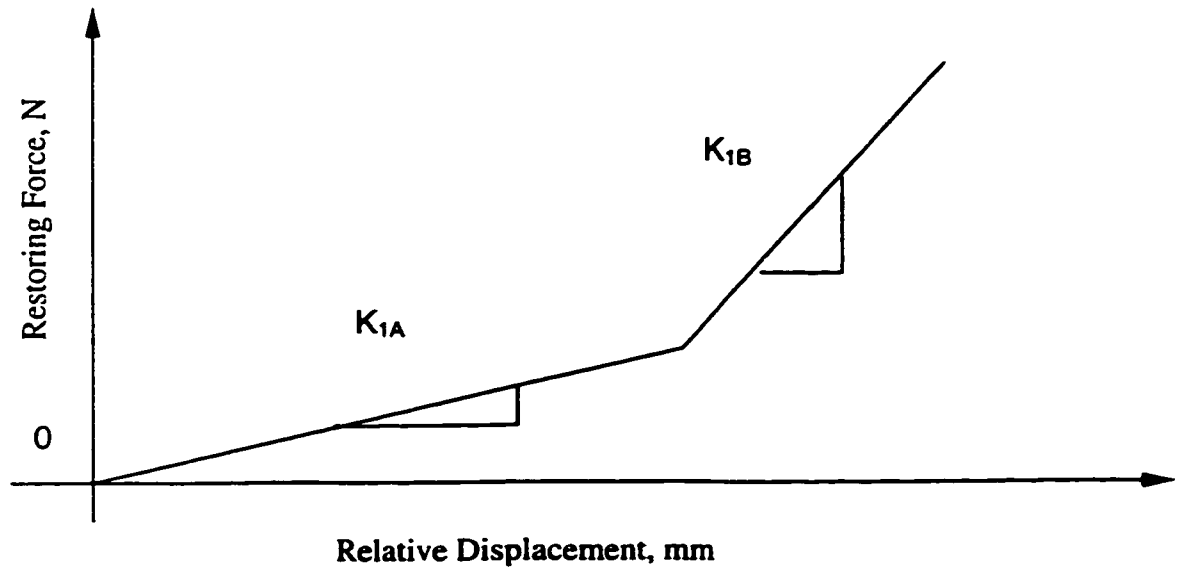

Figure 4.11: Typical Force-Deflection Characteristics of a Seat-Suspension.

The seat suspension system, considered in this study, is equipped with two soft elastic bump stops mounted on the suspension frame (*lowplatform*) to limit the downward motion in the compression stroke. Two relatively stiff bump stops are mounted within the roller guides (*upperplatform*) to limit the upward motion during extension or rebound of suspension mass. The force-deflection characteristics of two soft bump stops can be derived from the measured static force-deflection characteristics of the suspension shown in Figure 4.4. Such force-deflection properties are conveniently modeled in ADAMS as VFORCE "low_bump". This force becomes activated when the distance between *upperplatform* and *lowplatform* is less than 25 mm, which corresponds to the permissible travel of the suspension from the mid-ride level to the upper edge of the rubber bump stop.

The interactions between the guided rollers of *link1* and *link2* and almost rigid bump stops integrated within the *upperplatform* are modeled in ADAMS employing an IMPACT function. The IMPACT function models collisions between two objects and is activated when the axial distance between the objects approaches a value lower than a user-specified reference distance. Otherwise, the force function returns a value of 0.0. The IMPACT function yields two components of force arising from a spring or stiffness component, and a damping or viscous component. The spring force may be expressed by a linear or nonlinear function of the deflection and stiffness coefficient. While the IMPACT function yields an immediate spring force in an almost discontinuous manner, the dissipative or damping portion of the force is varied in a gradual manner. The magnitude of the damping force is considered as a linear function of the rate of change of the distance between the two objects. It also depends on a damping coefficient and the

penetration distance, which is used to define the interval over which the force ramps up to its maximum value.

Suspension damping force: The suspension damper yields variable damping characteristics associated with bleed- and blow-off control. Furthermore, the force-velocity characteristics of the suspension damper are asymmetric in compression and rebound, as illustrated in Figure 4.5. The shock absorber provides high damping constant corresponding to bleed-control at low piston velocity, and low damping constant due to blow-off control at high piston velocity. The transition from high to low constants occurs at a preset velocity. The damping coefficients in rebound are higher than those in compression. The damping force due to the shock absorber can thus be expressed as:

$$F(x,\dot{x},t)=\begin{cases} C_{1A}\dot{x}; if\, 0 \le \dot{x} \le V_1 \\ C_{1A}V_1 + C_{1B}(\dot{x}-V_1); \dot{x} > V_1 \\ C_{2A}\dot{x}; if V_2 \le \dot{x} < 0 \\ C_{2A}V_2 + C_{2B}(\dot{x}-V_2); \dot{x} < V_2 \end{cases} \tag{4.1}$$

where C_{1A} and C_{2A} are low speed damping constants corresponding to bleed control in compression and rebound, respectively. C_{1B} and C_{2B} are the damping constants in compression and rebound, respectively, corresponding to blow-off control. V_1 and V_2 are the transition velocities in compression and rebound and $\dot{x}$ is the relative velocity along the damper axis. In the ADAMS environment, the damping force between *upper-* and *lowplatform* due to the shock absorber, is represented by an action–reaction translational SFORCE function, referred to as "non_lin_damp". The magnitude and direction of nonlinear force is completely user-defined and may be expressed as a general function expression consisting of any combination of displacements, velocities, external forces,

etc. A set of equations (4.1) is then used to define the damping force, while its direction is determined from the instantaneous coordinates of the damper attachment points.

Suspension Friction force: The seat-suspension linkage exhibits dry or Coulomb friction due to rollers and pin-joints. It has been established that the magnitude of friction force depends mostly upon the preload and also upon the properties of the sliding surfaces [21]. Although Coulomb friction within the suspension system provides the necessary damping to suppress the resonant peaks, too large a value of Coulomb friction deteriorates the suspension performance in the isolation region. Furthermore, high friction tends to limit the effective seat travel due to its lock-up behavior. For the seat-suspension system, selected in this study, the coefficient of friction (ratio of friction force to the preload) was obtained to be approximately 0.1 [21].

While majority of the reported suspension seat models assumes negligible contributions due to friction, only few studies have incorporated friction assuming ideal characteristics [21,22]. Under the low amplitude and low excitation frequency, the suspension exhibits lock-up due to low resultant inertia force. However, as the inertia force exceeds the static friction force, the coulomb damper provides a constant force independent of the response velocity except for the sign.

The ADAMS software provides a possibility to represent joint friction forces more accurately, using the instantaneous reaction forces acting on the joints. The internal reaction forces are thus extracted at each integration time step to compute the instantaneous friction force. The magnitudes and directions of reaction forces due to algebraic constraints for revolute joints (1), (2), and (3), and inplane joints (1) and (2) for suspension system model, are retrieved through defining an ADAMS element-specific

JOINT function. Each of the element specific reaction force functions provides instantaneous response for a single constraint element. The forces due to dry or Coulomb friction within a roller or pin-joint in a seat-suspension linkage is then computed from the magnitude of the reaction force at the particular joint and the friction coefficient. Consequently, the joint friction forces are computed as functions of the element specific reaction forces.

For the inplane joints (1) and (2), the friction forces are represented by an SFORCE statement. The magnitude of each force is calculated at each integration stepsize according to:

$$F_F = \mu N ; \tag{4.2}$$

where F_F is the magnitude of the friction force, μ is the friction coefficient and N represents an element specific reaction force at corresponding joint, which is accessed through JOINT statement in ADAMS. The direction of F_F for inplane joint (1) or (2) is always horizontal but opposite to an instantaneous direction of a velocity vector of a corresponding guided roller.

Employing the above-described modeling technique, the rotational friction torques are also incorporated within revolute joints (1), (2) and (3). The magnitude of the friction torque during simulation is determined according to equation:

$$T_F = \mu T ; \tag{4.3}$$

where T_F is the magnitude of the friction torque, T is the magnitude of the element-specific reaction torque at the specific revolute joint and μ is the friction coefficient.

4.4 Verification of the ADAMS Model

The validity of suspension seat model, developed using ADAMS software, is examined by comparing its vibration transmission response with the laboratory measured data. The model, when validated, can serve as an important design tool not only for the energy restoring and dissipative components, but also for the suspension linkage. The ADAMS model is analyzed with a rigid load and a driver model, under deterministic and stochastic excitations. The response characteristics are compared with the measured data to examine its validity.

4.4.1 Dynamic Seat with Rigid Load

The mechanical seat-suspension system, loaded with a sandbag, was tested under sinusoidal excitations in the 0.5-8.0 Hz frequency range [21]. The vertical vibration transmissibility of the suspension and the seat are evaluated as the ratio of amplitude of response acceleration to the amplitude of input acceleration at each excitation frequency. The vibration transmissibility is expressed in terms of acceleration transmissibility of the suspension mass, and that of the seat. The tests were performed under sinusoidal displacement excitations of 12.5 mm amplitude. Owning to the small amplitude of horizontal acceleration measured at the seat, the discussions on the horizontal acceleration response are omitted.

The ADAMS model of a seat-suspension system, incorporated a rigid load (56.2 kg) representation of a driver mass was analyzed for validation purposes. The sinusoidal excitations of 12.5 mm amplitude at discrete frequencies in the 0.5-8 Hz range served as

input for simulations. The acceleration transmissibility characteristics of the suspension mass are computed as the ratio of suspension mass acceleration to the excitation acceleration magnitude. The acceleration transmissibility of the seat is also computed as the ratio of driver mass acceleration to the excitation acceleration magnitude. The acceleration transmissibility characteristics of the suspension mass and seat are compared with those derived from the laboratory test data to examine the validity of the model. Validations are initially performed for seat-suspension model without a shock absorber (force "non_lin_damp" is deactivated during simulations). Figures 4.12 and 4.13 present a comparison of the analytical and experimental vibration transmissibility characteristics of the suspension and driver mass, respectively. The measured acceleration transmissibility characteristics reveal that the seat-suspension system resonates near1.4 Hz. The excessive relative motion of the suspension mass around the natural frequency yields repetitive impacts against the bump stops, which was observed during experiments [21]. The undamped seat suspension system exhibits a high resonant peak around its resonant frequency due to repetitive impacts of suspension frame against the bump stops, as shown in the vibration transmissibility characteristics of both the suspension and the seat. The analytical vibration transmissibility characteristics of the suspension system are in good agreement with those established via laboratory experimentation.

The vibration transmissibility characteristics of the damped suspension system, established via ADAMS simulations and laboratory experiments, are presented in Figures 4.14 and 4.15. The shock absorber parameters are derived form the nonlinear force-velocity characteristics, as discussed in section 4.3.2. These figures clearly illustrate that

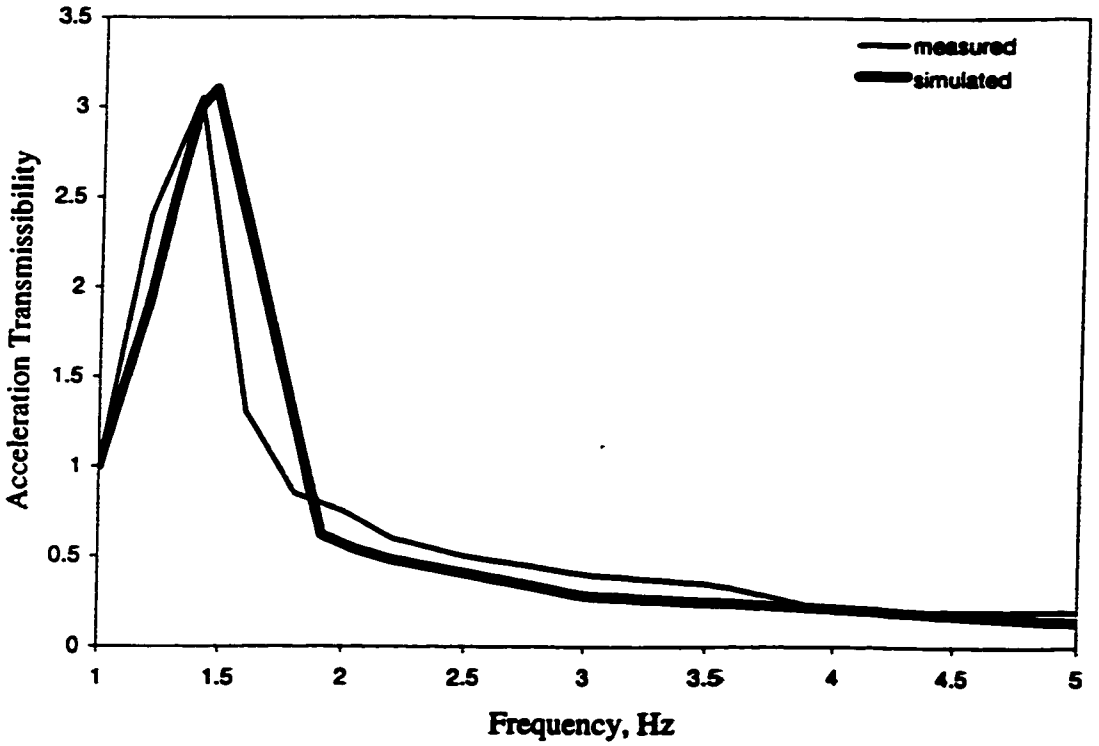

Figure 4.12: Comparison of Measured and Simulated Suspension Transmissibility Characteristics (Shock-Absorber Removed).

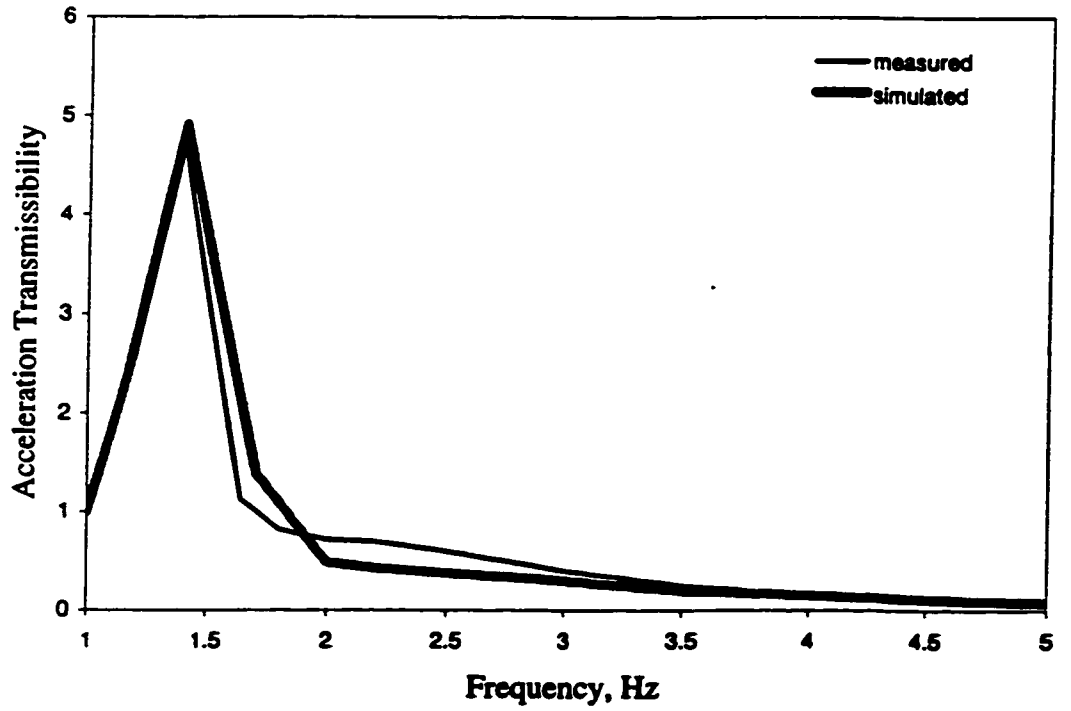

Figure 4.13: Comparison of Measured and Simulated Seat Acceleration Transmissibility Characteristics (Shock-Absorber Removed).

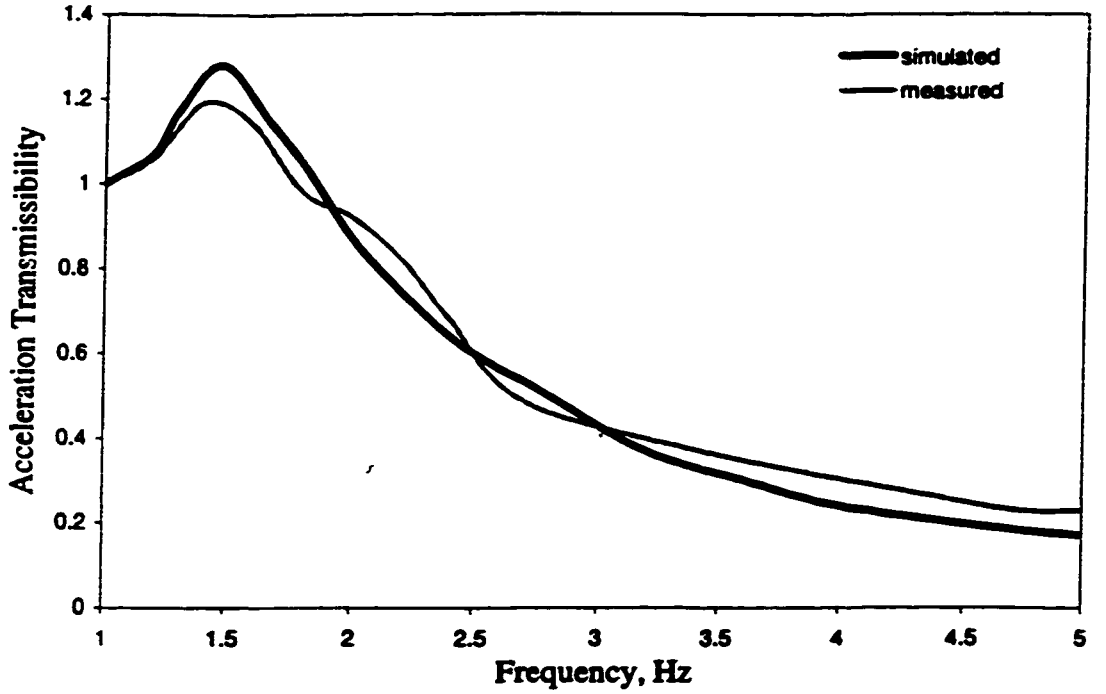

Figure 4.14: Comparison of Measured and Simulated Acceleration Transmissibility Characteristics at the Suspension for Damped ISRI-Mechanical Seat-Suspension System.

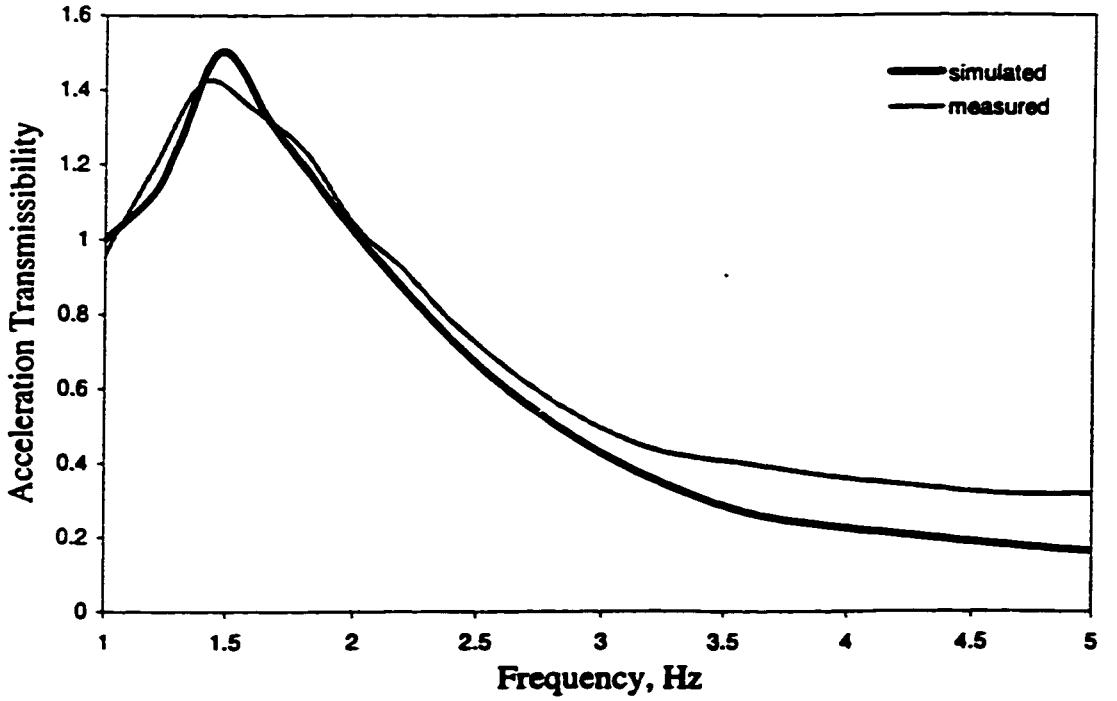

Figure 4.15: Comparison of Measured and Simulated Acceleration Transmissibility Characteristics at the Seat for Damped ISRI-Mechanical Seat-Suspension System.

the analytical acceleration transmissibility characteristics correlate quite well with those established from the laboratory measurements.

The validity of the ADAMS model is further examined under random excitations. The acceleration response of the ADAMS seat-suspension model is evaluated under excitations due to Class2 and ISO2 excitations defined earlier in section 4.2.4, while the driver is represented as a rigid mass. The acceleration response of the ADAMS model is analyzed to derive its power spectral density (PSD). The PSD of the acceleration response of the seat under ISO2 and Class2 excitation are compared with those derived from the laboratory tests performed using the WBVVS, in order to demonstrate the validity of the analytical model. Since the random excitations predominate in a relative narrow frequency band, depending upon the excitation class, the suspension seat response tends to be quite pronounced in that particular band. Outside this frequency band, the acceleration response tends to be masked by excessive noise due to very low level excitations. The acceleration transmissibility characteristics under such excitations have little significance, and thus not presented.

Figures 4.16 and 4.17 illustrate the comparison between measured and computed PSD acceleration response at the driver mass-seat interface derived under ISO2 and Class2 random excitation classes. Under ISO2 excitation, the computed model response is in close agreement with the measured response. The model, however, tends to overestimate the response, particularly at the predominant excitation frequency. This tendency is also observed under Class 2 excitations, although the overestimation is more pronounced. In the 1.8-2 Hz frequency band the difference between the model and measured response is observed to be as high as 100%. Outside this particular band, the

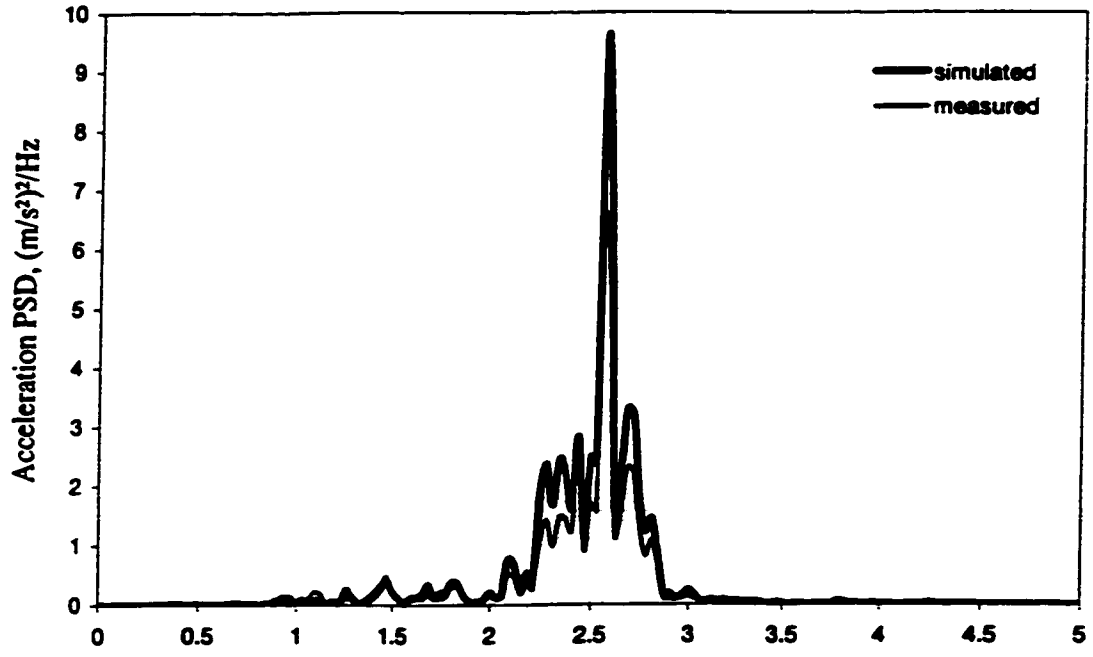

Figure 4.16: Comparison of Measured and Simulated Response Characteristics for ISRI-Mechanical Seat-Suspension System Loaded with a Rigid Body under ISO2 Class Random Excitations.

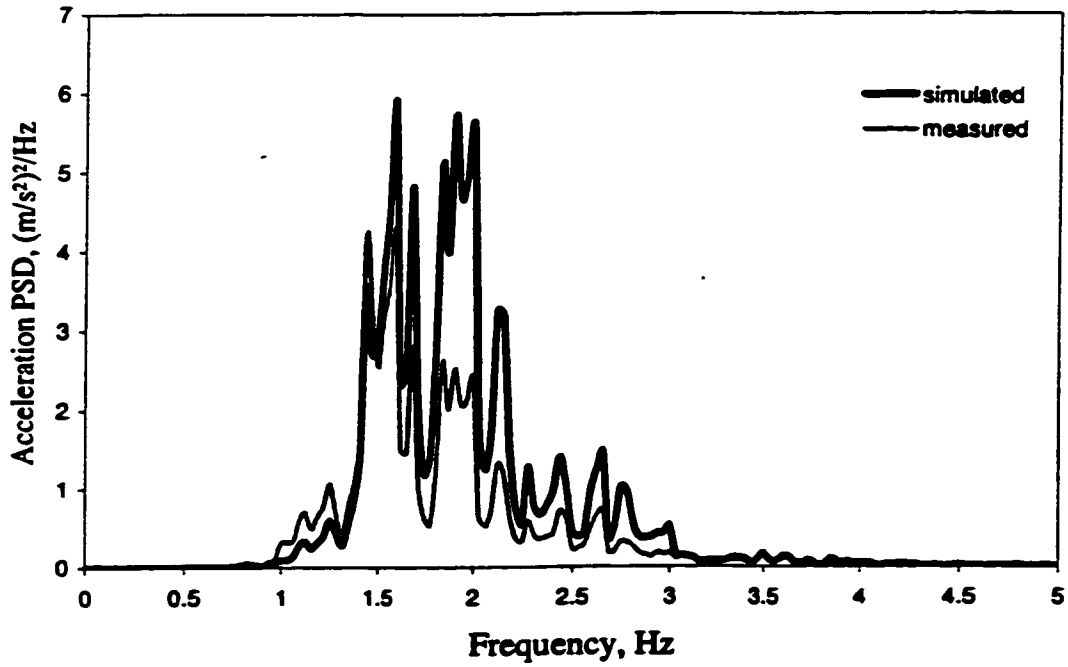

Figure 4.17: Comparison of Measured and Simulated Response Characteristics for ISRI-Mechanical Seat-Suspension System Loaded with a Rigid Load under Class2 Random Class

degree of correlation can be considered to be relatively good.

4.4.2 Dynamic Seat with Occupant

The seat-suspension system performance is influenced not only by the suspension design and parameters but also by the dynamics of the suspended mass of the driver. It is thus essential to incorporate the appropriate human body model into the seat-suspension model in order to investigate the performance characteristics of the total driver-seat-suspension system. The relative performance characteristics of three different seated human body models were investigated in Chapter 2. From the results it was concluded that the single-DOF driver model, proposed by Griffin [39], allows the most effective evaluations of the driver's contribution.

A combined ADAMS suspension-seat-human driver model is thus developed upon integrating the suspension-seat model, presented in section 4.3, with the linear single-DOF seated human body model. The simulations were performed under sinusoidal excitations swept in the 0.5-10 Hz frequency range, and ISO2 and Class2 random excitations. The computed vibration response characteristics of this combined model are compared with those derived from the laboratory tests performed using WBVVS for a seat loaded with human subject, to demonstrate the validity of the model. The tests were performed with a male seated subject 'A' with feet resting flat on the WBVVS platform and hands in contact with a steering wheel with the mass supported by the seat equal to 55.6 kg (73.2 kg while standing). The results of the comparison are discussed below.

Sinusoidal excitations: Figure 4.18 illustrates a comparison of the suspension seat acceleration transmissibility measured with subject 'A' under sine sweep excitation with

the response characteristics computed from the ADAMS combined suspension-seat-occupant model. The analytical results exhibit trends similar to those observed in the measured response, certain deviations between the response magnitudes are also observed. The largest deviations between the model response and the measurements are observed at frequencies above 4 Hz, while a relatively good agreement between the computed and measured results is observed in the 1-4 Hz frequency range. At frequencies above 4 Hz, the model provides an underestimation of the measured seat transmissibility

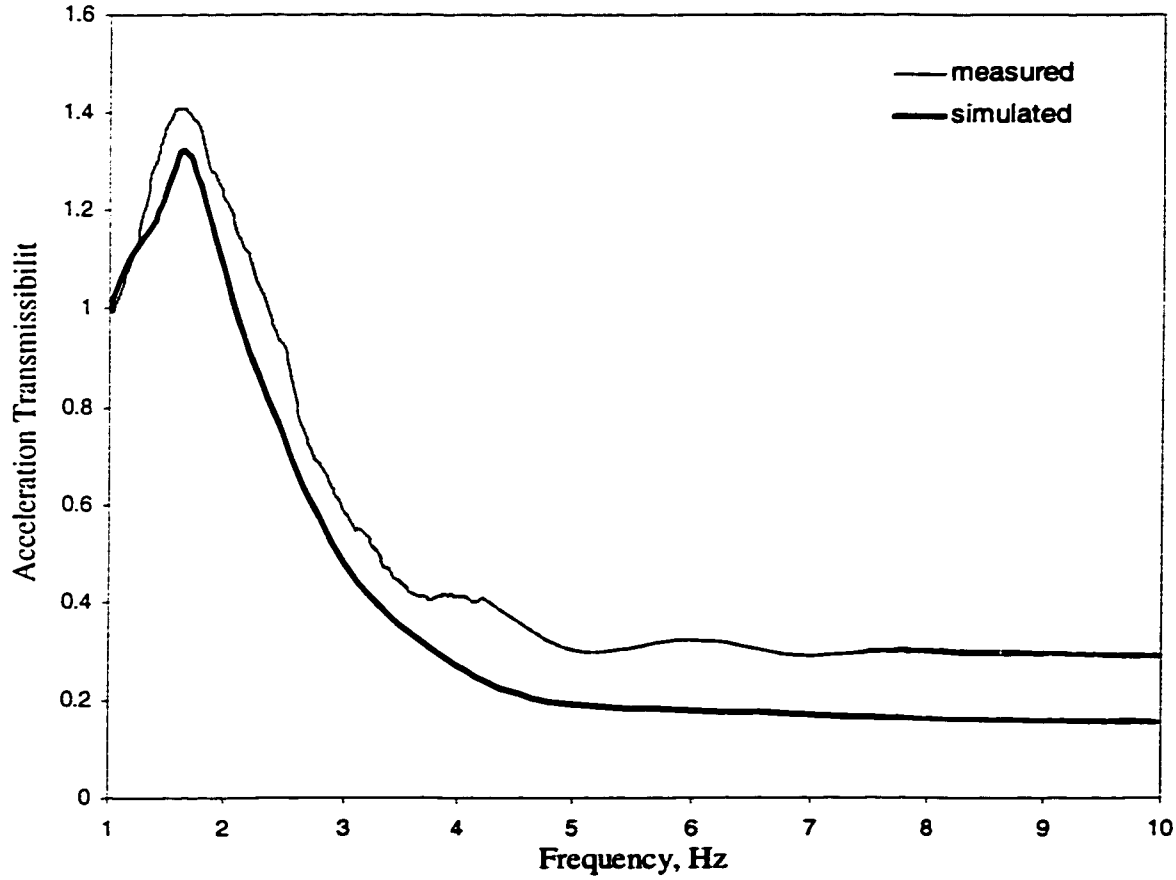

Figure 4.18: Comparison of Measured and Simulated Acceleration Transmissibility Characteristics of ISRI-Mechanical Seat-Suspension System Loaded with a Human Body.

magnitude by as much as 100% at some particular frequencies.

Random excitations: The PSD of acceleration response derived from the ADAMS model using local equivalent linearization technique under different random excitations, are compared with the PSD of measured acceleration response under identical excitations to examine model validity. Figures 4.19 and 4.20 illustrate the comparison of PSD of measured and computed acceleration response under ISO2 and Class2 random excitations. The analytical response characteristics under ISO2 input are observed to be in good agreement with measured response, except for slight deviations in the vicinity of predominant excitation frequency of 2.65 Hz. For the Class 2 excitation, the model generally tends to underestimate the response, particularly in the vicinity of suspension resonant frequency (1.4-1.6 Hz). In view of high level of difficulty involved in determining the model parameters, the degree of correlation between computed and measured response can be considered relatively good under the two classes of off-road vehicle vibration selected. The error associated with the ADAMS model may be considered within tolerable limits. The proposed model may thus be considered as a useful design tool to further investigate the response behavior of coupled driver-suspension-seat system, the influence of the suspension parameters on the vibration attenuation performance, and the optimal suspension design to minimize the whole-body vibration exposure.

4.5 Summary

A two-DOF nonlinear suspension-seat model is formulated using ADAMS software. A single-DOF occupant model is integrated to derive a coupled suspension-seat-occupant model. The proposed models with rigid and seated body model are

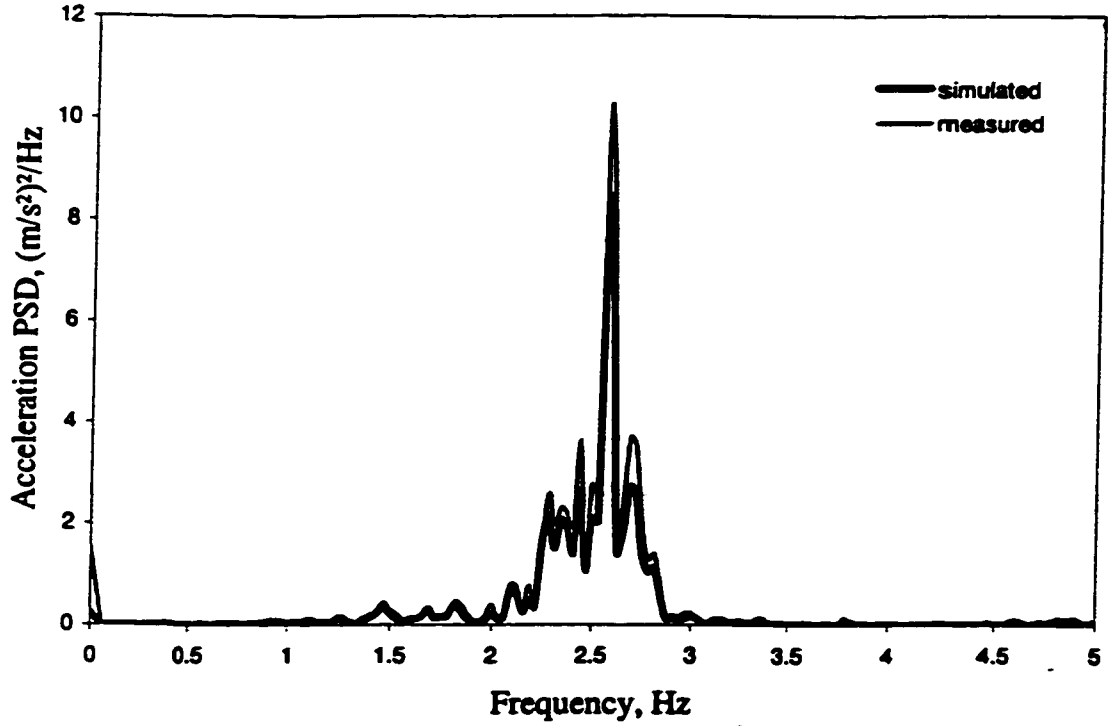

Figure 4.19: Comparison of Measured and Simulated Response Characteristics for ISRI-Mechanical Seat-Suspension System Loaded with a Human Body under ISO2 Random Class

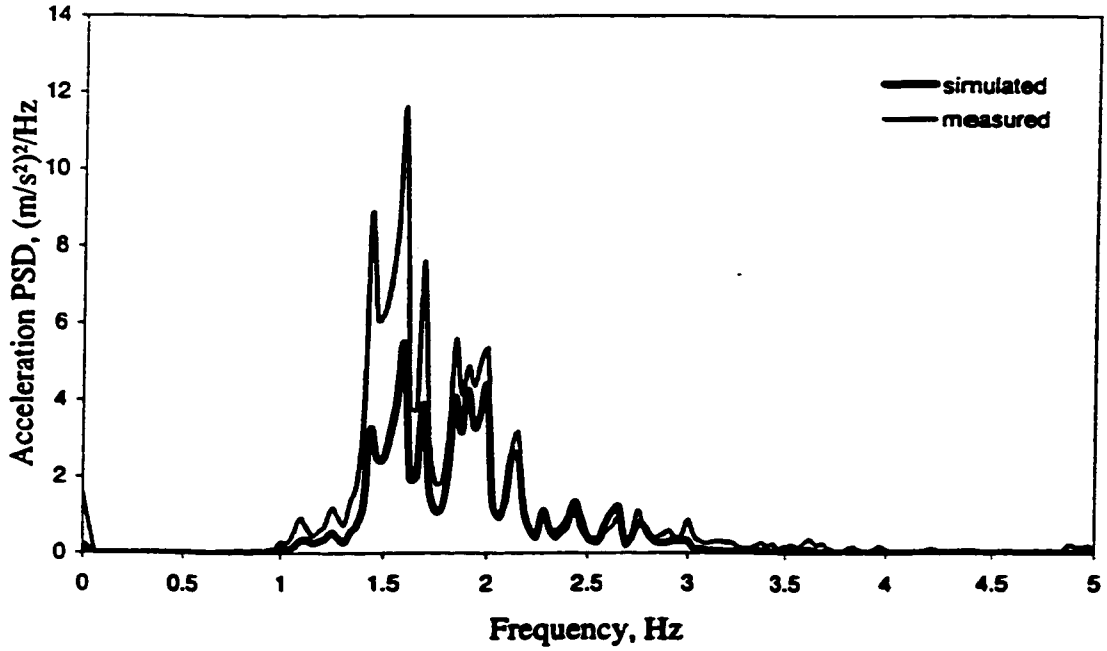

Figure 4.20: Comparison of Measured and Simulated Response Characteristics for ISRI-Mechanical Seat-Suspension System Loaded with a Human Body under Class2 Random Excitation.

analyzed under deterministic and random excitation. The acceleration response characteristics of the models are compared with the data acquired from laboratory measurements performed on a suspension seat loaded with a sand bag and a human subject. The comparison revealed relatively good agreement between the measured and model response characteristics. The proposed model resulted in reasonably accurate estimation of the response under excitations, which are predominant at relatively higher frequencies, such as ISO2. The model resulted in poor correlation with the measured data under excitations, which predominate at frequencies closer to the suspension resonant frequency.

CHAPTER 5

CONCLUSIONS AND RECOMMENDATIONS FOR THE FUTURE WORK.

5.1. Highlights of the Investigation

The thesis research was formulated to develop analytical and experimental tools to effectively analyze and assess the performance characteristics of automotive and suspension seats. The major highlights of the thesis include:

- Development of seat-occupant mathematical models incorporating single-, two- and four-DOF human body models, and nonlinear static and dynamic properties of the seat cushion.

- Identification of seat cushion properties through static and dynamic tests performed on the seats.

- Derivation of response characteristics of the seat-human and seat-passive load systems through laboratory tests performed under harmonic and random excitations.

- Formulation and implementation of the local equivalent linearization technique to represent nonlinear force-displacement and force-velocity behavior of seat cushions by arrays of local equivalent spring and damping constants.

- Validation of analytically derived vibration transmission characteristics against the experimental results under different excitations, and selection of the most appropriate human body model.

- Development of methodology for estimation of seat performance and the Human body Response Function.

- Response analysis of the seat-human system incorporating the Human Response Function under sinusoidal and random input excitations.

- Determination of vibration transmissibility characteristics and parametric sensitivity analysis of seat-human body model.

- Development of an ADAMS model of dynamic suspension seat and a combined dynamic suspension seat-occupant system and validation of the models against experimental data.

5.2. Conclusions

The following conclusions are drawn from the experimental and analytical studies conducted in this investigation.

- Human body is most sensitive to vertical whole-body vibrations in the 1-8 Hz frequency range, and the automobile vibrations mostly dominate in same frequency range.

- From the analysis of the measured data, it is concluded that:

(i) static stiffness of a seat cushion is a strong nonlinear function of its deflection and hysteretic properties of the foam cushion;

(ii) the dynamic force-deflection characteristics of seats 'A' and 'B' revealed that seats in-general become stiffer at higher excitation frequencies, and the capability of the seats to dissipate energy strongly depends on the excitation frequencies;

(iii) the equivalent viscous damping coefficient derived from the force-deflection characteristics revealed nearly constant coefficient at frequencies above 3 Hz and only minimal dependency upon deflection amplitude.

- From the analyses of the measured data obtained from laboratory testing of seat-human and seat-passive load systems, it is concluded that:

(i) the acceleration transmissibility characteristics for seats 'A' and 'B' show considerable variations among the measurements performed with different subjects, belonging to 50^{th} percentile male category. The acceleration transmissibility curves reveal seat-subject system natural frequency in 2.5-3.5 Hz frequency range for both seats;

(ii) for the seats loaded with a passive load (sandbag) both the peak acceleration transmissibility and natural frequency decrease with increase in the excitation amplitude. Fundamental frequencies are observed to be in 5.5-6.5 Hz range and the magnitudes of peak acceleration transmissibility obtained with a sandbag are considerably larger than those obtained with human subjects. It is apparent that the human body contributes considerably in reducing the fundamental frequency, peak acceleration transmissibility and the vibration transmission in the isolation frequency range.

- The comparative analysis of simulation results for seat-occupant systems incorporating different human body models revealed that the vehicle seat-occupant system can be characterize by a two-degrees-of-freedom dynamic system incorporating linear single-DOF human body model and nonlinearities due to seat cushion.

- The results obtained through analysis of the coupled human-seat model also reveal that the human body dynamics contributes considerably to the overall performance.

- Since the assessment methods of seat performance using human subjects pose many ethical and safety risks, the alternative method based upon the measurement with passive load offers considerable advantages in eliminating the need to repetitively expose human subjects to vibration environment.

- A Human Response Function can be identified through analysis of the vibration response behavior of the seat-human and seat-load systems. The overall performance of the seat-human system is then evaluated upon integrating the Human Response Function into the dynamic response behavior of the seat-load system.

- The implementation of Human Response Function resulted in reasonable correlation between estimated and measured performance characteristics for seats 'A' and 'B'. The Human Response Function can then serve as a very important tool to assess the overall performance of the seats, while eliminating the complex testing involving human subjects.

- The parametric studies conducted on the seat-human body models illustrate that the ride performance characteristics can be improved by reducing the seat cushion stiffness.

- The kinematic and dynamic response characteristics of a suspension-seat system can be effectively investigated through development and analysis of an ADAMS model. The model allows for the assessment of various geometric nonlinearities and suspension nonlinearities due to bump stops, joint friction and shock absorber, in view of the seat comfort performance.

5.3. Recommendations for Further Investigation

The experimental and analytical studies performed in this investigation focus on the development of methodologies for objective assessment of comfort performance of automotive and dynamic seats. However, the ride perceived by the car occupant is a

function of the road roughness, vehicle dynamics, occupant enclosure, and seat location within the vehicle. Therefore, studies incorporating a full-scale vehicle model are recommended in order to study the performance characteristics of the seat-human body system in a realistic environment of multiple axes vibration.

Further studies in development of nonlinear human body models that could closely approximate the characteristics of human body under vehicular vibration environment is recommended for more realistic assessment of vibration transmission performance of seat-human system.

The effectiveness of the proposed methodology and Human Response Function needs to be evaluated for a large group of automotive seats and human subjects in conjunction with representative excitations and adequate seat load.

The kinematic behavior of a suspension seat and thus the design of its linkages needs to be further investigated using the ADAMS based design tool formulated in this study. The model may be further explored as a design tool to tune the suspension for different kinds of excitation arising from varying classes of vehicles.

REFERENCES

1. Wong, J. "Theory of Ground Vehicles", Wiley Interscience, New York, 1978, 330 pp.

2. Rosegger, R., and Rosseger, S. "Health Effects of Tractor Driving", J. Agr Eng Res, Vol.5, 1960, pp. 241-275.

3. Coermann, R.R., "The Mechanical Impedance of the Human Body in Sitting and Standing Position at Low Frequencies", *Human Factors*, 1962, pp. 227-253.

4. Ograwa, S. "Study of Riding Quality With New Concept", Japanese Railway Engineering, Vol. 21, No. 1, 1991, pp. 16-22.

5. Griffin, M. J. "Evaluation of Vibration with Respect to Human Response", SAE Paper No. 860047, 1986.

6. Miwa, T. "Evaluation Methods for Vibration Effect: Part 8, The Vibration Greatness of Random Waves", Industrial Health, Vol. 7, 1969, pp. 89-115.

7. Oborne, D.J. "Techniques Available for the Assessment of Passenger Comfort", Applied Ergonomics, Vol. 9, No. 1, March 1978, pp. 211-225.

8. Van Deusen, B.D. "Human Response to Vehicle Vibration", Transaction SAE, Vol. 77, No. 1, 1968, pp. 328-345.

9. Verein Deutscher. "Assessing the Effects of Vibration on Human Beings", VDI-2057. Translated and Published by Peter Peregrinus Ltd. Stevenge, Herts, U.K., 1963.

10. Janeway, R.N. "Passenger Vibration Limits", SAE Journal Vol. 77, No. 1, 1968, pp. 346-370.

11. Society of Automotive Engineers. "Measurement of Whole-Body Vibration of the Seated Operator of Off-Highway Work Machines", SAE J1013, January 1980.

12. Murphy, N.R. "Further Developments in Ride Quality Assessment", ISTVS 8th International Conference, Cambridge, 1992.

13. Goldman, D.E. "A Review of Subjective Responses to Vibratory Motion of the Human Body in the Frequency Range 1-70 cps", Naval Med. Res. Institute, Report No. 4, March 1948.

14. International Standard Organization ISO-2631/1. "Mechanical Vibration and Shock-Evaluation of Human Exposure to Whole-Body Vibration", Part 1: General Requirements, First Edition, 1985, 17 pp.

15. Lee, R. A. and Pradko, F. "Analytical Analysis of Human Vibration", SAE Paper No. 680091, January 1968.

16. British Standard Guide to "Measurement and Evaluation of Human Exposure to Whole-Body Mechanical Vibration and Repeated Shock", BS 6841: 1987.

17. International Standard Organization ISO-2631 / 1. "Mechanical Vibration and Shock-Evaluation of Human Exposure to Whole-Body Vibration", Part 1: General Requirements, 1994, 33 pp.

18. Boileau, P.E. "Evaluation of Human Exposure Using Fourth Power Method and Comparison with ISO-2631", Journal of Sound and Vibration, Vol. 129, No. 1, 1989, pp. 143-154.

19. Varterasian, J.H. "On Measuring Automobile Seat Ride Comfort", SAE Technical Paper No. 820309, February 1982.

20. Stikeleather, L.F. and Timithy, L.F. "Simulation of Seat Ride Performance by the Mechincal Impedance of the Test Load", SAE Paper No. 891161, 1989, pp. 371-382.

21. Afework, Y., "An Analytical and Experimental Study of Driver-Seat-Suspension Systems", M.A.Sc. Thesis, Concordia University, Montreal, 1991.

22. Boileau, P.E. "A Study of Secondary Suspension and Human Driver Response to Whole-Body Vehicular Vibration and Shock", Ph.D. Thesis, Concordia University, March 1995, pp. 200-305.

23. Griffin, M.J., "Handbook of Human Vibration", Academic Press, London, 1990.

24. Fairley, T.E. and Griffin, M.J. "Modeling a Seat-Person System in the Vertical and Fore-and-Aft Axes", Vehicle Noise and Vibration Conference, Institution of Mechanical Engineers, London, 1984.

25. Claar, P., Buchele, W.F., Marley, S.J., and Seth, P.N. "Off-Road Vehicle Ride: Review of Concepts and Design Evaluation with Computer Simulation", SAE Paper No. 801023, 1980.

26. Rakheja, S., Ahmed, A.K.W. "Ride Performance Characteristics of Seat-Suspension Systems and Influence of the Seated Driver", ASAE Paper No 917569, Chicago, Illinois, 1991, 26 pp.

27. Suggs, C.W., Stikeleather, L.E., Harrison, J.Y. and Young, R.E. "Application of a Dynamic Simulator in Seat Testing", Annual Meeting American Society of Agricultural Engineers, Purdue University, Indiana, 1969.

28. Fairley, T.E., Griffin, M.J. "A Test Method for the Prediction of Seat Transmissibility", SAE Paper No. 860046, January, 1986.

29. Matthew, J. "Progress in the Application of Ergonomics to Agricultural Engineering", Agricultural Engineering Symposium of the Institution of Agricultural Engineers, NCAE, Silsoe, 1967.

30. Rakheja, S. and Sankar, S. "An Optimum Seat-Suspension for Off-Road Vehicles", The Shock and Vibration Bulletin 53, 1983, pp. 19-34.

31. Patil, M.K., Palanichamy, M.S. and Ghista, D.N. "Tractor Occupant Dynamics and Optimal Seat Suspension for Riding Comfort", *Proceeding of the 6 th Canadian Congress of Applied Mechanics*, Vancouver, May 1977, pp. 347-348.

32. Patil, M.K., Palanichamy, M.S. and Ghista, D.N., "Man-Tractor System Dynamics: Toward a Better Suspension System for Human Ride", *Journal of Biomechanics 11*: 1978, pp. 397-406.

33. Patil, M.K., Palanichamy, M.S. and Ghista, D.N., "Minimization of Tractor-Occupant's Vibrational Response by Means of "Patil-Palanichamy-Ghista" (PPG) Tractor Seat Suspension", *Proceedings of the International CISM-IFToNN-WHO Symposium*, Udine, April 1979.

34. Meinecke, E.A. and Clark, R.C., "Mechanical Properties of Polymeric Foams", Technomic Publishing Co., 1973.

35. Hilyard, N.C. and Cillier, P. "Effect of Vehicle Seat Cushion Material on Ride Comfort", Plastic on Road: The Plastic and Rubber Institute International Conference, London, December 1984.

36. Fairley, T.E., "Predicting Seat Transmissibilities: the Effect of the Legs", *Preceedings of Joint Frech-English Meeting, Groupe Francais des Etudes des Effets des Vibrations sur l'Homme and U.K. Informal Group on Human Response to Vibvation,* INRS, Vandoeuvre, France, September 1988.

37. Chen, C.Y. and Griffin, M.J., "The application of Non-Linear Least Squares Methods to Predicting Seat Transmissibility", Technical Report No. 173. Institute of Sound and Vibration Research, The University, Southampton.

38. Payne, P.R., "Method to Quatify Ride Comfort and Allowable Accelerations", Aviation, Space, and Environmental Medicine, pp. 262-269, 1978.

39. Fairley, T.E. and Griffin, M.J., "The Apparent Mass of the Seated Human Body: Vertical Vibration", J. Biomechanics, Vol. 22, No. 2, 1989, pp. 81-94.

40. Suggs, C.W., Stikeleather, L.F *"Application of a Dynamic Simulator in Seat Testing"*, Trans. of ASAE, Vol. 13, 1970, pp. 378-381.

41. Suggs, C.W., Abrams, C.F. and Stikeleather, L.F., "Application of a Damped Spring-Mass Human Vibration Simulator in Vibration Testing of Vehicle Seats", *Ergonomics*, Vol. 12, 1969, pp. 79-90.

42. Wambold, J.C. and Park, W.H., "A Human Model for Measuring Objective Ride Quality", ASME Paper 75-DET-6, Design Engineering Technical Conference, Washington, D.C., September 1975, pp. 17-19.

43. Allen, G., "A Critical Look at Biodynamic Modeling in Relation to Specifications for Human Tolerance of Vibration and Shock", Paper A25, AGARD Conference Proceeding No. 253 "Models and Analogues for the Evaluation of Human Biodynamic Response, Performance and Protection", Paris, France, 6-10 November 1978, pp. A25-5-A25-15.

44. Mertens, H., "Nonlinear Behavior of Sitting Humans Under Increasing Gravity", Aviation, Space, and Environmental Medicine, 1978, pp. 287-298.

45. Mertens, H. and Vogt, L., "The Response of a Realistic Computer Model for Sitting Humans to Different Types of Shocks", Paper A26, AGARD Conference Proceeding No. 253 "Models and Analogues for the Evaluation of Human Biodynamic Response, Performance and Protection", Paris, France, 6-10 November 1978, pp. A26-1-A26-16.

46. ISO Committee Draft CD 5982 ., " Mechanical Driving Point Impedance and Transmissibility of the Human Body", Document ISO/TC 108/SC 4N226, 1993, 21pp.

47. Rakheja, S., Sankar, S., and Bhat, R.B., "Ride Vibration Levels at the Driver-Seat Interface", CONCAVE Research Center: Report, November 1987.

48. Claar II, P.W. and Sheth, P., "Off-Road Vehicle Ride: Review of Concepts and Design Evaluations with Computer Simulations", SAE Paper No. 801023, 1980.

49. Stikeleather, L.F., "Operator Seats for Agriculture Equipment", ASAE Distinguished Lecture Series, No. 7, 1981.

50. Gillespie, T.D., "Heavy Truck Ride", SAE/SP-85/607, 1985.

51. Stikeleather, L.F. and Suggs, C.W., "An Active Suspension System for Off-Road Vehicles", Trans. of ASAE, Vol. 13, No. 1, 1970, p. 99.

52. Young, R.E. and Suggs, C.W., "Seat-Suspension System for Isolation of Roll and Pitch in Off-Road Vehicles", Trans. of ASAE, Vol. 16, No. 5, 1973, p. 876.

53. Rakheja, S., "Computer Aided Dynamic Analysis and Optimal Design of Off-Road Tractors", Ph.D. Thesis Concordia University, Montreal, 1983.

54. Kyeong, K.K., "Ride Simulation of Passive, Active and Semi-Active Seat-Suspensions for Off-Road Vehicles", Ph.D. Thesis, University of Illinois at Urbana-Champaign, 1981.

55. Kjellberg, A. "Whole-Body Vibration: Exposure Time and Acute Effects – Experimental Assessment of Discomfort", Ergonomics, vol. 28, 1985, pp. 545-554.

56. Rakheja, S., Peijun Liu, Ahmed, A.K.W. and Su, H., "Analysis of an Interlinked Hydro-Pneumatic Suspension", *Advanced Automotive Technologies*, DSC-Vol. 52, *Proc. of ASME Winter Ann. Meet.*, New Orleans, Nov. 1993, pp. 279-288.

57. Wu, X., Rakheja, S., Boileau, P.-E., "Study of Human-Seat Interface Pressure Distribution under Vertical Vibration", International Journal of Industrial Ergonomics 0169-8141, 1997.

58. Oborne, D.J., and Boarer, P.A., "Subjective Response to Whole-Body Vibration. The Effect of Posture", Ergonomics, Vol. 25, 1982, pp. 673-681.

59. Bowers-Carnahan, R., Carnahan, T., Sanford, L., and Walters, J.,"User Perspective on Seat Design", International Truck and Bus Meeting and Exposition. Winston-Salem, North Carolina, SAE No. 952679, 1995.

60. Styner, R.M. and Whyte, R.T., "Design Criteria for Tractor Seats", In Noise and Vibration in Agriculture and Forestry. Proceedings of the 8 th Joint Ergonomic Symposium, Sisole, Bedford Shire, UK, September 1985.

61. Stikeleather, L.F., "Operator Seats for Agricultural Equipment", ASAE Distinguished Lecture Series, No. 7, 1981.

62. Bush, C.A., "Study of Pressures on Skin under Ischium Tuberosities and Thighs During Sittings", Archives of Physical Medicine and Rehabilitation, 60: 1969, pp. 207-213.

63. Griffin, M.J., "Biodynamic Response to Whole-Body Vibration", Shock and Vibration Digest, Vol. 13, No. 8, August 1981, pp. 3-12.

64. SAE J1051, "Force Deflection Measurement of Cushioned Components of Seats for Off-Road Work Machines", SAE J1051, December 1988.

65. Neirovitch, L., "Elements of Vibration Analysis", 2 nd ed. New York, McGraw-Hill, 1986.

66. Zwillinger, D., "Handbook of Differential Equations", Academic Press Inc., San Diego, 1989.

67. Van Vliet, M., "Computer Aided Dynamic Analysis and Design of Off-Road Motorcycle Suspensions", Ph.D. Thesis Concordia University, 1983.

68. Beucke, K.E. and Kelly, J.M., "Equivalent Linerization for Practical Hysterical Systems", Journal of Nonlinear Dynamics, July 1990, pp. 213-229.

69. Boileau, P.E. "A Study of Secondary Suspension and Human Driver Response to Whole-Body Vehicular Vibration and Shock", Ph.D Thesis, Concordia University, March 1995, pp. 310-314.

70. Sandover, J., "Measurement of the Frequency Response Characteristics of Men Exposed to Vibration", Ph.D. Thesis, Loughborough University of Technology, 1981.

71. Boileau, P.E. and Scory, H., "Les Lombalgies chez les Conducteurs de Debusqueuses: Etude des Vibrations Appliquees au Corps Entier dans les Chantiers Forestiers du Quebec", Arch. Mal. Prof., 1988, 49 (5) pp. 305-314.

72. SAE J1384., "Classification of Agricultural Wheeled Tractors for Vibration Tests of Operator Seats", SAE Hand Book, 1988, pp. 40.334-40.335.

73. ISO Technical Report 5007., "Agricultural Wheeled Tractors-Operator Seat-Measurement of Transmitted Vibration", ISO/TR 5007-1980(E), 1980, 29pp.

74. International Standard ISO 7096., "Earth-Moving Machinery-Operator Seat-Transmitted Vibration", First Edition, 1982, 14 pp.